The Nonlinear Schrödinger Equation as Both a PDE and a Dynamical System

David Cai * **and David W. McLaughlin** †

Courant Institute of Mathematical Sciences

New York University

New York, New York 10012

Kenneth T. R. McLaughlin

Department of Mathematics

University of Arizona

Tucson, Arizona 85721

March 8, 2001

*Sloan Foundation Grant #96-3-1

†Funded in part by NSF DMS 9600128, AFOSR-49620-98-1-0256, and Sloan Foundation Grant #96-3-1.

Abstract

Nonlinear dispersive wave equations provide excellent examples of infinite dimensional dynamical systems which possess diverse and fascinating phenomena including solitary waves and wave trains, the generation and propagation of oscillations, the formation of singularities, the persistence of homoclinic orbits, the existence of temporally chaotic waves in deterministic systems, dispersive turbulence and the propagation of spatiotemporal chaos.

Nonlinear dispersive waves occur throughout physical and natural systems whenever dissipation is weak. Important applications include nonlinear optics and long distance communication devices such as transoceanic optical fibers, waves in the atmosphere and the ocean, and turbulence in plasmas. Examples of nonlinear dispersive partial differential equations include the Korteweg de Vries equation, nonlinear Klein Gordon equations, nonlinear Schrödinger equations, and many others.

In this survey article, we choose a class of nonlinear Schrödinger equations (NLS) as prototypal examples, and we use members of this class to illustrate the qualitative phenomena described above. Our viewpoint is one of partial differential equations on the one hand, and infinite dimensional dynamical systems on the other. In particular, we will emphasize global qualitative information about the solutions of these nonlinear partial differential equations which can be obtained with the methods and geometric perspectives of dynamical systems theory.

The article begins with a brief description of the most spectacular success in pde of this dynamical systems viewpoint — the complete understanding of the remarkable properties of the soliton through the realization that certain nonlinear wave equations are completely integrable Hamiltonian systems. This complete integrability follows from a deep connection between certain special nonlinear wave equations (such as the NLS equation with cubic nonlinearity in one spatial dimension) and the linear spectral theory of certain differential operators (the "Zakharov-Shabat" or "Dirac" operator in the NLS case). From this connection the "inverse spectral transform" has been developed and used to represent integrable nonlinear waves. These representations have provided a full solution of the Cauchy initial value problem for several types of boundary conditions, a thorough understanding of the remarkable properties of the soliton, descriptions of quasi-periodic wave trains, and descriptions of the formation and propagation of oscillations as slowly varying nonlinear wavetrains.

In addition, more recent developments are described, including: (i) the formation of singularities and their relationship to dispersive turbulence; (ii) weak turbulence theory; (iii) the persistence of periodic, quasi-periodic, and homoclinic solutions, by methods including normal forms for pde's, Melnikov measurements, and geometric singular perturbation theory; (iv) temporal and spatiotemporal chaos; (v) long-time and small dispersion behavior of integrable waves through Riemann-Hilbert spectral methods. For each topic, the description is necessarily brief; however, references will be selected which should enable the interested reader to obtain more mathematical detail.

Contents

1 Introduction

Geometric viewpoints have proven to be extremely useful for understanding qualitative behavior of finite dimensional dynamical systems [153, 85, 191], particularly behavior over long (infinite) durations of time. We believe that viewpoints which combine geometry and dynamics will prove to be equally useful for understanding qualitative long-time results for evolutionary partial differential equations (pde's). Even though pde's are infinite dimensional dynamical systems, we also believe that their deep fundamental properties will not be understood solely through natural extensions of finite dimensional methods to abstract infinite dimensional settings. Pde, computational, and stochastic methods will be essential in this process.

Our purpose here is to expose graduate students, as well as other researchers in partial differential equations, to this qualitative and geometric view of partial differential equations through a brief overview of one specific class of nonlinear wave equations. We will emphasize global qualitative behavior of solutions. We will try to select references which develop the material in an accessible, even tutorial, manner. Some of these will contain extensive references to the original work. Here, we will make no effort toward historical referencing — leaving that to other more detailed review articles. However, some sample general references include: [178, 190] for nonlinear waves; [120, 156, 56] for introduction to solitons; [181] for nonlinear lattices; [64, 11] for inverse scattering transform; [158, 161] for periodic inverse spectrum transform; [72] for recent developments. (see also extensive annotated bibiography [44].) We intend this brief overview to provide an outline or "study guide" for a graduate course which develops this qualitative viewpoint for the analysis of nonlinear waves, with the references leading to more detailed study.

This article will illustrate this viewpoint for one class of nonlinear wave equations — nonlinear Schrödinger (NLS) equations,

$$iq_t = \nabla^2 q \mp (q\bar{q})^\sigma q, \tag{1.1}$$

$\sigma \geq 0$, as well as some of its natural extensions.

This class of equations can be used to illustrate many striking features of nonlinear waves, each of which has been understood by a combination of methods from scientific computation and from the theory of pde's and geometric dynamical systems. These features include solitary waves and solitons; response of solitons to external perturbations; periodic waves and quasi-periodic wavetrains; the slow modulation of wavetrains; long-time asymptotics, including a decomposition of the field into solitons and radiation; finite-time blow up; instabilities and representations of unstable manifolds; chaotic evolution in deterministic pde's; spatiotemporal chaos and dispersive turbulence; nonlinear localization in random environments.

After touching upon the pde properties of solutions of NLS in Section 2, we begin the overview in Section 3 with a brief summary of a most spectacular success of the dynamical systems viewpoint for pde's — the complete integrability of soliton equations as infinite dimensional Hamiltonian systems. Established through the deep connection between spectral theory of certain linear differential operators and specific nonlinear wave equations, this complete integrability unveils and demystifies the mysteries of solitons. It also provides

representations of important classes of nonlinear waves — including N-solitons in interaction and multi-phase wave trains, as well as the full solution of Cauchy initial value problems. Long-time asymptotic descriptions of the nonlinear waves, including dispersive spreading, scattering, and a decomposition of the field into solitons and radiation, follow from these representations, as well as small dispersion (semi-classical) asymptotics. Under periodic spatial boundary conditions, Floquet theory of the linear differential operators provides a proof of almost-periodic behavior in time of the general solution to the periodic Cauchy problem. For NLS with focusing nonlinearity, this work under periodic boundary conditions culminates in the identification and complete classification of all instabilities, and in the complete representation of their associated unstable manifolds and homoclinic orbits. Such detailed information is unprecedented for finite dimensional dynamical systems, let alone for nonlinear pde's — and indicates the power of the connection between linear spectral theory and certain nonlinear wave equations.

In Section 4 we consider perturbations of the integrable NLS equation — damped-driven perturbations under spatially periodic boundary conditions. The instabilities in the integrable focusing case can generate chaotic behavior when the system is perturbed. First, numerical experiments showing temporal chaos are summarized, which are then correlated with integrable instabilities. Then the persistence of homoclinic orbits under perturbations is established with mathematically rigorous analytical arguments. Finally, the connection of these persistent homoclinic orbits with long complex transients and with symbol dynamics is briefly summarized.

In Section 5, spatiotemporal chaos is found for these same perturbations by breaking the even spatial symmetry of the system. The concept of spatiotemporal chaos is defined, characterized in terms of "mutual information" at two separated spatial locations, and studied numerically. Then, in Section 6, macroscopic descriptions of the spatiotemporal chaotic state are briefly summarized, including equilibrium statistical mechanics, weak-turbulence theories, and "effective stochastic dynamics". Section 6 concludes with sample effects of random coefficients such as "nonlinear localization" — emphasizing distinctions between the linear case and those of focusing or defocusing nonlinearities.

In Section 7, we return to the integrable case and describe a powerful analytic method which has recently been developed to extract asymptotic information from the linear spectral representations of integrable nonlinear equations — the Riemann-Hilbert method. First, we define the representations developed by this approach and indicate their use for long-time asymptotics. We then outline the asymptotic method, which exploits rapidly oscillating kernels in the Riemann-Hilbert integral equations. Finally we describe the success of this approach by stating a theorem which provides the complete long-time asymptotics of NLS waves.

In Section 8, semiclassical behavior of the NLS wave is described — first by numerical experiments which illustrate the sharp distinctions between linear, defocusing, and focusing behavior, and then by a formal modulation theory. We then mention the use of the Riemann-Hilbert approach to obtain "semiclassical" asymptotic behavior in the defocusing case. The section concludes with a brief description of a beautiful representation of the resulting modulation equations in terms of Abelian differentials and its use in unifying

other equivalent representations.

In this article we illustrate the potential power of the combination of pde methods with those from geometric dynamical systems. But we also emphasize the importance of a totally new and unexpected idea in the creative process of mathematical discovery — in this case the deep connection between linear spectral theory and certain special nonlinear wave equations. And we emphasize that the full use of such key new mathematical ideas requires further new analytical developments — in this case the Riemann-Hilbert representations of inverse spectral theory and their use for asymptotics. Riemann-Hilbert methods realize the power and breadth of integrable methods for modern analysis of asymptotic limits — for nonlinear waves and far beyond. This point is elaborated upon in the Conclusion, where we also mention the many open problems for research, once rigid integrability is relaxed. It is in resolving these that we expect the interplay between pde and geometric-dynamical systems to play an essential role.

2 Pde Properties

Energy methods can be used to establish the following global existence result[36, 178]:

Theorem 2.1 *Consider the Cauchy problem for*

$$\begin{aligned} iq_t &= \nabla^2 q - g(q\bar{q})^\sigma q, \quad g = \pm 1, \\ q(t=0) &= q_0 \in H^1(\mathbb{R}^N). \end{aligned}$$

1. *Assume either a) $g > 0$ and $0 \le \sigma < 2/(N-2)$, or b) $g < 0$ and $0 \le \sigma < 2/N$.*

   Then $\forall q_0 \in H^1(\mathbb{R}^N)$, $\exists!\ q \in C[\mathbb{R}; H^1(\mathbb{R}^N)]$ which solves the initial value problem for the NLS equation.

2. *For $g < 0$ and $\sigma = 2/N$, $\forall q_0 \in H^1(\mathbb{R}^N)$, $|q_0|_2 < |R|_2$*

   $\Rightarrow$ $\exists!\ q \in C[\mathbb{R}; H^1(\mathbb{R}^N)]$ which solves the initial value problem for the NLS, where R denotes the solitary wave solution (2.2) of the critical NLS equation.

3. *For $g < 0$ and $\sigma = 2/N$, if the energy (2.1) $H(q_0) < 0$, then*

   (a) $\exists$ a finite time T^* such that $\lim_{t \uparrow T^*} |q(t)|_{H^1} = +\infty$.

   (b) $\exists$ a finite time T^{**} such that $\lim_{t \uparrow T^{**}} |q(t)|_\infty = +\infty$.

Similar results hold for a larger, more general class of NLS equations and boundary conditions. Here the Sobolev space $H^1(\mathbb{R}^N)$, consisting of functions which are square integrable with square integrable first derivatives, is natural because of the energy invariant of NLS,

$$H(q) \equiv \int \left[|\nabla q|^2 + \frac{g}{\sigma+1} |q|^{2(\sigma+1)} \right] d^N x, \tag{2.1}$$

which can be used to provide global control. Recently, solutions with "rough data" have also become important — for example, for statistical solutions (see below). For recent existence results for data rougher than H^1, see [19, 21, 26, 27].

It is clear from this existence theorem that the sign of nonlinearity is important, with $g = -1(+1)$ called *focusing* (*defocusing*) nonlinearity, respectively. In the defocusing case, the energy (2.1) is positive definite and can be used for global control of the existence estimates. In the focusing case, the energy (2.1) is indefinite, and need not provide sufficient control if the nonlinearity is too strong, i.e., $\sigma \geq 2/N$. In this case, the focusing nonlinearity can cause the solution to blow-up in finite time. To see this, consider the following differential inequality which follows from the focusing NLS equation:

$$\frac{d^2}{dt^2} V(q) \leq 4H(q), \quad \sigma \geq 2/N,$$

where the variance V is defined by the functional

$$V(q) \equiv \int \left[|\vec{x}|^2 \ |q|^2 \right] \ d^N x,$$

and where $q = q(\vec{x}, t)$ denotes any solution in $H^1[\mathbb{R}^N]$ for which the variance $V(q)$ is well defined. This differential inequality immediately shows that, for initial data with negative energy $[H(q_{in}) < 0]$, the positive definite variance must become negative in finite time. Clearly, this contradiction implies a breakdown in the solution. Sobolev arguments then show that the solution blows-up by leaving H^1, and L^∞, in finite time. Such matters are discussed with mathematical rigor in references [79, 36, 178].

This blow-up can be understood intuitively, as follows: The focusing nonlinear medium acts as a lens which focuses more and more strongly, the more intense and focused the wave; hence, a catastrophic blow-up of intensity of the wave results, accompanied by the collapse of its spatial extent. In applications such as the propagation of a laser beam, this produces the striking effect of extremely intense, very sharply focused, spots of light. (These spots of light are called "filaments" in the nonlinear optics literature, and the laser beam is said "to filament.")

The NLS equation (1.1) is a *conservative* wave equation. In addition to the energy (2.1), the L^2 norm

$$I(q) \equiv \int |q|^2 \ d^N x$$

and linear momentum

$$\vec{P}(q) \equiv \int \frac{q \nabla \bar{q} - \bar{q} \nabla q}{2i} \ d^N x$$

are also invariants — associated to the symmetries of time translation, phase translation, and space translation. In addition, (1.1) admits the important *Galilean and scaling symmetries*: If $q(x,t)$ denotes a solution, so does

$$\begin{aligned} Q(x,t;v) &= q(x - vt, t) \exp\left(\frac{i}{4} [v^2 t - 2vx] \right), \\ Q(x,t;\lambda) &= \lambda^{1/\sigma} q(\lambda x, \lambda^2 t). \end{aligned}$$

The NLS equation is classified as a *dispersive nonlinear wave equation* [190] because its linearization about $q = 0$,

$$iq_t = \Delta q,$$

has Fourier solutions of the form

$$A \exp\{i[\vec{k} \cdot \vec{x} + \omega(\vec{k})t]\}, \quad \forall \vec{k} \in \mathbb{R}^N,$$

with real dispersion relation

$$\omega(\vec{k}) = |\vec{k}|^2.$$

Thus, different Fourier components travel at different speeds — leading to dispersive spreading, algebraic (in t) decay, and the concept of a *group velocity*, which for this linear equation is given by

$$\vec{v}_{gp}(\vec{k}) = \nabla_{\vec{k}}\omega = 2\vec{k}.$$

Focusing nonlinearity acts against this dispersive spreading mechanism, can completely overwhelm spreading and produce singularities in finite time, or it can exactly balance the spreading mechanism and produce persistent solitary waves which are localized in space. Which of these alternatives occurs depends upon details of the competition between nonlinearity and dispersion. For example, consider the case of cubic nonlinearity,

$$iq_t = \Delta q + 2(q\bar{q})\, q,$$

for which solitary waves exist of the form

$$q(\vec{x}, t) = \exp(-it) R(|\vec{x}|),$$

where R(r) is defined as the *positive* solution of

$$\Delta R + \left(2R^2 - 1\right) R = 0, \tag{2.2}$$

$$\begin{aligned} R_r(0) &= 0, \\ R(r) &\to 0 \text{ as } r \to +\infty. \end{aligned}$$

In dimension $N = 1$, these localized waves are stable, while for dimension $N \geq 2$ they are unstable; in fact, severely unstable to blow-up in finite time.

When combined with Galilean invariance, a four parameter representation of solitary waves results, which in dimension 1 takes the form

$$q(x, t; \lambda, v, \gamma, x_0) = \lambda \operatorname{sech}[\lambda(x - x_0 - vt)] \exp\left[\frac{i}{4}\Big((v^2 - 4\lambda^2)t - 2vx + \gamma\Big)\right]. \tag{2.3}$$

This wave is (exponentially) localized in space, and has many of the characteristics of a "particle". The parameters $(\lambda, v, \gamma, x_0)$ represent its amplitude [inverse-width], velocity, phase, and spatial location, respectively. This particle-like wave travels at constant velocity v and is very stable to perturbations of both the initial data and the equation. The stability and properties of this solitary wave have been established with many numerical experiments in the physical literature, with formal asymptotics [101], and with rigorous pde analysis [83, 84, 187].

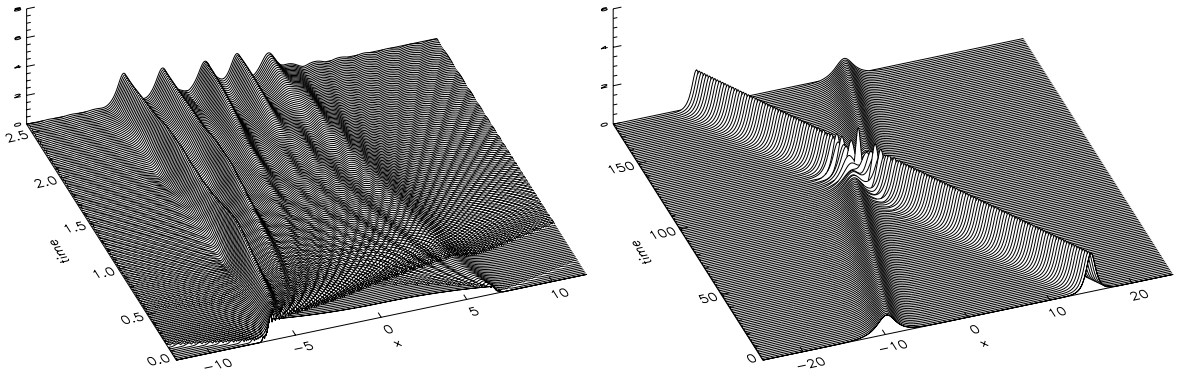

Figure 1: Left panel: solitons emerge out of an initial wave packet; Right panel: collision of two solitons.

These solitary waves are the most striking and important component of the solution of the NLS equation — as is clearly seen in numerical simulations. Emerging from generic Cauchy data (which vanishes sufficiently rapidly as $|x| \to \infty$) are a finite number of solitary waves (see Fig. 1), traveling to both the left and right, ordered by the magnitude of their velocities — together with a finite number of "nonlinear bound states" of these solitary waves. In addition, an algebraically decaying (in t) component is present which resembles dispersive radiation of the linear Schrödinger equation. These solitary waves are remarkably robust. They exist for a large class of nonlinearities, persist (but slowly deform) under small perturbations of the equation, and can survive collisions with other solitary waves. In the case of cubic nonlinearity, no radiation emerges from these direct collisions. Rather, the two solitary waves emerge from the collision unscathed, with the same velocities and with no generation of additional radiation. The only change the wave experiences as a result of collisions between solitary waves is a shift in their relative phases. In effect (see Fig. 1), for the cubic nonlinearity, NLS solitary waves travel and interact as particles experiencing elastic collisions. For other nonlinearities, very stable solitary waves exist, but radiation (at times slight and at times significant) is generated by collisions. These remarkable stability properties for localized waves of NLS make them potentially important in many physical and technological applications — including laser beams [157, 90] and transoceanic telephone communication [152].

Understanding these stability properties has also generated considerable mathematical research. Formal asymptotic methods can be used to study linearized stability of the solitary wave [101, 186, 187] and its response to perturbations [101, 146]. For the latter, the NLS equation is perturbed by the addition of small $O(\epsilon)$ terms such as dissipation. Then approximate solutions are constructed from the solitary waveform, with two modifications: (i) the replacement of its constant parameters (such as the velocity v) with (slowly varying) functions of time; and (ii) the addition of a small correction to the solitary wave. Demanding that this correction remains small over times of $O(\epsilon^{-1})$ identifies the correct slow modulations of the parameters.

For example, small dissipation causes the velocity $v(\epsilon t)$ to slowly decay as a function of time. Some of these formal calculations have been made rigorous mathematically: Nonlinear stability of the solitary wave has been established [83, 84, 187]; while modulation theory has led to some of the most successful combinations of pde scattering theory with geometric dynamical systems [188, 173, 174, 175] for the study of the interaction of solitary waves with radiation. In this work, the evolution equations for the nonlinear wave are decomposed into discrete solitary and continuous radiative components; and the equations are then analysed with a combination of methods from scattering theory for pde's with center manifold-like arguments from dynamical systems theory. A global characterization of the interaction of solitary with radiation results [188, 173, 174, 175, 59, 160].

But the understanding of the remarkable elastic collision properties of solitary waves for the 1-D cubic NLS equation required totally new mathematical ideas [77, 78, 151, 196] — ideas which are very different from classical pde and dynamical systems methods. One description of these begins from the realization that the NLS equation (1.1) is a Hamiltonian system,

$$iq_t = \frac{\delta H}{\delta \bar{q}},$$

which for the 1-D cubic case is a very special Hamiltonian system. In the next section we will describe those new mathematical ideas which identify the very special nature of this 1-D cubic NLS equation, and the reasons for the remarkable elastic scattering properties of its solitary waves.

3 The Integrable NLS Equation

The 1-D cubic NLS equation,

$$iq_t = q_{xx} \mp 2\left(q\bar{q}\right) q, \tag{3.1}$$

is equivalent to the following linear system [77, 121, 196]

$$\begin{aligned} \varphi_x &= U^{(\lambda)}\,\varphi, \\ \varphi_t &= V^{(\lambda)}\,\varphi, \end{aligned} \tag{3.2}$$

where

$$U^{(\lambda)} \equiv i\lambda\sigma_3 + i\begin{pmatrix} 0 & q \\ \mp\bar{q} & 0 \end{pmatrix};$$

$$V^{(\lambda)} \equiv i\left[2\lambda^2 + \omega^2 \pm (q\bar{q} - \omega^2)\right]\sigma_3 + \begin{pmatrix} 0 & 2i\lambda q + q_x \\ \mp(-2i\lambda\bar{q} + \bar{q}_x) & 0 \end{pmatrix},$$

and where σ_3 denotes the third Pauli matrix $\sigma_3 \equiv diag(1, -1)$. This equivalence follows from the integrability condition for the overdetermined linear system (3.2): Note that system (3.2) consists in two equations for only one unknown φ. As such, it is overdetermined and will possess a solution iff $\varphi_{t,x} = \varphi_{x,t}$. Explicitly calculating this condition, using system (3.2), shows that the integrability condition is equivalent to the NLS equation (3.1).

The linear system (3.2) is known as the "Lax pair for NLS" [121, 196]. From it, the nonlinear Schrödinger equation (3.1) inherits a "hidden linearity" which is the key to an explanation of the truly remarkable properties of 1-D NLS. And it is this relationship between linear equations (3.2) and nonlinear wave equations (3.1) which is the "new mathematical idea" to which we referred at the end of the last section.

The primary way this equivalence has been used to study 1-D NLS begins from the "x-flow" of (3.2):

$$\hat{L}\,\varphi = \lambda\varphi, \tag{3.3}$$

where

$$\hat{L} \equiv -i\sigma_3 \frac{d}{dx} - \begin{pmatrix} 0 & q \\ \pm\bar{q} & 0 \end{pmatrix}. \tag{3.4}$$

We view this linear "x-flow" as a Sturm-Liouville eigenvalue problem, with eigenvalue parameter λ. For example, consider the 1-D NLS equation (3.1) on the whole line ($-\infty < x < +\infty$), for smooth rapidly decaying functions of x; i.e., in Schwarz class. [Actually, in the defocusing case $|q(x)| \to c > 0$, while in the focusing case, the limit c vanishes.] Consider the operator $\hat{L}$, equation (3.4), as an (unbounded) differential operator on $L^2(\mathbb{R})$, which is known as the "Zakharov-Shabat" operator. Denote its point spectra (eigenvalues with $L^2(\mathbb{R})$ eigenfunctions) by $\{\lambda_1, \lambda_2, \ldots, \lambda_N\}$. As the coefficients $q(x,t)$ of this differential operator evolve in time t according to 1-D NLS equation (3.1), one expects the eigenvalues $\lambda_j(t)$ to change with time. But they do not! A simple calculation using the Lax pair (3.2) shows that the eigenvalues are constant in t. These eigenvalues provide N invariants for the 1-D NLS equation (3.1) – where the number N, as determined by the initial data, can be very large and often exceeds the number of classical invariants of L^2 norm, energy, and linear momentum. Thus, the 1-D NLS equation possesses some unusual invariants, in addition to the classical ones.

These invariants arise after considering the eigenvalues as functionals of the coefficients $q(\cdot, t)$:

$$\lambda_j(t) = \lambda_j[q(\cdot, t)].$$

This viewpoint leads one to consider determining $q(\cdot, t)$ from spectral data of the differential operator (3.4). Clearly a finite number N of eigenvalues will be insufficient data to determine the function $\{q(x,t)\ \forall x \in (-\infty, +\infty)\}$, and the eigenvalues will have to be augmented with additional spectral data. But this is a well known problem in mathematical physics known as "inverse scattering theory" — particularly so for the Schrödinger operator of nonrelativistic quantum mechanics, but also for the operator (3.4) which is a form of the Dirac operator of relativistic quantum mechanics.

The appropriate spectral data (see, for example, [78, 64, 10, 11]) is

$$S \equiv \{\lambda_j, c_j,\ j = 1, 2, \cdots, N;\ \ r(\lambda)\ \forall \lambda \in (-\infty, +\infty)\ \}, \tag{3.5}$$

where λ_j denotes the eigenvalues, c_j denotes certain norming constants of the associated L^2 eigenfunctions, and $r(\lambda)$ denotes the "reflection coefficient" defined through the asymptotic behavior (as $|x| \to \infty$) of the generalized eigenfunctions for the continuous spectrum: if $\psi^{(\pm)}$ are matrix solutions of equation (3.3), normalized by

$$\vec{\psi}^{(\pm)}(x, \lambda) \ \simeq \ e^{i\lambda x \sigma_3}, \ \ x \to \pm\infty, \tag{3.6}$$

then from the transition matrix (which is independent of x)

$$\left[\vec{\psi}^{+}\right]^{-1} \vec{\psi}^{-} = \begin{pmatrix} a(\lambda, t) & \overline{b}(\lambda, t) \\ b(\lambda, t) & \overline{a}(\lambda, t) \end{pmatrix}, \tag{3.7}$$

one defines the reflection coefficient as follows:

$$r(\lambda) \equiv \frac{b(\lambda)}{a(\lambda)} \tag{3.8}$$

(see, for example, [64]).

Each member of the spectral data S is viewed as a functional of q, and the data S uniquely determines q by the integral equations of inverse scattering theory [50, 78]; that is, the correspondence between q and S is one-to-one and invertible [50]. There exist several equivalent formulations of the integral equations of inverse scattering theory, including the Gelfand-Levitan equations [78] and the equations of Riemann-Hilbert theory [52, 54]. The latter have proven to be the most powerful for mathematical analysis of asymptotic behavior. (See Sections 7 and 8.) While these integral equations are difficult to solve analytically, they do provide explicit representations of special solutions which consist of N-solitary waves in interaction, in the absence of any radiation $r(\lambda) \ \equiv 0\ \forall \lambda$. These representations have the functional form of a "log-determinant", which leads to interesting analysis as N (the number of solitary waves) tends to infinity. (See Section 8.)

As $q(x, t)$ evolves in time according to 1-D NLS, one can use the Lax pair (3.2) calculate the time evolution of the spectral data S:

$$\begin{aligned} \lambda_j(t) &= \lambda_j(0); \\ c_j(t) &= \exp\left[4i\lambda_j t\right] c_j(0); \end{aligned} \tag{3.9}$$

$$\begin{aligned} a(\lambda, t) &= a(\lambda, 0); \\ b(\lambda, t) &= \exp\left[-4i\lambda^2 t\right] b(\lambda, 0). \end{aligned} \tag{3.10}$$

Thus,

$$r(\lambda, t) = \exp\left[-4i\lambda^2 t\right] r(\lambda, 0),$$

and we have the following (infinite!) number of constants of motion:

$$\left\{\lambda_j(q)\ \forall j=1,\cdots,N;\ \ |r(\lambda;q)|\ \forall\lambda\in(-\infty,+\infty)\right\}. \tag{3.11}$$

Thus, 1-D NLS (3.1) is an infinite dimensional Hamiltonian system with an infinite number of constants of motion. Indeed, exactly one-half of the spectral data is invariant $\{\lambda_j\ \forall j=1,\cdots,N;\ \ |r(\lambda)|\ \forall\lambda\in(-\infty,+\infty)\}$, while the other half evolves linearly with t: $\{\log(c_j)\ \forall j=1,\cdots,N;\ \ \log r(\lambda)\ \forall\lambda\in(-\infty,+\infty)\}$. Thus, using the inverse spectral representation, one establishes that 1-D NLS (3.1) is a *completely integrable Hamiltonian system*.

This infinite collection of constants of motion explains the remarkable stability and elastic collision properties of solitary waves: First, one must understand the connection between spectral data and solitary waves. The log-determinant formula for N-solitary waves, together with the invertibility of the map to scattering data [50], establishes that there is a one-to-one correspondence between the solitary waves in the spatial profile and the bound state eigenvalues in the spectral data. The N eigenvalues correspond to N solitary waves, with the amplitude and speed of each fixed by the real and imaginary part of the associated eigenvalue. Moreover, the reflection coefficient $r(\lambda)$ fixes the amplitude of the λ^{th} radiative component of the nonlinear wave. The temporal behavior of the spectral data (3.10) shows that the speeds and amplitudes of the solitary waves are invariant in time, and are not altered by "interactions of the solitary waves". And, since $|r(\lambda,t)|=|r(\lambda,0)|$, no radiation can be generated by these interactions. In other words, the infinite number of invariants so rigidly constrain the solution that the elastic collision properties of 1-D NLS (3.1) result! Solitary waves which satisfy the elastic collision property are called *solitons*, to emphasize the remarkable particle-like properties of these nonlinear waves.

3.1 Periodic Spatial Boundary Conditions

In our overview, we have focused upon solutions of 1-D NLS on the whole line, which decay rapidly as $|x|\to\infty$. Now we turn to solutions of (3.1) under periodic boundary conditions of (spatial) period ℓ, $q(x+\ell,t)=q(x,t)$. NLS is still equivalent to the Lax pair (3.2), and it is still relevant to view the Zakharov-Shabat operator (3.4) as an (unbounded) operator on $L^2(\mathbb{R})$, even though its coefficients $q(x,t)$ are ℓ-periodic functions of x.

Since its coefficients are periodic in x, Floquet theory can be used to understand the spectral theory of the differential operator (3.4). The well known Floquet procedures for Hill's operator [135, 161] readily extend to the Zakharov-Shabat operator (3.4). Note that this operator is self-adjoint in the defocusing case, but it is not self-adjoint in the case of focusing nonlinearity. This lack of self-adjointness is the only real difficulty for its Floquet theory, and is also the source of the most interesting phenomena of the NLS equation under periodic boundary conditions [130].

The spectrum of the Zakharov-Shabat operator (3.4) with periodic coefficients, when viewed as an unbounded operator on $L^2(\mathbb{R})$, consists entirely of continuous spectrum which resides on a countable number

of curves in the complex plane, called "bands of spectrum". In the self-adjoint case, these bands lie on the real axis, while in the nonself-adjoint case, they are not so constrained. In both cases, the bands terminate at periodic and antiperiodic eigenvalues, which typically have multiplicity one. However, for certain special coefficients, these bands can join at eigenvalues of higher multiplicity. (Consider, for example, the simplest case, $q(x) = 0$, for which all bands join at eigenvalues with multiplicity 2, and the continuous spectrum consists of the entire real axis.)

Again, calculations using the Lax pair (3.2) show that the eigenvalues provide a (countably infinite) collection of constants of motion. Moreover, inverse spectral theory [130] (although not as complete for the nonself-adjoint Zakharov-Shabat operator (3.4) as for the Hill's operator [161]) shows that 1-D NLS (3.1) under periodic boundary conditions is a completely integrable Hamiltonian system. Its integration is accomplished through "Louiville's method" [5, 4], as realized by an Abel-Jacobi transformation and theta functions. This procedure amounts to a transformation from $q(x)$ to action-angle variables [99, 98], a beautiful procedure which is most easily described for soliton equations in the case of the Toda lattice [69, 71, 43].

Generically, the level sets of this countable collection of eigenvalue invariants, $\{q \in H^1 \mid \lambda_j(q) = \lambda_j(q_0)\ \forall j\}$, are infinite dimensional tori. The solutions to the NLS equation under periodic boundary conditions wind around this torus, executing almost-periodic motion in time t. One should think of the nonlinear Schrödinger wave as being decomposed into a countable number of oscillators (called "degrees of freedom"), one for each dimension of the torus. Each oscillator has both an amplitude and angle of oscillation, with the amplitudes fixed by the constants of motion and the angles providing coordinates on the infinite dimensional torus. As the values of the constants of motion change, the tori deform and fill out (or "stratify") the function space H^1.

As noted above, for special choices of coefficients q_*, bands of spectrum can join. As the coefficient approaches a special q_*, two eigenvalues coalesce. As this occurs, the torus become degenerate in that its dimension decreases by one. (Intuitively, the amplitude for one of the oscillators vanishes, and the system loses one of its degrees of freedom.) In the self-adjoint case, the pinched torus which results is always stable, in the sense that nearby coefficients have tori for which the oscillatory degree of freedom that was "pinched away" at q_* now executes small amplitude oscillations [140]. In this stable case the singular level set $\{q \in H^1 \mid \lambda_j(q) = \lambda_j(q_*)\ \forall j\}$, consists only in the degenerate torus itself.

On the other hand, in the nonself-adjoint case, the degenerate torus T_* can be unstable. When it is unstable, the singular level set is larger than the torus itself, containing the unstable manifold $W^u(T_*)$ as well as the torus T_*. Intuitively, the circle which is "pinched" becomes one lobe of a "figure eight," rather than just a point. (See [63, 130] for pictures.) A homoclinic orbit results which approaches the degenerate torus T_* as t approaches infinity:

$$q_{hom}(x,t) \to T_* \quad \text{as } t \to \pm\infty.$$

Inverse spectral theory establishes that these unstable tori cannot result from eigenvalues which coalesce on the real axis; hence, instabilities and homoclinic orbits must be associated with complex valued multiple

eigenvalues, which must be finite in number. Hence, the dimension of the unstable manifold $W^u(T_*)$ must be finite. Such spectral matters are discussed in detail in [130, 149].

An elementary example which illustrates these instabilities and their associated integrable geometry begins from the trivial x-independent solution of NLS equation (3.1):

$$q_c(x,t;c,\gamma) = c\exp\left[-i(2c^2t+\gamma)\right], \tag{3.12}$$

where (c,γ) denote two real parameters. This solution is a single circle. It has only one degree of freedom, with the remaining (countable number) of degrees of freedom all "pinched away". In other words, the torus $T_* = S^1$, is one-dimensional; hence, extremely degenerate.

The linear stability of solution (3.12) is easy to study:

$$\begin{aligned} q(x,t) &= q_c(x,t) + \delta f(x,t)\exp\left[-i(2c^2t+\gamma)\right]; \\ if_t &= f_{xx} + 2c^2 f + 2c^2\bar{f} + O(\delta); \\ f(x,t) &= \hat{f}(k)\exp\left[i(kx-\omega(k)t)\right]; \\ \omega^2(k) &= k^2[k^2-4c^2]. \end{aligned}$$

Thus, the wave (3.12) is unstable to fluctuations with wave numbers $0 < k^2 < 4c^2$; while shorter wavelength fluctuations are neutrally stable according to linear stability theory. The "quantization condition" which ensures spatial periodicity,

$$k_j = \frac{2\pi j}{\ell}, \quad j = \ldots, -1, 0, +1, \ldots,$$

shows that the number of unstable Fourier modes scales linearly with the size ℓ of the periodic spatial domain. This instability of the plane wave (3.12) to long-wave fluctuations is a special case of a famous instability in nonlinear dispersive wave theory, known as the "Benjamin-Feir instability" [12] in the context of water waves and as the "modulational instability" in the context of plasma physics [199]. It is now understood to be the fundamental cause of solitary wave formation, of self-focusing and filamentation of a laser beam, and, more generally, of blow-up in finite time.

This calculation of the tangent space to the unstable manifold of the circle $S = q_c$ shows

$$dim\ W^u(S) = 2N+1,$$

where the "$2N$" comes from the $\{\cos(k_j x), \sin(k_j x),\ j = 1, \ldots, N\}$ basis of the unstable tangent space, and the "1" is the dimension of the circle S itself.

Using integrable theory, one can identify all unstable tori T_{**} for 1-D NLS, and construct rather explicit representations of their unstable manifolds $W^u(T_{**})$, which for the integrable NLS equation equal their stable manifolds $W^s(T_{**})$. This beautiful representation results from Bäcklund (Darboux) transformations — a construction which we now describe in its generality [60, 130, 149]:

First, one [60, 130, 149] establishes that, for each instability, there is an associated complex eigenvalue of with multiplicity at least two. Thus, there is a correspondence between instabilities and complex multiple

points in the periodic and antiperiodic spectrum of the Zakharov-Shabat operator (3.4) — a correspondence which enables us to classify the unstable tori.

Fix a periodic solution of NLS which is quasiperiodic in t, unstable, and for which the instability is associated to a complex double point ν with multiplicity 2, for the operator $\hat{L}(q)$. We denote two linearly independent Zakharov-Shabat eigenfunctions at (ν, q) by $(\vec{\phi}^+, \vec{\phi}^-)$. Thus, a general solution of the Zakharov-Shabat linear eigenvalue problem at (q, ν) is given by

$$\vec{\phi}(x,t;\nu;c_+,c_-) = c_+\vec{\phi}^+ \ + \ c_-\vec{\phi}^-.$$

We use $\vec{\phi}$ to define a *transformation matrix* G by

$$G = G(\lambda;\nu;\vec{\phi}) \equiv N \begin{pmatrix} \lambda-\nu & 0 \\ 0 & \lambda-\bar{\nu} \end{pmatrix} N^{-1}, \tag{3.13}$$

where

$$N \equiv \begin{bmatrix} \phi_1 & -\bar{\phi}_2 \\ \phi_2 & \bar{\phi}_1 \end{bmatrix}.$$

Then we define Q and $\vec{\Psi}$ by

$$Q(x,t) \equiv q(x,t) \ + \ 2(\nu-\bar{\nu}) \ \frac{\phi_1\bar{\phi}_2}{\phi_1\bar{\phi}_1+\phi_2\bar{\phi}_2} \tag{3.14}$$

and

$$\vec{\Psi}(x,t;\lambda) \ \equiv \ G(\lambda;\nu;\vec{\phi}) \ \vec{\psi}(x,t;\lambda), \tag{3.15}$$

where $\vec{\psi}$ solves the Zakharov-Shabat linear system at (q, ν). Formulas (3.14) and (3.15) are the Bäcklund transformations of the potential and eigenfunctions, respectively. We have the following

Theorem 3.1 *Define $Q(x,t)$ and $\vec{\Psi}(x,t;\lambda)$ by (3.14) and (3.15). Then*

(i) $Q(x,t)$ is a solution of NLS, with spatial period ℓ;

(ii) The spectrum $\sigma(\hat{L}(Q)) = \sigma(\hat{L}(q))$;

(iii) $Q(x,t)$ is homoclinic to $q(x,t)$ in the sense that $Q(x,t) \longrightarrow q_{\theta_\pm}(x,t)$, exponentially as $\exp(-\sigma_\nu|t|)$ as $t \longrightarrow \pm\infty$. Here $q_{\theta_\pm}$ is a "torus translate" of q, σ_ν is the nonvanishing growth rate associated to the complex double point ν, and explicit formulas can be developed for the growth rate σ_ν and for the translation parameters $\theta_\pm$.

(iv) $\vec{\Psi}(x,t;\lambda)$ solves the linear system (3.15) at (Q,λ).

This theorem is quite general, constructing homoclinic solutions from a wide class of starting solutions $q(x,t)$. Its proof is one of direct verification, following the sine-Gordon model [60, 139]. Periodicity in x is achieved by choosing the transformation parameter $\lambda = \nu$ to be a double point.

Several qualitative features of these homoclinic orbits should be emphasized: (i) $Q(x,t)$ is homoclinic to a torus which itself possesses rather complicated spatial and temporal structure, and is not just a fixed point;

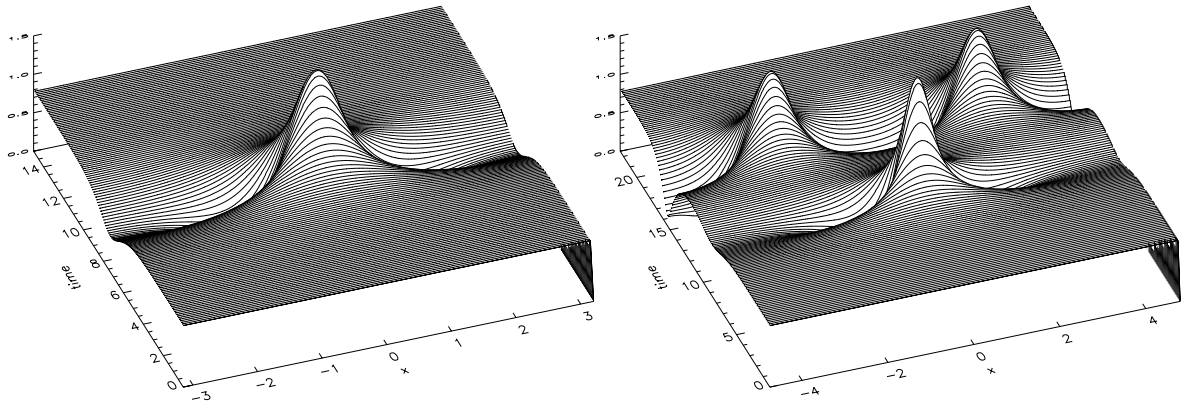

Figure 2: Homoclinic orbits associated with one instability (left panel) and two instabilities (right panel).

(ii) nevertheless, the homoclinic orbit typically has still more complicated spatial structure than its "target torus". (iii) When there are several complex double points, each with nonvanishing growth rate, one can iterate the Bäcklund transformations to generate more complicated homoclinic manifolds. (iv) The number of complex double points with nonvanishing growth rates counts the dimension of the unstable manifold of the critical torus in that two unstable directions are coordinatized by the complex ratio c_+/c_-. Under even symmetry only one real dimension satisfies the constraint of evenness, as will be clearly illustrated in the example below. (v) These Bäcklund formulas provide coordinates for the stable and unstable manifolds of the critical tori; thus, they provide explicit representations of the critical level sets which consist in "whiskered tori" [3].

An Example: The Spatially Uniform Plane Wave. As a concrete example, we return to the spatially uniform plane wave q_c, equation (3.12), for which the entire construction can be carried out explicitly: A single Bäcklund transformation at one purely imaginary double point yields $Q = Q_H(x,t;c,\gamma;k=\pi,c_+/c_-)$:

$$Q_H = \left[\frac{\cos 2p - \sin p \ \ \mathrm{sech}\tau\cos(2kx+\phi) - i\sin 2p\tanh\tau}{1+\sin p \ \ \mathrm{sech}\tau\cos(2kx+\phi)}\right] c e^{-i(2c^2t+\gamma)} \tag{3.16}$$
$$\to e^{\mp 2ip} c e^{-i(2c^2t+\gamma)} \qquad \text{as } \tau \to \mp\infty$$

where $c_+/c_- \equiv \exp(\rho + i\beta)$ and p is defined by $2c\exp(ip) = (1+i\sigma)$, $\sigma = \sqrt{4c^2-1}$, $\tau \equiv \sigma t - \rho$, $\phi \equiv p - (\beta + \pi/2)$, and where the spatial period $\ell = 1$. (see Fig. 2)

Several points about this homoclinic orbit need to be made:

(i) The orbit depends only upon the ratio c_+/c_-, and not upon c_+ and c_- individually.

(ii) Q_H is homoclinic to the plane wave orbit; however, a phase shift of $-4p$ occurs when one compares the asymptotic behavior of the orbit as $t \to -\infty$ with its behavior as $t \to +\infty$.

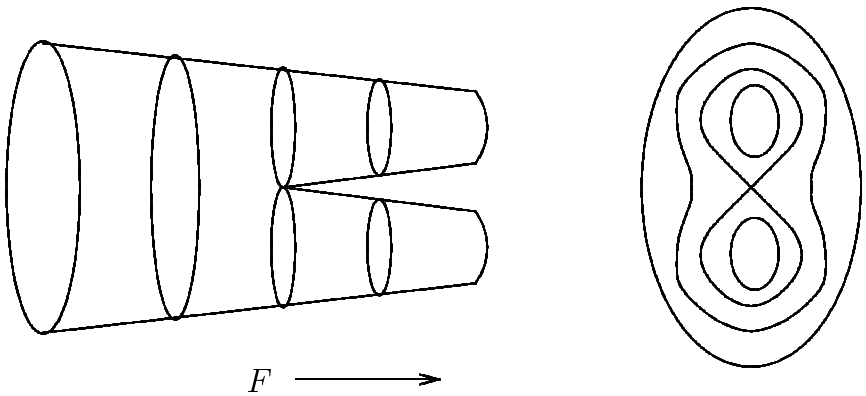

Figure 3: Trouser diagram

(iii) For small p, the formula for Q_H becomes more transparent:

$$Q_H \simeq \Big[(\cos 2p - i\,\sin 2p\,\tanh\tau) - 2\sin p\ \ \mathrm{sech}\tau\cos(2kx+\phi)\Big]ce^{-i(2c^2t+\gamma)}.$$

(iv) The complex transformation parameter $c_+/c_- = \exp(\rho + i\beta)$ can be thought of as $S \times R$. In the formula an evenness constraint about $x = 0$ can be enforced by restricting the phase ϕ to one of two values — $\phi = 0, \pi$. In this manner, evenness reduces the formula for Q_H from $S \times R$ to two copies of R. In this manner, the even symmetry disconnects the level set. Each component constitutes one "whisker" of the "whiskered circles". While the target q is independent of x, each of these whiskers has x dependence through $\cos(2kx)$. One whisker has exactly this dependence and can be interpreted as a spatial excitation located near $x = 0$ [Fig. 2 (left panel)] — while the second whisker (not shown) has the dependence $\cos(2k(x - \pi/2k))$, which we interpret as spatial structure located near $x = 1/2$. In this example, the disconnected nature of the level set is clearly related to distinct spatial structures on the individual whiskers.

In this example the target is always the plane wave; hence, it is always a circle of dimension one, and here we are really constructing only whiskered circles. On the other hand, in this example the dimension of the whiskers need not be one, but is determined by the number of purely imaginary double points, which in turn is controlled by the amplitude c of the plane wave target and by the spatial period. (The dimension of the whiskers increases linearly with the spatial period.) When there are several complex double points, Bäcklund transformations must be iterated to produce complete representations of the unstable manifold. While these iterated formulas are quite complicated, their parameterizations admit rather direct qualitative interpretations [see Fig. 2 (right panel)].

Thus, Bäcklund transformations give global representations of the critical level sets. The level sets in the neighborhood of these of critical ones have fascinating topological structure [63, 130]. The plane wave example under even symmetry and with only one instability provides the simplest case. Here, $dim W^u(q = S) = 2$ — the dimension of each homoclinic orbit, plus the dimension of the target circle $q = S$. In addition, NLS also

possesses a four dimensional invariant manifold which contains $W^u(q = S)$, and which can be viewed as the result of "shutting-off" all degrees of freedom except for the spatial mean and the "first radiation mode." In this four dimensional space, the fixed energy level sets topologically form a trouser diagram shown in Fig. 3. (The "trouser $\times S^1$" forms the three dimensional, fixed energy manifold.) Note in particular the symmetric pair of homoclinic orbits and their relationship to the two legs, one of which represents a (periodic) soliton located at the center of the periodic domain at $x = 0$, and the other a soliton located one-half period away at $x = \ell/2$. When all other radiation degrees of freedom are excited, each forms a small disc (a center for each additional radiation degree of freedom), and the full phase space can be represented topologically (locally, near the trouser) as the product of the trouser with a countable number of discs. More complex examples are described in [130].

4 Temporally Chaotic Behavior

The existence of instabilities and their associated homoclinic orbits for the integrable NLS equation indicates that external perturbations could induce chaotic responses in the perturbed deterministic pdes. Moreover, the trouser topology nearby critical level sets, together with the correlation of the two legs of the trouser with two distinct spatial locations for a soliton ("center" and "edge" of the periodic domain), indicates that chaotic behavior under deterministic perturbations might involve a "random jumping" of a solitary wave between these two spatial locations. An exciting possibility arises — Smale horseshoes [171] and chaotic symbol dynamics [191] in a pde setting. Moreover, this temporal chaos — involving interactions of solitary waves with each other, with radiation, and with external perturbations — should be easily observed in numerical simulations, and even in laboratory experiments. And indeed this type of chaos does appear to exist for certain near-integrable systems — temporal chaos resulting from competitions between, and instabilities of, spatially coherent solitary waves.

4.1 Numerical Experiments

As described in the references [15, 149], we designed some numerical experiments to investigate this exciting possibility. For example, we considered a damped-driven perturbation of an NLS equation in the form:

$$-2iq_t + q_{xx} + (\frac{1}{2}q\bar{q} - 1)q = i\ \alpha q - \sqrt{2}\Gamma e^{-i\gamma}, \tag{4.1}$$

with periodic boundary condition

$$q(x + \ell, t) = q(x, t), \tag{4.2}$$

and initial condition a periodic extension of the single soliton waveform

$$q(x, 0) = 4e_m e^{-2ie_r x}\mathrm{sech}(2e_m x). \tag{4.3}$$

where $e = e_r + ie_m$, with e_r chosen so that $e^{-2ie_r x}$ is periodic of period ℓ (usually $e_r = 0$ and $e_m = 1/2$).

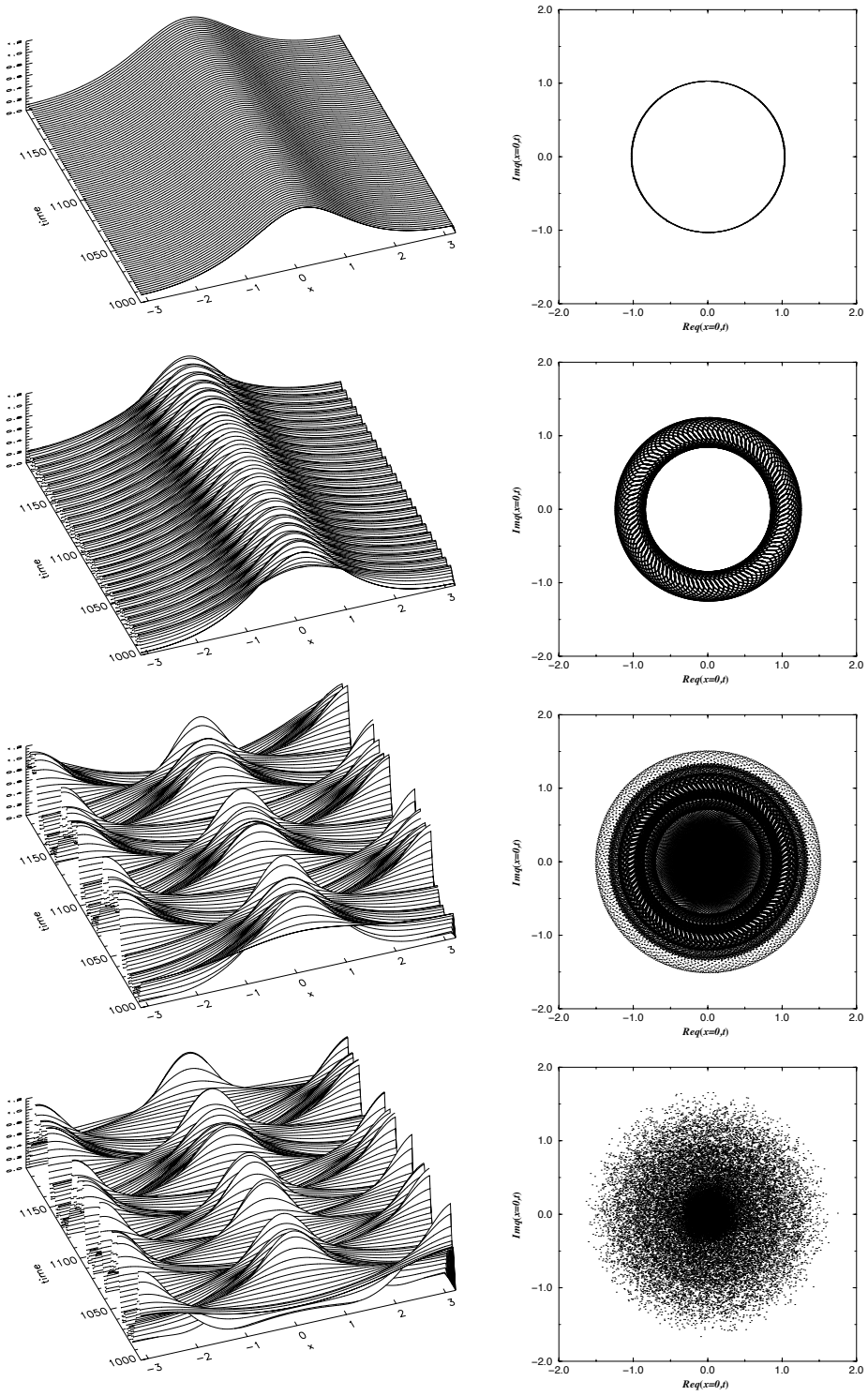

Figure 4: Perturbed solitonic dynamics. From top to bottom: 1) locked state, 2) periodic state, 3) quasiperiodic state and 4) temporal chaotic state. Plotted here are $|q(x,t)|$. The right panels are the corresponding surface cross sections $\{\mathrm{Re}\ q(0,t), \mathrm{Im}\ q(0,t) \forall t\}$. Note that for the case of the quasiperiodic and chaotic dynamics shown here, the values of the driving Γ differ only by 0.4%.

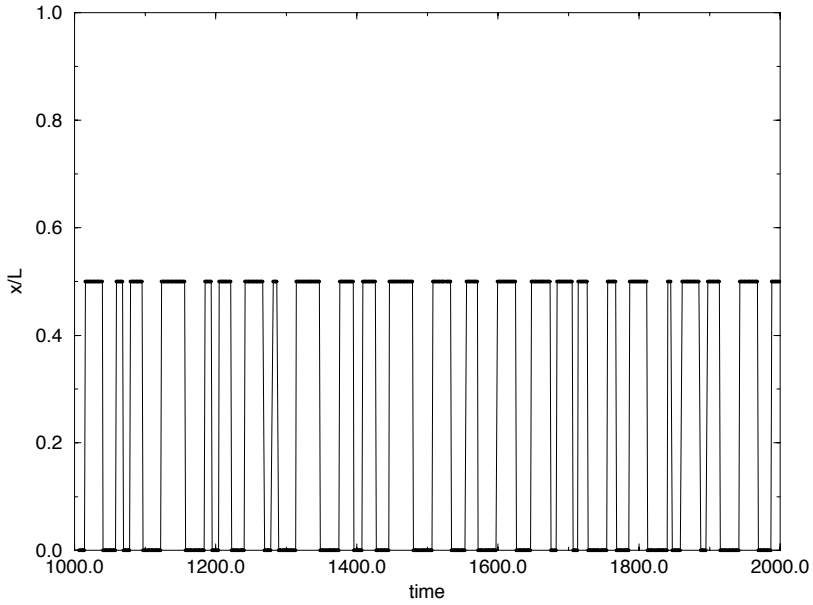

Figure 5: Center-edge jumps of soliton in the chaotic state. The dark line segments are the temporal traces of the maximum of $|q(x,t)|$.

These numerical experiments are described in detail in the survey [149], including: (i) the numerical algorithms and their validation, which is essential when studying long-time temporal integrations of chaotic behavior of unstable orbits; (ii) the collection of chaotic diagnostics with which we post-processed the numerical data; and (iii) a detailed discussion of our numerical observations. Here we only give a brief description of typical observations, for the simplest case where temporal chaos was observed.

We organized our numerical studies into *bifurcation experiments* in which all parameters were fixed (dissipation strength α, spatial period ℓ), except for the amplitude of the driving force Γ, which was increased from experiment to experiment as a "bifurcation parameter". In the simplest case, we set $\alpha \approx 0.1538$ and choose the spatial period $\ell \approx 6.12$, for which only one instability is present. (For larger periods ℓ more complicated behavior was observed.)

Sample results are pictured in Fig. 4. While the details of the bifurcation sequence are somewhat involved [149], the general pattern may be summarized as follows. As Γ increases, the long-time behavior of the wave undergoes the following sequence of changes in $|q(x,t)|$: (i) spatially flat, time independent; (ii) "sech-like" in space, time independent; (iii) sech-like in space, but time periodic; (iv) sech-like in space, quasiperiodic in time; (v) chaotic in time, with the sech-like excitation jumping from center to edge of the periodic spatial domain.

We used standard chaotic diagnostics to identify chaotic behavior — including Poincaré sections, power spectra, Lyapunov exponents, and information dimension. Each of these diagnostics is defined and discussed in detail in [149]. In Fig. 4, we show four sample "cross sections" — for time-independent, periodic, quasiperiodic, and chaotic temporal behavior.

We emphasize that this experiment, which is the simplest that we have found which has chaotic behavior,

is extremely important for our theoretical studies. In it, the chaotic state contains only one spatially localized coherent structure. At times this solitary wave is located at the center, and at other times it is seen at the edges of the periodic spatial domain. These two locations are the only two allowed under even boundary conditions. We believe that one source of the chaotic behavior is an irregular (random?) jumping of the solitary wave between center and edge locations (see Fig. 5). This center-edge jumping of the solitary wave through homoclinic transitions forms the basis for the simplest description and model of chaotic behavior.

4.2 Persistent Homoclinic Orbits

The first step toward analytical descriptions of such chaotic behavior is to assess the persistence of homoclinic orbits. These can provide a "skeleton" for chaotic trajectories. That is, persistent stable and unstable manifolds, and their intersections, provide a framework with which chaotic behavior can be described. Procedures for this description are well known for finite dimensional dynamical systems [85, 191], and have recently been developed for the NLS pde [131]. See also [147] for a rather detailed overview of these mathematical arguments. Here we present a brief sketch of the arguments, taken from [147], and state the persistence theorem.

Specifically, we study a perturbed nonlinear Schrödinger equation (PNLS) of the form

$$iq_t \;=\; q_{xx} + 2\left[q\bar{q} - \omega^2\right] q \;+\; i\epsilon\left[\hat{D}q - 1\right], \tag{4.4}$$

where the constant $\omega \in (\frac{1}{2}, 1)$, ϵ is a small positive constant, and $\hat{D}$ is a *bounded* negative definite linear operator on the Sobolev space $H^1_{e,p}$ of even, 2π periodic functions. Specific examples of the dissipation operator $\hat{D}$ include the discrete Laplacian and a "smoothed Laplacian" given by

$$\hat{D}q = -\alpha q - \beta \hat{B} q, \tag{4.5}$$

where the operator $\hat{B}$ has symbol given by

$$b(k) = \begin{cases} k^2 & k < \kappa, \\ 0 & k \geq \kappa. \end{cases}$$

This pde is well posed in $H^1_{e,p}$, and the solution

$$q(t;\epsilon) \;=\; F^t_\epsilon(q_{in})$$

has several derivatives in q_{in}, and in the parameters such as ϵ, with the exact number of derivatives increasing with decreasing ϵ.

Our analysis of this equation begins with two observations: *First*, when $\epsilon = 0$, the unperturbed NLS equation is a completely integrable soliton equation. *Second*, the "plane of constants" Π_c,

$$\Pi_c \equiv \{q(x,t) \,|\, \partial_x q(x,t) \equiv 0\},$$

is an invariant plane for PNLS. In each of these two cases, [$\epsilon = 0$ or $q \in \Pi_c$], the behavior of solutions $q(\cdot, t)$ can be described completely. In the first case, this description is described in Section 3.1; in the second case, it is accomplished through "phase plane analysis". In the jargon of the theory of dynamical systems, our methods will be a form of "local-global" analysis, where at times the term "local" will mean close to the plane Π_c, and at other times "local" will mean close to integrable solutions. In any event, throughout our global arguments, control is achieved either because of proximity to (i) the plane Π_c or (ii) $\epsilon = 0$.

4.2.1 Motion on the Invariant Plane

On the invariant plane Π_c, the equation takes the form

$$iq_t \;=\; 2\left[q\bar{q} - \omega^2\right] q \;-\; i\epsilon\left[\alpha q + 1\right], \tag{4.6}$$

where it is assumed that the dissipation operator $\hat{D}$ acts invariantly on Π_c as

$$\hat{D}q = -\alpha q,$$

for α a positive constant. Equivalently, in terms of polar coordinates

$$q \equiv \sqrt{I}\, \exp i\theta,$$

these equations take the form

$$\begin{aligned} I_t &= -2\epsilon\left[\alpha I + \sqrt{I}\cos\theta\right], \\ \theta_t &= -2(I - \omega^2) + \frac{\epsilon}{\sqrt{I}}\sin\theta. \end{aligned} \tag{4.7}$$

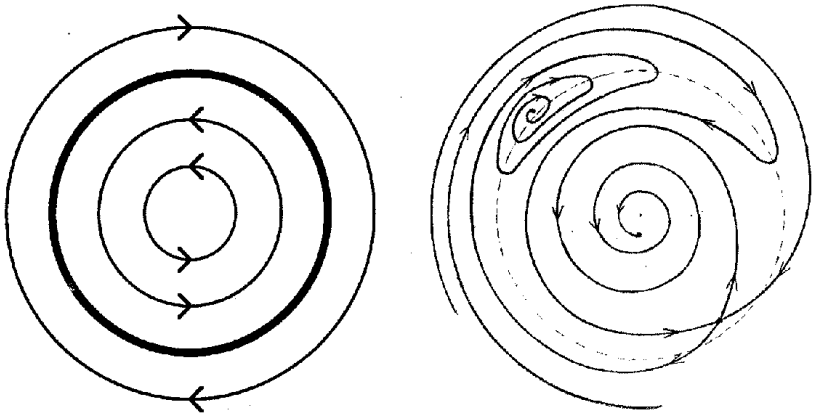

Figure 6: Phase Plane Diagram of the ODE

When $\epsilon = 0$, the unperturbed orbits on Π_c are nested circles, with S_ω a circle of fixed points given by $I = \omega^2$. For $\epsilon > 0$, the perturbed orbits on Π_c are very different (see Fig. 6). First, only three fixed points

exist: O, which is a deformation of the origin; Q, a saddle which deforms from the circle S_ω; and P, a spiral sink which also deforms from the circle S_ω.

While the circle of fixed points S_ω for the unperturbed ($\epsilon = 0$) problem does not persist as a circle of fixed points, motion near S_ω remains slow for small positive ϵ. We introduce the variable J,

$$J = I - \omega^2,$$

and, in order to describe the slow flow close to this circle S_ω, we rescale the coordinates

$$\begin{aligned} \tau &= \nu t, \\ J &= \nu j. \end{aligned} \tag{4.8}$$

where $\nu = \sqrt{\epsilon}$. In these scaled coordinates, equations (4.7) on the plane Π_c take the form of an $O(\nu)$ perturbation of the conservative system

$$\begin{aligned} j_\tau &= -2(\alpha\omega^2 + \omega\cos\theta), \\ \theta_\tau &= -2j\ . \end{aligned}$$

Thus, we see that near the circle S_ω, the slow motion is approximated as a driven pendulum, with energy

$$E(j,\theta) \equiv \frac{1}{2}j^2 - \omega(\sin\theta + \alpha\omega\theta)\,. \tag{4.9}$$

4.2.2 Integrable Homoclinic Orbits

The unperturbed (ϵ=0) focusing NLS equation is a completely Hamiltonian system,

$$-iq_t = \frac{\delta}{\delta\bar{q}}\ H, \tag{4.10}$$

with the Hamiltonian H given by

$$H = \int_0^{2\pi} \left[q_x\bar{q}_x - (q\bar{q})^2 + 2\omega^2 q\bar{q}\ \right] dx.$$

Consider the two parameter family of plane wave solutions, independent of x:

$$q(x,t;c,\gamma) = c\exp\{-i[2(c^2-\omega^2)t - \gamma]\}.$$

Linearizing NLS about $q(x,t;c,\gamma)$ shows that this plane wave is linearly unstable, with positive growth rate σ for the linearized "$\cos x$ mode" given by

$$\sigma = \sqrt{4c^2 - 1}.$$

As described in Section 3.1, a Bäcklund transformation will produce an orbit homoclinic to this plane wave:

$$q_h^{\pm} = \left\{ \frac{\cos 2p - i\sin 2p\tanh\tau \pm \sin p\ \mathrm{sech}\ \tau\cos x}{1 \mp \sin p\ \mathrm{sech}\ \tau\cos x} \right\} q\ , \tag{4.11}$$

where

$$\begin{aligned} \tau &= \sigma(t+t_0), \\ e^{ip} &= \frac{1+i\sigma}{2c}\,. \end{aligned}$$

Here $\pm$ labels a symmetric pair of homoclinic orbits. (Recall that $-\cos x = \cos(x+\pi)$, which shows that one sign $(+)$ represents an excitation centered at $x=0$, while the other sign $(-)$ represents an excitation centered at $x=\pi$.)

If we specialize to $c=\omega$, q lies on the circle of fixed points S_ω, and the orbit q_h is homoclinic to this circle. Thus, from one point of view, (4.11) provides an explicit representation of a "whiskered circle"; while from another viewpoint, it provides an explicit representation of the unstable manifold

$$W^u(S_\omega) = W^s(S_\omega) = \bigcup_{\gamma,\, t_0, \pm} q_h^{\pm}\,(t;\,\gamma,\,t_0,\,c)\,.$$

4.2.3 Melnikov Integrals

Next, we define the Melnikov integral which will be used to establish persistence. First, we write the perturbed NLS equation in the form

$$q_t \;=\; iH'(q) + \epsilon G(q), \tag{4.12}$$

where $H'(q) = \; -q_{xx} - 2\,[q\bar{q} - \omega^2]\,q$ and where $G(q)$ denotes the perturbation:

$$G(q) = -\alpha\, q - \beta\, \hat{B}\, q - 1. \tag{4.13}$$

Let I denote a (real valued) constant of motion for the unperturbed ($\epsilon = 0$) system.

Definition: The Melnikov function (based on I) is defined by

$$\begin{aligned} M_I &\equiv \int_{-\infty}^{\infty} \Big\langle I'[q_h(t)],\, G[q_h(t)] \Big\rangle\, dt \\ &= \int_{-\infty}^{\infty} \left\{ \left[G\,\frac{\delta}{\delta q} I \;+\; \bar{G}\frac{\delta}{\delta \bar{q}} I \right] \Big|_{q_h(t)} \right\} dt. \end{aligned} \tag{4.14}$$

In this definition, we assume that the integrals converge (which they do for our choices of constant I).

Melnikov integrals, *together with geometric analysis*, are used to assess the fate of the orbit $q_h(t)$ under the perturbation. As is clear from its definition, the Melnikov integral M_I provides an estimate of the change in the value of the constant of motion I over the perturbed orbit. Without an additional geometric setting, this change provides very little information about persistence. When this integral does not vanish, one can establish no persistence [42]. However, in particular geometric settings, a simple zero of the Melnikov function with respect to one of its parameters can insure the intersection of certain stable and unstable manifolds, and the persistence which follows as a consequence of this intersection.

Next we specialize the orbit $q_h(t)$ to one homoclinic to the circle of fixed points S_ω. Setting $c=\omega$ produces orbits homoclinic to S_ω, which we denote by q_ω:

$$q_\omega(t) = \left[\frac{\cos 2p - i \sin 2p\, \tanh\tau + \sin p\, \operatorname{sech}\tau \cos x}{1 - \sin p\, \operatorname{sech}\tau \cos x} \right]\, \omega \exp i[\theta_b - 2p], \tag{4.15}$$

where $\tan p = \sqrt{4\omega^2 - 1}$ and $\tau = (\tan p)(t + t_o)$. While the orbit q_ω approaches the circle S_ω as $t \to \pm\infty$, it approaches the fixed point $\omega \exp i\theta_b$ as $t \to -\infty$ and, as $t \to +\infty$,

$$q_\omega(t) \longrightarrow \omega\, e^{i(\theta_b - 4p)}.$$

Thus, the (heteroclinic) orbit experiences a *phase shift* of $-4p$

$$e^{-4ip} = \left[\frac{1 - i\sqrt{4\omega^2 - 1}}{2\omega}\right]^4.$$

It will be sufficient to use the the Melnikov integral based on the energy H. With these ingredients, we assemble the final expression for this Melnikov integral:

Proposition: For the specific perturbation (4.13) and homoclinic orbit q_ω, equation (4.15), the Melnikov integral takes the form

$$\begin{aligned} M_H = M_H(\alpha, \beta, \theta_b) &= \int_{-\infty}^{\infty} \Big\langle H'(q_\omega(t)),\, G(q_\omega(t)) \Big\rangle\, dt \\ &= [\alpha M_\alpha + \beta M_\beta + M(\theta_b)], \end{aligned} \tag{4.16}$$

where

$$\begin{aligned} M_\alpha &= \int_{-\infty}^{\infty} \Big\langle H'(q_\omega(t)),\, q_\omega(t) \Big\rangle\, dt \\ M_\beta &= \int_{-\infty}^{\infty} \Big\langle H'(q_\omega(t)),\, \hat{B} q_\omega(t) \Big\rangle\, dt \\ M(\theta_b) &= \int_{-\infty}^{\infty} \Big\langle H'(q_\omega(t)),\, 1 \Big\rangle\, dt\,. \end{aligned}$$

More explicitly,

$$\begin{aligned} M_\alpha &= \int_{-\infty}^{\infty} d\tau \int_0^{2\pi} dx\, \frac{4\pi\,\omega^2 \sin^2 p_o\, \operatorname{sech}\,\tau}{\sigma\, A^3} \times \\ &\quad \big[\operatorname{sech}\,\tau + \sin p_o \tanh^2\tau \cos x - \sin^2 p_o\, \operatorname{sech}\,\tau(2 + \cos^2 x) \\ &\qquad + 2\sin^3 p_o\, \operatorname{sech}^{\,2}\tau \cos x\big], \end{aligned}$$

$$\begin{aligned} M_\beta &= \int_{-\infty}^{\infty} d\tau \int_0^{2\pi} dx\, \frac{4\pi\omega^2 \sin^2 p_o\, \operatorname{sech}\,\tau}{\sigma A^5}\, \times \\ &\quad \big[\sin p_o\, \operatorname{sech}\,\tau \cos x - \sin^2 p_o\, \operatorname{sech}^{\,2}\tau(1 + \sin^2 x)\big] \times \\ &\quad \big[2\, \operatorname{sech}\,\tau - 2\sin p_o\, \operatorname{sech}^{\,2}\tau \cos x - 2\sin^2 p_o\, \operatorname{sech}\,\tau \\ &\qquad + 2\sin^3 p_o\, \operatorname{sech}^{\,2}\tau \cos x\big] + O(\sin^{\kappa-2} p_o), \end{aligned}$$

$$\begin{aligned} M(\theta_b) &= \cos(\theta_b - 2p_o) \int_{-\infty}^{\infty} d\tau \int_0^{2\pi} dx\, \frac{4\pi\omega \sin^2 p_o\, \operatorname{sech}\,\tau}{\sigma A^2} \times \\ &\quad [\,\operatorname{sech}\,\tau - \sin p_o \cos x\,], \end{aligned}$$

where $p_o = \tan^{-1}\sqrt{4\omega^2 - 1}$, $A = [1 - \sin p_o \text{ sech } \tau \cos x]$ and where the $O(\sin^{\kappa-2} p_o)$ term in the M_β equation is due to the fact that we used $-\partial_x^2$ instead of $\hat{B}$ in our calculation. Thus, the final expression for the Melnikov integral is of the form

$$M(\alpha, \beta, \theta_b) = \alpha M_\alpha + \beta M_\beta + M_1 \cos(\theta_b - 2p_o), \tag{4.17}$$

where M_α, M_β, and M_1 are functions of ω only.

Clearly, for small α and β, this Melnikov function has simple zeros as a function of θ_b. At issue, of course, is the geometric meaning of these zeros.

4.2.4 Persistent Homoclinic Orbits for PNLS

Simple zeros of the Melnikov function (4.17) enable us to prove the following persistence theorem for the pde:

Theorem 4.1 *The perturbed NLS equation (4.4) possesses a symmetric pair of orbits which are homoclinic to the saddle fixed point Q, provided the parameters lie on a codimension 1 set in parameter space which is approximately described by*

$$\alpha = E(\omega)\beta.$$

$E(\omega)$ can be computed explicitly to leading order ϵ. In addition, various properties of persistent homoclinic orbit (such as a "take-off" angle) can be precisely characterized.

These two homoclinic orbits differ by the location of a transient spatial structure — a solitary wave which is located either at the center ($x = 0$) or the edge ($x = \pi$) of the periodic box. As such, this theorem provides a key step toward a symbol dynamics for the pde.

The proof of this theorem is described in mathematical detail in [131], and a detailed overview of the argument is presented in [147]. It is organized with "local-global" analysis, and it involves normal forms for the perturbed NLS equation, invariant manifold theory for NLS and geometric singular perturbation theory, combined with integrable theory and Melnikov analysis. It is important to keep in mind that, throughout the proof, control is obtained in one of two ways — either the orbits are (i) close to the invariant plane Π_c, or they are (ii) close to the integrable case. Also keep in mind that the arguments will be a form of "shooting", where the goal will be to force an orbit to "hit" target manifolds of high dimension, but in an infinite dimensional space. To make these manifolds easy targets, we make them very large in the sense that they will be codimension 1.

The steps in the proof are as follows:

1. **Preliminary set up** including (i) motion on Π_c, (ii) coordinates near Π_c, (iii) linear stability and time scales, and (iv) a normal form.

2. **Local arguments** including (i) persistent invariant manifolds, (ii) fiber representations, and (iii) the height of the stable manifold $W^s(Q)$.

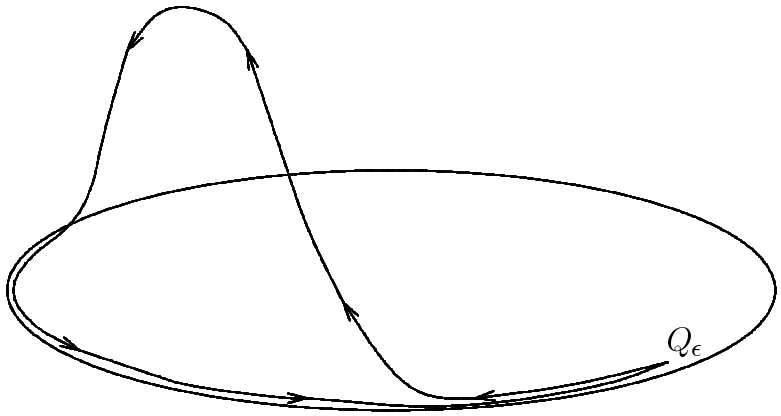

Figure 7: Schematic Diagram of the Homoclinic Orbit

3. **Global arguments** which describe the first and second Melnikov measurements.

Here we restrict ourselves to a few remarks about these steps:

Remark 1: In the local arguments for persistence of stable and unstable manifolds, and for their representations with "fiber coordinates", we use integral equation methods rather than more geometric ones [9, 133] from dynamical systems theory. These integral equation methods are natural for pde's. Their use is consistent with our view that intuition, taken from finite dimensional dynamical systems, should structure the arguments — which should then be implemented with methods which are natural for pde's.

Remark 2: Fiber-represention are constructions from geometric singular perturbation theory which permit one to follow the long-time fate of the full motion with an orbit totally restricted to a slow manifold. These were developed by Fenichel [65, 66, 67, 68] to provide a geometric understanding of singular perturbation methods, such as those of Howard and Kopell [110, 92]. Recent descriptions of these fibrations, with explicit examples, may be found in [97, 145, 147].

Remark 3: The argument is a "shooting method", with the final target the stable manifold of the saddle Q, $W^s(Q)$. To ensure that this "target is hit", this stable manifold must have sufficient height above the plane Π_c. For this estimate, the effects of quadratic nonlinearities must be controlled. An elegant normal form transformation for the pde is used to control these quadratic nonlinearities by transforming them into cubics.

Remark 4: The shooting arguments make use of two distinct time scales in the problem — a slow scale for motion near the plane Π_c, and a fast scale for motion away from Π_c. These arguments are organized into two measurements, associated with these two time scales. This organization of the argument follows some earlier work [145], in which the pde was truncated to a four dimension model problem. A particularly clear description of these finite dimensional arguments may be found in [111].

Remark 5: Intuitively (see Fig. 7), the persistent homoclinic orbit will "leave the saddle point Q, creep slowly near the plane Π_c along the unperturbed circle of fixed points S_ω to a location near the "take-off" angle, rapidly fly away and return along a global orbit which is close to one of the integrable homoclinic

orbits $q_\omega(t;\gamma)$. Upon its return near Π_c, it will slowly creep back to the saddle Q, again near the circle S_ω."

Remark 6: The first measurement determines the intersection of the unstable manifold $W^u(Q)$ with a persistent center-stable manifold W^{cs}, which is codim 1. This is accomplished with the Melnikov function $M_H = M_H(\gamma_T)$, viewed as a function of the "take-off" angle γ_T. This Melnikov function measures the distance between these manifolds,

$$d\{W^u(Q), W^{cs}\} = \epsilon M_H(\gamma_T) + O(\epsilon^{3/2}).$$

Remark 7: *Within* the persistent W^{cs}, the stable manifold $W^s(Q)$ is codim 1. Thus, once the orbit is known to reside in W^{cs}, a single measurement can ensure that it returns to the saddle Q. This "second measurement" is accomplished using the pendulum energy (4.9) and the fact that the stable manifold $W^s(Q)$ is tall enough, as established by the normal form transformation.

Remark 8: Once the persistence of one homoclinic orbit is established, the symmetry $x \to x + \pi$ shows the persistence of a second homoclinic orbit, and the ingredients for a "center-edge" symbol dynamics are in place.

4.3 Chaotic Behavior

The simplest chaotic behavior which was observed in the numerical experiments for the perturbed NLS equation consists of a single solitary spatial excitation which jumps, irregularly in time, between the two distinct spatial locations at $x = 0$ and $x = \pi$. These numerical experiments, together with the persistence of a *symmetric pair* of homoclinic orbits, suggests a "symbol dynamics" explanation of this phenomena.

4.3.1 Symbol Dynamics

More precisely, the term "symbol dynamics" refers to the existence of an invariant set in the phase space which is topologically equivalent to a set of all 2-symbol valued sequences. In our setting, these sequences would take the values of C (center) or E (edge), and the dynamics would be represented as a shift on this sequence space. As such, the dynamics, when restricted to the invariant set, is as random as a sequence of "coin tosses".

In finite (usually very small) dimensions, the existence of such an invariant set is established by constructing a "Smale horseshoe" [171, 153, 85, 191]. Such constructions have been carried out for orbits homoclinic to the saddle Q for the four dimensional truncation [145], for a $2N+2$ dimensional truncation in [132], and most recently for an infinite dimensional model of the pde [129]

Symbol dynamics is very appealing because it demonstrates the existence of chaotic motions which last for all time. However, it has some drawbacks: First, it occurs on a very small set in phase space, which is not shown to be (and is likely not) a stable set. As such, this type of chaos may not be observable. Moreover, the behavior depends on parameters in a bifurcation fashion. Often the parameter values required to show the existence of the horseshoe are very far from the values of the parameters at which chaotic behavior is

observed in numerical experiments. (For example, in our analytical results [131], an additional dissipation $\beta > 0$ is required which satisfies a codim 1 constraint. However, in the numerical experiments [149], chaotic behavior is observed for $\beta = 0$, over a range of α values.) Finally, the construction of the horseshoe is almost always performed for generic abstract models, rather than for a fixed specific dynamical system. To us, this generic situation seems to be a severe limitation of the practice of the method — and particularly so for the NLS pde with its singular, two-time scale, homoclinic orbits.

4.3.2 Long Complex Transients

Recently, Haller has been developing an alternative perspective, which he has applied to finite dimensional discretizations of the perturbed NLS equation [88, 87], and to the pde [86]. In his work, using very similar geometric perturbation methods, he constructs a large class of heteroclinic orbits from the saddle Q to (for example) the sink P. These orbits have complex patterns of center-edge jumps, finite in number. While only transient behavior, the length of the transients is arbitrarily long. In any case, this set of heteroclinic orbits certainly demonstrates very complicated dynamics which depends sensitively upon initial conditions. Moreover, these orbits are associated with a "mixing and entangling" of the unstable manifolds. And, as the second measurement is not required to force the orbit to return to the saddle Q, these heteroclinic orbits exist for a full open set of external parameter values, without any codim 1 restriction.

4.4 Very Recent Work

Our proof [131] of persistence of homoclinic orbits for dissipative, driven perturbations of NLS is very geometric. While beautiful, this geometric framework can be cumbersome and somewhat tedious. We continue to develop methods which rely upon geometric intuition, but which implement the actul calculations "more mechanistically" — within an integral equation framework, together with natural pde estimates. In [148] we prove the persistence of an orbit homoclinic to an isolated unstable fixed point for a nonlinear Klein Gordon equation (a simpler situation than the orbit homoclinic to a circle of fixed points treated in [131]) by replacing Melnikov methods with a Lyapunov Schmidt framework for the pde, together with pde scattering theory.

Normal forms, while beautiful when they work as in the NLS case, often depend upon conditions which are extremely difficult to verify — as, for example, in the case of the persistence of an orbit homoclinic to a periodic solution in the sine-Gordon setting. Recently Shatah and Zeng [168] have used integral equation estimates to replace the normal form argument. They also have extended our NLS results [131] to include *unbounded* dissipative perturbations such as diffusion. They accomplished this extension by replacing our "fiber" representation of the stable manifold with long-time, integral equation estimates. Such improvements in the methods, while technical, are essential for the development of general procedures to establish qualitative results, valid globally in time, for pde's — such as the persistence of homoclinic orbits for pde's.

Another set of related questions concerns persistent tori, and persistence of associated periodic and quasi-periodic solutions, for Hamiltonian perturbations of integrable systems. This well studied "KAM" behavior in finite dimensional dynamical systems has recently been extended to infinite dimensional pde settings. While we will not describe these extensions in this review, we do note several representative references: [114, 115, 40, 20, 21, 22, 25, 13, 17, 48, 185, 54].

An important example is the persistence of the sine-Gordon "breather". The sine-Gordon equation on the whole line ($-\infty < x < +\infty$) has exact solutions which are periodic in time, exponentially localized in space, and which can be viewed as nonlinear bound states which consist of two solitons. The question of the survival of such temporally periodic solutions to small Hamiltonian perturbations is known as the "persistence of the breather". For perturbations which do not depend upon derivatives of the field, the breather does not persist [167, 166, 14]. Rather it decays extremely slowly, generating radiation as it decays at a rate which is exponentially small in the perturbation parameter. The work of Segur and Kruskal [167, 166] uses formal "asymptotics beyond all orders" [165] to capture this decay rate, while that of [14] proves that the breather does not persist with mathematical arguments which begin from formulas of "soliton perturbation theory" [146]. This persistence problem provides one example of the important interactions between solitary waves and radiation in nonintegrable situations. (See [173, 174, 30] for others.)

5 Spatiotemporal Chaos

5.1 Intuition

In Section 4, we have discussed the existence and nature of *temporal chaos* which consists of spatially coherent localized waves which dance chaotically in time. As Fig. 4 clearly indicates, these waves are very regular in space. Their time series at location x, $\{q(x,t)\ \forall t\}$, appears to be statistically well correlated to the time series at location $y \neq x$, $\{q(y,t)\ \forall t\}$. On the other hand, waves of *dispersive turbulence* should behave chaotically in both space and time. At least the time series $\{q(x,t)\ \forall t\}$ and $\{q(y,t)\ \forall t\}$ should become statistically independent as the distance from x to y increases.

Intuitively, this independence might be achieved by increasing the size ℓ of the spatial domain. The numerical data shown in Section 4 was for small spatial domains, with only one instability and only one solitary wave under even, periodic boundary conditions. Recall that the number of instabilities, and hence the number of solitary waves present in the spatial domain, scales linearly with ℓ. Moreover, with an increasing number of linearly unstable modes, there is, correspondingly, an increasingly large number of distinct classes of spatial excitations in the form many types of quasi-solitons — standing waves, waves traveling to the left and right, bound states which are quasiperiodic in time, etc. Therefore, increasing ℓ will place more, and more complex, solitary wave structures into the spatial domain, and should decorrelate in space. Moreover, relaxing even symmetry enlarges the number of spatial locations at which these solitary waves can reside (from a discrete set to the continuum) (See [1] for fascinating effects which result from

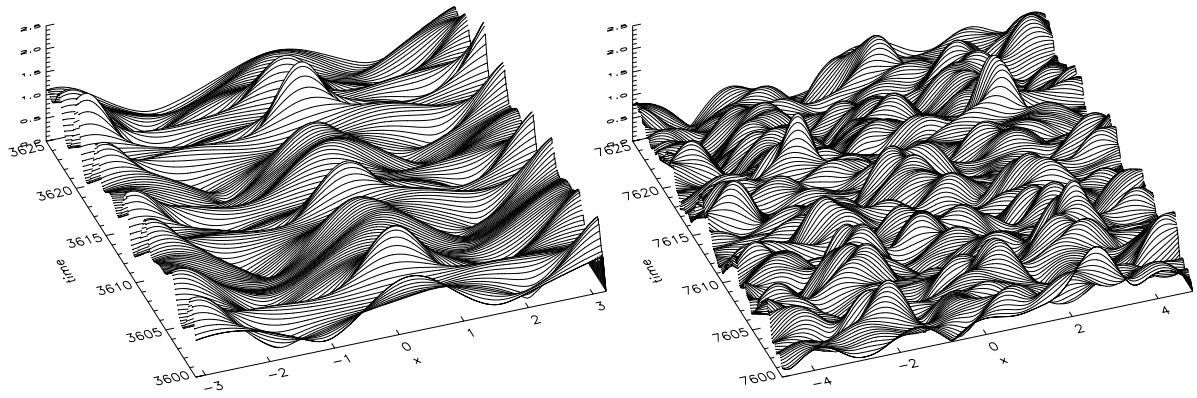

Figure 8: Evolution of system (5.1) with $\alpha = 0.004$, $\Gamma = 0.144$, $\omega = 1$. The initial condition $q = c + \epsilon \exp(i2\pi x/\ell)$, $c = 0.8$, $\epsilon = 2 \times 10^{-5}$. Plotted here is $|q(x,t)|$. Left panel: Temporal chaos in the presence of one linearly unstable mode, $\ell = 6.4$; Right panel: Spatiotemporal chaos in the presence of two linearly unstable modes, $\ell = 9.6$.

relaxing even symmetry). Indeed, this decorrelation is seen in our NLS numerical experiments [35, 34], provided the constraint of even symmetry is removed. And, similar phenomena occur much more widely than just for near-integrable waves. For example, a similar scenario occurs in studies of purely spatially chaotic, stationary waves [7, 80], in which the temporal access of all of these stationary states remains to be fully addressed [41].

Specifically, we will describe spatiotemporal chaos for the driven, damped NLS equation,

$$iq_t + q_{xx} + 2|q|^2 q = -i\alpha q + \Gamma e^{i(\omega t + \gamma)}, \tag{5.1}$$

with periodic boundary conditions,

$$q(x + \ell) = q(x), \tag{5.2}$$

where ℓ is the system length, and ω and γ are the driving frequency and phase, respectively. The damping coefficient α and the driving strength Γ will be small.

A natural question: Given a temporally chaotic solution of the perturbed NLS equation, how large a spatial domain, or how many instabilities, is required for effective decorrelation in space? An example with only one instability is shown in Fig. 8 (left panel), while one with two instabilities in Fig. 8 (right panel). Clearly, the two figures display drastically different spatial patterns.

Before investigating such questions further, we need first to formulate a precise definition of the concept of spatiotemporal chaos.

5.2 A Definition of Spatiotemporal Chaos

There have been many definitions proposed to capture the essence of spatiotemporal chaos [41]. We prefer a "working definition" which includes two points: (i) A temporally chaotic wave $q(x,t)$, (ii) for which the time

series $\{q(x,t)\ \forall t\}$ and $\{q(y,t)\ \forall t\}$ become statistically independent as the distance from x to y increases.

For a definition, we must make precise the meanings of "temporal chaos" and "statistical independence". For *temporal chaos* we will accept any common definition, such as a bounded attractor with positive Lyapunov exponents.

Statistical independence is often estimated through the decay of the two-point correlation function:

$$C(x-y) \equiv \lim_{T\to\infty} \frac{1}{T-T_0} \int_{T_0}^{T} \left[(q(x,t)-\langle q\rangle)(\bar{q}(y,t)-\langle\bar{q}\rangle)\right]\, dt, \tag{5.3}$$

where $\langle\cdot\rangle$ denotes the temporal mean, and where we have assumed translational invariance of the system. However, the vanishing of the two-point correlation function is only a necessary condition for statistical independence; thus, we prefer to base the definition upon *mutual information*.

For two stochastic variables U and V, with probability density functions $p(u)$ and $p(v)$, respectively, and with joint probability density function $p(u,v)$, the mutual information between these two variables U and V is defined as [16]

$$\mathcal{I}(U,V) = \int du\ dv\ p(u,v)\ \log \frac{p(u,v)}{p(u)\ p(v)}. \tag{5.4}$$

In this application of spatiotemporal chaos, the probability distributions will be generated by the chaotic time series:

$$\begin{aligned} p_x(q) &: \{q(x,t)\ \forall t\} \\ p_y(q) &: \{q(y,t)\ \forall t\} \\ p_{x,y}(q,r) &: \{[q(x,t), r(y,t)]\ \forall t\}, \end{aligned}$$

where $r(y,t) = q(y,t)$. Intuitively, $p_x(q)\ dq$ is the fraction of time that $q(x,\cdot) \in (q, q+dq)$, etc. Thus, we define the mutual information between points x and y by

$$\mathcal{I}(x,y) = \int dq\ dr\ p_{x,y}(q,r)\ \log \frac{p_{x,y}(q,r)}{p_x(q)\ p_y(r)}. \tag{5.5}$$

In terms of this mutual information between spatial points, we arrive at our

Working Definition: A wave $q(x,t)$ is *spatiotemporally* chaotic if

1. $q(x,t)$ is a temporally chaotic orbit (for example as characterized by positive Lyapunov exponents);
2. its mutual information between two spatial points, $\mathcal{I}(x,y)$, decays exponentially for large separatons, i.e., as $|x-y| \gg 0$.

It is well known that temporal chaos signifies a loss of information in time. (This loss of temporal information can be quantified by a positive Kolmogorov-Sinai entropy, which in turn can be estimated by the sum of positive Lyapunov exponents.) It is our view that a key feature of spatial chaos is a similar loss of information, but over space. Mutual information provides a natural measure.

First, mutual information is closely related to entropy:

$$\mathcal{I}(x,y) = \mathcal{H}(x) + \mathcal{H}(y) - \mathcal{H}(x,y),$$

where $\mathcal{H}(\cdot)$ denotes the entropy. Here, $\mathcal{H}(x)$ is the entropy of $q(x,t)$ at the space point x, and $\mathcal{H}(x,y)$ is the total entropy of $q(x,t)$ and $q(y,t)$ between the two spatial points. This relation shows that the mutual information $\mathcal{I}(q(x,t),q(y,t))$ measures the shared information between the two spatial points (x,y).

Mutual information more faithfully captures the notion of statistical independence than does the two-point correlation, since the vanishing of mutual information is a necessary and sufficient condition for statistical independence. (The factorization of the complete infinite hierarchy of correlation functions to all orders is required for statistical independence — not just the factorization of two point correlations.) In addition, unlike the correlation functions, mutual information is invariant under invertible coordinate transformations. Thus, it provides an intrinsic description of the information propagated under the chaotic dynamics.

Unfortunately, the numerical computation of mutual information is far more involved than the correlation functions. However, we stress the conceptual advantage of mutual information over correlation functions since it renders a unified picture of chaos in time and space — spatiotemporal chaos giving rise to a loss of information in both time and space.

5.3 Information Propagation in Linear Stochastic Dynamics

Before turning to the discussion of mutual information for chaotic NLS waves, we develop some intuition about the behavior of mutual information for several distinct classes of linear waves. In particular, we describe examples which illustrate very distinct behavior for the propagation of information in space for diffusive, wave, and dispersive systems.

We need the mutual information between two random variables (X,Y), each individually normal with means m_x, m_y and variances σ_x^2 and σ_y^2, respectively, and whose joint probability density is Gaussian

$$\begin{aligned} p(x,y) &= \frac{1}{2\pi\sigma_x\sigma_y(1-\rho^2)^{1/2}} \\ &\quad \times \exp\left\{-\frac{1}{2(1-\rho^2)}\left[\left(\frac{x-m_x}{\sigma_x}\right)^2 - 2\rho\left(\frac{x-m_x}{\sigma_x}\right)\left(\frac{y-m_y}{\sigma_y}\right) + \left(\frac{y-m_y}{\sigma_y}\right)^2\right]\right\}. \end{aligned}$$

Here ρ is the correlation coefficient, i.e., $\rho = \mathrm{Cov}(x,y)/(\sigma_x\sigma_y)$. In this case, definition (5.4) becomes

$$\begin{aligned} \mathcal{I}(X,Y) &= \int_{-\infty}^{\infty} dxdy\; p(x,y)\left\{-\frac{1}{2}\ln(1-\rho^2)\right. \\ &\quad \left. -\frac{1}{2(1-\rho^2)}\left[\rho^2\left(\frac{x-m_x}{\sigma_x}\right)^2 - 2\rho\left(\frac{x-m_x}{\sigma_x}\right)\left(\frac{y-m_y}{\sigma_y}\right) + \rho^2\left(\frac{y-m_y}{\sigma_y}\right)^2\right]\right\} \\ &= -\frac{1}{2}\ln(1-\rho^2). \end{aligned} \tag{5.6}$$

First, consider diffusion dynamics:

$$u_t - Du_{xx} = f(t)\delta(x), \quad -\infty < x < +\infty,$$

where $f(t)$ is a Gaussian white noise with zero mean and δ-correlation:

$$\langle f(t)\rangle = 0,$$

$$\langle f(t)f(t')\rangle \quad = \quad \bar{\gamma}\delta(t-t'),$$

where $\langle\cdots\rangle$ denotes an average over noise. As any linear transformation of a Gaussian process remains a Gaussian process, the solution

$$u(x,t) = \int_0^t \frac{1}{\sqrt{4\pi D(t-t')}} \exp\left[-\frac{x^2}{4D(t-t')}\right] f(t')dt'$$

is a Gaussian process, whose correlation can be easily written as

$$\langle u(x,t)u(x',t)\rangle = -\frac{\bar{\gamma}}{4\pi D}\mathrm{Ei}\left(-\frac{\xi}{t}\right),$$

where Ei is the exponential-integral function

$$\mathrm{Ei}(z) = -\int_{-z}^{\infty} s^{-1}e^{-s}ds \quad \text{for } z<0,$$

and where

$$\xi = \left(\frac{x^2+x'^2}{4D}\right).$$

Therefore, according to equation (5.6), the mutual information between $u(x,t)$ and $u(x',t)$ in the case of diffusion is

$$\mathcal{I}(x,x') = -\frac{1}{2}\ln\left(1-\frac{\mathrm{Ei}^2(-\xi/t)}{|\mathrm{Ei}(-\xi_1/t)\mathrm{Ei}(-\xi_2/t)|}\right),$$

in which $\xi_1 = x^2/(2D)$ and $\xi_2 = x'^2/(2D)$. For a fixed time t and a fixed $x' \neq 0$, we have

$$\mathcal{I}(x,x') \sim \frac{C(x',t)}{x^2}, \tag{5.7}$$

for large x, i.e., $x \gg (2Dt)^{1/2}$ and $|x| \gg |x'|$. Here $C(x',t)$ is a positive constant depending on x' and t. Equation (5.7) shows that, in the *case of diffusion*, the mutual information decays with *a power law in space*.

Now we contrast this result with that for wave dynamics:

$$u_t - u_x = f(t)\delta(x), \quad -\infty < x < +\infty,$$

where $f(t)$ is again Gaussian white noise. Since the solution is

$$u(x,t) = f(t+x),$$

for x and t within the "light cone" such that $-t \leq x \leq 0$, we have

$$\langle u(x,t)u(x',t)\rangle = \bar{\gamma}\delta(x-x').$$

Thus, in the wave case, the mutual information between $u(x,t)$ and $u(x',t)$ for x and t in the light cone is

$$\mathcal{I}(x,x') = \begin{cases} 0, & x \neq x', \\ \infty, & x = x'. \end{cases} \tag{5.8}$$

(Note that the correlation coefficient $\rho = 1$ for $x = x'$ by definition). Therefore, *in the wave case*, spatially distinct points do not share any information when driven by Gaussian white noise which is δ correlated in time. If the noise is Gaussian but with a finite correlation function in time,

$$\langle f(t)f(t')\rangle = \bar{\gamma}\exp\left(-\frac{|t-t'|}{\tau}\right), \tag{5.9}$$

then the mutual information between $u(x,t)$ and $u(x',t)$ becomes

$$\mathcal{I}(x,x') = -\frac{1}{2}\ln\left[1-\exp\left(-\frac{2|x-x'|}{\tau}\right)\right]. \tag{5.10}$$

At large distances, $|x-x'| \gg \tau/2$, the mutual information decays exponentially in space, i.e.,

$$\mathcal{I}(x,x') \sim \exp\left(-\frac{2|x-x'|}{\tau}\right). \tag{5.11}$$

Note that the equal-time two-point correlation function for the wave is

$$C(x,x') = \langle u(x,t)u(x',t)\rangle \sim \exp\left(-\frac{|x-x'|}{\tau}\right). \tag{5.12}$$

Therefore, in this case, the lengthscale of the spatial decay of the correlation function is two times that of the mutual information. Numerical simulations have observed values of this ratio which are close to 2, even for nonlinear systems [192, 159].

For linear Schrödinger dispersive waves, i.e.,

$$iu_t + u_{xx} = f(t)\delta(x), \quad -\infty < x < +\infty,$$

where $f(t)$ is real Gaussian white noise, it can also be shown that the mutual information between $u(x,t)$ and $u(x',t)$ is

$$\mathcal{I}(x,x') = \begin{cases} 0, & x \neq x', \\ \infty, & x = x'. \end{cases} \tag{5.13}$$

That is, the information is not shared between any spatially distinct points.

These discussions show clearly that the propagation of information in space depends distinctly on the class of linear pde. Moreover, for linear Gaussian processes, these calculations illustrate the sufficiency of two-point correlations to compute mutual informations. In contrast, for the information propagation in the situation of spatially extended *deterministic nonlinear* dynamics, mutual information, in general, requires a full knowledge of joint probability distributions — and not just the two-point correlation functions [183].

5.4 Numerical Measurements of Spatiotemporal Chaos for NLS Waves

Now we return to chaotic NLS waves (5.1), and use mutual information to establish the existence of spatiotemporal chaos. First, we calculate numerically the spatial correlation function $C(x)$ [Eq. (5.3)]. Fig. 9 (left panel) shows the dependence of the correlation function $C(x)$ on the system length. For $\ell = 6.4$, which corresponds to the one linearly unstable mode, clearly, the whole system is correlated. This is intuitively

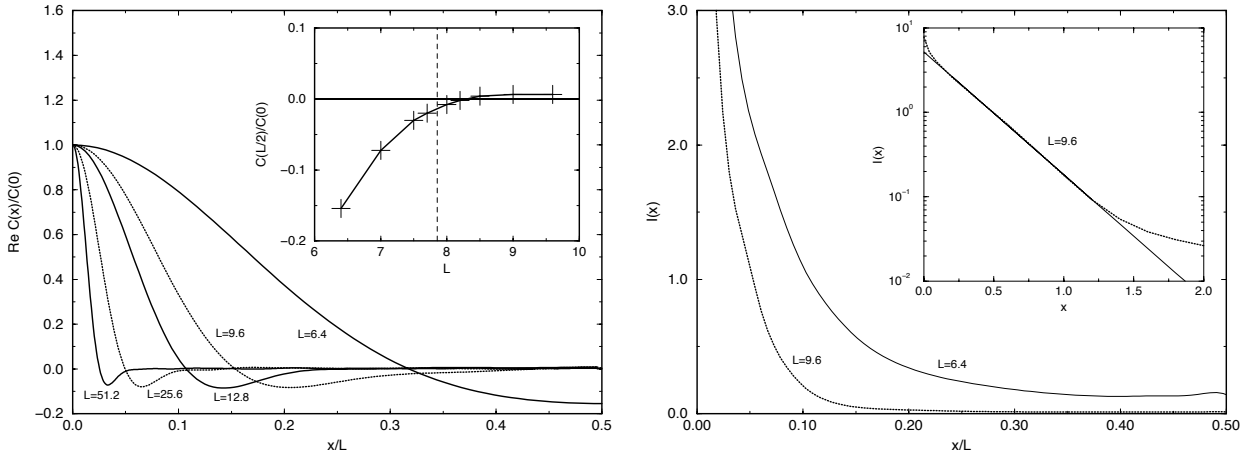

Figure 9: Numerical measurements. Left panel: Dependence of the correlation $C(x)$ on the system size L. Inset: Transition of $C(L/2)$ around $L_{\rm th} = 2\pi/c$ (dashed line) [cf. Eq. (3.12)]. Right panel: Mutual information $\mathcal{I}(x)$. Fine line: one linearly unstable mode; Dotted line: two linearly unstable modes, as also shown in the inset on the linear-log scale (the straight line is a fit to an exponential form).

consistent with what one would conclude by observing the spatial structures of Fig. 8, since, for the most times of the evolution, there is only one quasi-soliton in space. When the system size is increased so that there are higher numbers of linearly unstable modes present, Fig. 9 (left panel) shows that their correlation functions rapidly vanish. Therefore, the system becomes increasingly decorrelated, indicating an onset of spatiotemporal chaos. As shown in the inset of Fig. 9 (left panel), the correlation at the half system length as a function of ℓ displays a clear transition around the threshold $\ell_{\rm th} = 2\pi/c$, above which the second linearly unstable mode enters [see Eq. (3.12)].

According to our definition of spatiotemporal chaos, we use mutual information to further corroborate the preceding results. Figure 9 (right panel) summarizes the mutual information as a function of the distance x between any two points in space for both one and two linearly unstable modes, which corresponds to the cases in the left and right panel of Fig. 8, respectively. For one linearly unstable mode the mutual information remains nonzero across the system, signifying no sufficient loss of information over the whole system, while it vanishes rapidly for the case of two linearly unstable mode. It can be further determined that this decay is *exponential* as shown in the inset of Fig. 9 (right panel); that is,

$$\mathcal{I}(x) \to \exp(-\frac{x}{\xi}) \quad \text{for large } x \tag{5.14}$$

with a decay length $\xi \sim 0.30$. As solitons are phase-locked to the external driver, we anticipate that the driving frequency ω controls this decay length, i.e., the soliton's frequency determines its spatial width, the coherence length in space.

These results establish that spatiotemporal chaos exists for NLS waves, with the transition from temporal chaos to spatiotemporal chaos occurring at the system size at which a second instability arises. Only *two*

instabilities seem to be required. Spatiotemporal chaos in such small systems is somewhat unexpected, as the prevalent belief in the physical literature requires very large systems with many unstable modes [41, 89, 82, 57, 58, 170, 137, 200, 172, 38, 112, 91, 176, 39]. (See, however, the recent work [80]).

6 Descriptions of the Chaotic State

Given a chaotic state, one seeks ways to describe and to understand it. For *temporal chaos*, dynamical systems theory has provided a framework and some concepts, including: "strange" attractors, horseshoes and symbol dynamics, Lyapunov exponents, different dimensions, and universal routes to chaos — as well as more statistical descriptions of the attractor, including invariant measures and entropy. The application of some of these concepts to temporally chaotic dispersive waves is described in the survey [149].

For *spatiotemporal chaos* much less is known, and we believe that statistical representation will be essential for its description. For waves which occur in nature, such as waves on the surface of the ocean, statistical behavior and properties in the mean become far more important than individual trajectories. Wave spectra are observable, and modelling these with deterministic initial-boundary problems seems unnatural and would be irrelevant. Spatiotemporal chaotic waves call for statistical descriptions. In this section, we briefly describe three such statistical theories — (i) invariant measures of equilibrium statistical mechanics, (ii) weak-turbulence theories, and (iii) effective stochastic dynamics.

6.1 Equilibrium Statistical Mechanics

Nonlinear dispersive waves are frequently related to conservative mechanical systems. The Toda lattice and the sine-Gordon equation (as a continuum limit of coupled pendula) provide two examples. Equilibrium statistical mechanics is the traditional description of conservative mechanical systems with a large number of degrees of freedom; hence, it provides a natural starting point for a statistical description of conservative waves.

We view the 1-D NLS equation under periodic boundary conditions,

$$\begin{aligned} iq_t &= q_{xx} - 2g\left(q\bar{q}\right)q \\ q(x,t) &= q(x+\ell,t), \end{aligned}$$

as a Hamiltonian system

$$iq_t = \frac{\delta H}{\delta \bar{q}},$$

with Hamiltonian

$$H(q) \equiv \int_0^\ell \left[|q_x|^2 + g|q|^4\right] dx.$$

Statistical mechanics of NLS is the study of the *Gibbs measure* based upon this Hamiltonian. This measure, on the space of continuous functions, can be written formally in terms of the Hamiltonian H as

$$\frac{1}{Z}\ \exp\left\{-\beta H\big[u(\cdot),v(\cdot)\big]\right\}\ Du(\cdot)Dv(\cdot), \tag{6.1}$$

where $q(x) = u(x) + iv(x)$, and where the normalization constant (partition function) Z is defined as

$$Z \equiv \int_{C(0,\ell)} \exp\{ -\beta H[u(\cdot), v(\cdot)] \} \; Du(\cdot) Dv(\cdot).$$

Here $C(0,\ell)$ denotes the space of continuous, periodic functions in which $[u(x), v(x)]$ reside, and the positive parameter β denotes inverse temperature.

For those not familiar with function space integrals, reference [102] provides an intuitive introduction which emphasizes a view of the integral over functions as a "sum over paths", and which makes concrete the notation $Du(\cdot)$, etc.

In the defocusing ($g > 0$) case, it is relatively easy to give precise meaning to these formal expressions by writing

$$\begin{aligned} \frac{1}{Z} \exp\{ -\beta H[u(\cdot), v(\cdot)] \} \; Du(\cdot) Dv(\cdot) & \\ = \; & \frac{1}{Z} \exp\Big\{ -\beta g \int_0^\ell [u^2 + v^2]^2 \, dx \Big\} \; \exp\Big\{ -\beta \int_0^\ell [u_x^2 + v_x^2] \, dx \Big\} \; Du(\cdot) Dv(\cdot) \\ = \; & \frac{1}{Z} \exp\Big\{ -\beta g \int_0^\ell [u^2 + v^2]^2 \, dx \Big\} \; D_w u(\cdot) D_w v(\cdot), \end{aligned} \tag{6.2}$$

where $D_w u(\cdot) D_w v(\cdot)$ denotes unnormalized Wiener measure:

$$D_w u(\cdot) D_w v(\cdot) \; \equiv \; \exp\Big\{ -\beta \int_0^\ell [u_x^2 + v_x^2] \, dx \Big\} \; Du(\cdot) Dv(\cdot).$$

With this observation, Wiener measure can be used to give a precise mathematical definition of the Gibbs measure for the defocusing case [19, 23, 142, 141, 143].

Wiener measure is supported on functions which are continuous, but no-where differentiable. As such, these functions are "very rough"; for example, the energy space H^1 has Wiener measure zero. For the Gibbs measure to be invariant, the NLS equation must be well-posed for such rough data. Clearly, energy arguments will not work for such rough data. Resolving these existence issues requires delicate and interesting mathematical arguments [19, 23, 142, 141, 143], which establish that the Gibbs measure exists and is invariant for the defocusing NLS case.

The focusing ($g < 0$) case is more subtle, as the formal expressions show. (Note, for $g < 0$ the integrand (6.2) is unbounded.) In one-dimension, control can be achieved by constraining with the L^2 norm (which is also invariant).

The goal of an equilibrium statistical mechanics of waves is to use these invariant measures to extract statistical properties of typical wave configurations. Rose, Leibowitz, and Speer introduced these NLS measures, studied them both numerically and in "mean field", and posed some fascinating problems [127, 128]. In particular, they conjectured a phase transition in the focusing case which involves solitons vs radiation — At high temperature (small β), the typical configuration would consist in radiation, while at low temperature, it would consist in a gas of solitons. While recent evidence seems against this conjecture, the extraction of qualitative information about the statistical ensemble of waves from the Gibbs measure

remains open mathematically. (There is a related calculation for the discrete Toda lattice which estimates the expected number of solitons as a function of the temperature, and which agrees well with numerical observations [155, 154, 138, 33, 179].)

There are many fascinating issues, including: the thermodynamic ($\ell \to \infty$) limit, together with the possibility of the coupling constant $g \to \infty$; the extraction of spectra and other mean properties of the waves from the measure; the use of the measure or its moments to produce effective integration schemes, constrained by partial data [37]; "fluctuation-dissipation theorems" for ensembles of waves; macroscopic transport [73]; the application of these ideas to vortex filaments of fluid mechanics [134] (which can be described by NLS and its perturbations [103, 104, 107, 105, 106]).

Although these issues are fascinating mathematically, the fact that the measure is concentrated on rough functions remains troublesome physically. Typically, dissipation dominates at small scales — exactly where this rough spatial behavior appears. And this description of waves as a conservative Hamiltonian system neglects dissipation. Descriptions which focus upon steady fluxes of excitations between the different spatial scales, rather than upon equilibrium behavior, may be more relevant for ensembles of nonlinear waves. One such description is "weak turbulence theory".

6.2 Weak-turbulence Theories

In order to understand dynamics of spatially extended, nonlinear wave systems, an important issue one must first address is the identification of fundamental excitations. In an appropriate coordinate system the fundamental excitations often acquire a very simple representation, such as a soliton in the nonlinear spectral representation, which is far simpler and more compact than its Fourier (plane wave) representation. Conceptually, these natural representations often allow us to capture the main dynamics of the system. The small residual interactions amongst the fundamental excitations can be then treated perturbatively. The theoretical power, as we demonstrated in preceding chapters, of the spectral representation toward understanding temporal chaos precisely lies in the fact that solitonic excitations and their interactions are the most important features in this dynamics.

In this section we present another important theoretical formalism for nonlinear phenomena — namely, weak-turbulence theories. The dynamical emphasis of this formalism is wave-wave interactions. One origin of this formalism was a description of nonlinear phenomena in plasmas [199, 198, 195], such as the processes of modulational instabilities, decay instabilities, and wave couplings. It turns out that a Hamiltonian formalism, together with normal form transformations, provides a natural language for weak-turbulence, in which dissipative effects can be taken into account as small corrections. The waves described by weak-turbulence must be of small amplitude; and the weak-turbulence formalism fails to capture strongly nonlinear effects such as wave collapse and self-focusing. This is to be expected since these nonlinear phenomena involve a different kind of coherent degrees of freedom than simple resonant wave interactions.

Weak-turbulence theories provide a statistical description for the kinetic evolution of correlation func-

tions which describe wave spectra. In the derivation of these kinetic equations, a random phase approximation (i.e., a Gaussian assumption), as well as some technical assumptions, are invoked for the interacting waves, resulting in a certain closure scheme for the weak-turbulence description of the dynamics. These are strong assumptions which are difficult to verify, and often are not valid. Therefore, the applicability of weak-turbulence closures should be carefully examined. We will describe an explicit toy model which was introduced [136] to illustrate the hazards of a blind application of the weak-turbulence formalism. We will also describe an alternative new closure scheme [136] which provides an accurate representation of the wave spectra for this model problem.

6.2.1 Formalism

If there is only one type of wave dispersion $\omega(k)$ present in a nonlinear medium, one can describe the waves in the absence of dissipation by the complex amplitude a_k satisfying the Hamiltonian system

$$i\frac{\partial a_k}{\partial t} = \frac{\delta H}{\delta \bar{a}_k}. \tag{6.3}$$

We consider Hamiltonians of the form

$$H = H_0 + H_{\rm int}, \tag{6.4}$$

where

$$H_0 = \int \omega(k) a_k \bar{a}_k dk \tag{6.5}$$

is the Hamiltonian of the linearized problem, and $H_{\rm int}$ is the perturbation describing the interaction amongst those degrees of freedom represented by a_k. Generally, $H_{\rm int}$ can be expressed in terms of power series in a_k, and $\bar{a}_k$, such as

$$\begin{aligned} H_{int} &= \int (P_{kk_1k_2}\ \bar{a}_k a_{k_1} a_{k_2} + \bar{P}_{kk_1k_2}\ a_k \bar{a}_{k_1} \bar{a}_{k_2}) \delta(k - k_1 - k_2)\ dk dk_1 dk_2 \\ &+ \int (Q_{kk_1k_2}\ a_k a_{k_1} a_{k_2} + \bar{Q}_{kk_1k_2}\ \bar{a}_k \bar{a}_{k_1} \bar{a}_{k_2}) \delta(k + k_1 + k_2)\ dk dk_1 dk_2 \\ &+ \int R_{kk_1k_2k_3}\ \bar{a}_k \bar{a}_{k_1} a_{k_2} a_{k_3} \delta(k + k_1 - k_2 - k_3)\ dk dk_1 dk_2 dk_3. \end{aligned} \tag{6.6}$$

The dispersion $\omega(k)$ determines the nature of wave interaction and its resulting turbulence properties. For example, if the following condition holds,

$$\begin{aligned} \omega(k) &= \omega(k_1) + \omega(k_2) \\ k &= k_1 + k_2 \end{aligned} \tag{6.7}$$

for some k, the wave interaction leads to the resonant interaction of the waves a_{k_1} and a_{k_2} into $a_{k_1+k_2}$. This situation is called *three-wave* resonance. If Eq. (6.7) does not have solutions, and if the following condition holds instead,

$$\begin{aligned} \omega(k_1) + \omega(k_2) &= \omega(k_3) + \omega(k_4), \\ k_1 + k_2 &= k_3 + k_4, \end{aligned} \tag{6.8}$$

then the four-wave resonance is responsible for the main energy transfer between weak dispersive waves. In this instance, it can be easily shown that a normal form transformation will place the Hamiltonian (6.4) in the form

$$H = \int \omega(k) a_k \bar{a}_k dk + \int S_{kk_1k_2k_3}\ \bar{a}_k \bar{a}_{k_1} a_{k_2} a_{k_3} \delta(k + k_1 - k_2 - k_3)\ dk dk_1 dk_2 dk_3. \tag{6.9}$$

This is the general Hamiltonian system with four-wave resonances. Clearly, the "particle" number

$$N = \int n_k dk = \int n_\omega d\omega, \tag{6.10}$$

is conserved, where $n_k = |a_k|^2$ and $n_\omega = n_k dk/d\omega$. In addition, the kinetic energy

$$E = \int \omega_k n_k dk = \int \omega n_\omega d\omega. \tag{6.11}$$

is an important quantity.

6.2.2 Direct and Inverse Cascades

These two conserved quantities under the four-wave resonance have direct implication on the flux of energy and wave number in the ω space, when the system is forced at some wave numbers and damped at others. This can be easily seen from a global balance of "particles" and energy. Consider an idealized situation in which N particles are being created per unit time at frequency ω, and N_- and N_+ particles are being removed at frequencies ω_- and ω_+. In a steady state, conservation of particles and energy leads to

$$\begin{aligned} N &= N_- + N_+, \\ \omega N &= \omega_- N_- + \omega_+ N_+. \end{aligned}$$

Solving for N_- and N_+, we have

$$N_- = \frac{N(\omega_+ - \omega)}{\omega_+ - \omega_-}, \tag{6.12}$$

$$N_+ = \frac{N(\omega - \omega_-)}{\omega_+ - \omega_-}. \tag{6.13}$$

Since $N_-, N_+ > 0$, ω has to lie between ω_- and ω_+. Without loss of generality, we choose $\omega_- < \omega < \omega_+$. As neither N_-, N_+ nor $\omega_- N_-$, $\omega_+ N_+$ vanish, there are fluxes of particles and energy in both directions from ω. If ω_- is near zero, there will be almost no energy removal at the low frequencies, and the energy will flow upward from ω to ω_+, resulting in an upward (direct) cascade of energy from the low frequencies to the high ones. If ω_+ is very large, Eq. (6.13) shows that the number of particles removed at ω_+ will be very small, and the particles have to flow from ω to ω_-, creating a downward (inverse) cascade of particle numbers. As a consequence, if the dissipation takes place only at frequencies near zero and at very high values, there is an "inertial" range in which the energy flows upward from its source to the sink at the high frequencies, whilst the particles flow downward from their source to the sink at the low frequencies. As we will see below, these cascades provide a physical basis for understanding (nonequilibrium) steady state solutions in weak-turbulence theories.

6.2.3 A Simple Model

To further illustrate detailed aspects (such as the closure issues and wave spectra) of weak-turbulence via four-wave resonances, we describe a model system introduced by Majda, McLaughlin and Tabak [136]. The governing equation of the system is

$$iq_t = |\partial_x|^\alpha q + |\partial_x|^{-\beta/4}\left(\left||\partial_x|^{-\beta/4}q\right|^2|\partial_x|^{-\beta/4}q\right). \tag{6.14}$$

The equation has two parameters $\alpha > 0$ and $\beta \geq 0$. For $\beta = 0$, a standard cubic nonlinearity results. The parameter β is introduced to effectively weaken this nonlinearity as a consequence of a nonlocal smoothing in space. The parameter α controls the dispersion relation

$$\omega(k) = |k|^\alpha, \tag{6.15}$$

which, for $\alpha < 1$, leads to resonance quartets in this one-dimensional model.

The essence of weak turbulence theory is a statistical description of weakly nonlinear dispersive waves in terms of a closed, kinetic equation for certain two-point spectral functions. Starting with the equation of motion for system (6.14) in the Fourier space, and introducing Gaussian randomness through the initial conditions, one has

$$n_t(k,t) = \int \frac{2\mathrm{Im}\langle a_{k_1}a_{k_2}\bar{a}_{k_3}\bar{a}_k\rangle}{|k_1|^{\beta/4}|k_2|^{\beta/4}|k_3|^{\beta/4}|k|^{\beta/4}}\delta(k_1+k_2-k_3-k)\,dk_1dk_2dk_3 \tag{6.16}$$

for the two-point function

$$n(k,t) = \langle a_k(t)\bar{a}_k(t)\rangle. \tag{6.17}$$

The evolution of the four-point functions depends on six-point functions. Under a Gaussian random phase approximation, and the assumption that

$$\frac{\partial}{\partial t}\langle a_{k_1}a_{k_2}\bar{a}_{k_3}\bar{a}_k\rangle = 0,$$

one obtains

$$\mathrm{Im}\langle a_{k_1}a_{k_2}\bar{a}_{k_3}\bar{a}_k\rangle \approx -2\pi\frac{n_2n_3n_k + n_1n_3n_k - n_1n_2n_k - n_1n_2n_3}{|k_1|^{\beta/4}|k_2|^{\beta/4}|k_3|^{\beta/4}|k|^{\beta/4}}\delta(\omega_1+\omega_2-\omega_3-\omega), \tag{6.18}$$

where $n_2 = n(k_2,t)$, etc. Using this *closure condition*, one can close Eq. (6.16) to arrive at

$$\dot{n}_k = 4\pi\int\frac{n_1n_2n_3n_k}{|k_1k_2k_3k|^{\beta/2}}\left(\frac{1}{n_k}+\frac{1}{n_3}-\frac{1}{n_2}-\frac{1}{n_1}\right)\delta(\omega_1+\omega_2-\omega_3-\omega)\delta(k_1+k_2-k_3-k)dk_1dk_2dk_3. \tag{6.19}$$

Eq. (6.19) is the *kinetic equation* for $n(k,t)$.

6.2.4 Zakharov's Solutions

For an angular averaged kinetic equation (6.19), the trivial time-independent solutions

$$n(\omega) = c, \tag{6.20}$$

and

$$n(\omega) = \frac{c}{\omega}, \tag{6.21}$$

correspond to equipartition of particle number and energy, respectively. Using a conformal mapping, Zakharov showed that the angular averaged kinetic equations often possess additional (Kolmogorov) power law solutions of the form [197]

$$n_K(\omega) = \frac{c}{\omega^\gamma}, \tag{6.22}$$

for $\gamma \neq 0$, or 1, which describes the spectra for the cascades in nonequilibrium situations. These solutions are intimately related to fluxes of particles and energy in ω or k space as we discussed previously [197]. For system (6.14), it can be shown that for $\alpha = 1/2$

$$\begin{aligned} n_K(\omega) &= c\omega^{4/3\beta - 5/3} \\ \text{i.e.,}\quad n_K(k) &= c|k|^{2/3\beta - 5/6} \end{aligned}$$

for the inverse cascade, and

$$\begin{aligned} n_K(\omega) &= c\omega^{4/3\beta - 2} \\ \text{i.e.,}\quad n_K(k) &= c|k|^{2/3\beta - 1} \end{aligned}$$

for the direct cascade.

6.2.5 Numerical Results and Failure of the Weak-turbulence Theory for the Model

In [136], numerical experiments were carried out for the direct cascade of energy from long waves to short waves. For $\alpha = 1/2$ and $\beta = 1$, the Komolgorov spectrum from the weak-turbulence theory is $n_K \sim |k|^{-1/3}$. However, numerically this spectrum was not observed. Instead, the numerical measurements yielded a much steeper spectrum $n \sim |k|^{-3/4}$ over large inertial ranges. Moreover, in contrast to the weak-turbulence prediction of the existence of a spectral bifurcation at a critical β, the experiment displayed no spectral bifurcations. Careful postprocessing of the numerical simulations shows clearly that the Gaussian approximation is satisfied. Therefore, one would expect that the weak-turbulence theory should work. It turns out that the failure of the weak-turbulence theory prediction for this one dimensional model can be traced to the breakdown of the closure condition (6.18). Using the insight derived from the numerical results, a new closure condition was proposed [136]:

$$\mathrm{Im}\langle a_{k_1} a_{k_2} \bar{a}_{k_3} \bar{a}_{k_4} \rangle \approx c \frac{(n_1 n_2 n_3 n_4)^{1/2}}{\omega_1 + \omega_2 - \omega_3 - \omega_4} \tag{6.23}$$

for the evolution of the two-point function $n(k)$. The scaling of the Komolgorov spectrum under this new closure is found to be in excellent agreement with numerical scalings for the model. In general, to find a good closure scheme is a difficult problem. As is demonstrated by our example, although weak-turbulence theories provide a systematic approach to the closure problem, the validity of the closure thus obtained still needs to be carefully tested for the applicability of the weak-turbulence theories.

Finally it is worth noting that the weak-turbulence theory for system (6.14) is insensitive to the sign of the nonlinear term. Recalling that modulational instabilities and solitons crucially depend on this sign, one appreciates that weak turbulence, when valid, must be restricted to nonlinear waves of very small amplitudes.

6.3 Effective Stochastic Dynamics

In weak-turbulence theories, one uses two-point correlations (6.17) to characterize the spectra of wave-wave interactions over many scales. However, one may also be interested in a "macroscopic" description of the longest waves in the spatiotemporal chaotic system. The long waves in the deterministic chaotic system will be effectively stochastic. One anticipates that their dynamical evolution will be described by a stochastic equation — in which the chaotic waves on intermediate spatial scales will act as both a "source of a random stirring force" on the longest waves, and a "sink for the dissipation" of the longest waves. That is, long-wave instabilities create chaotic shorter waves, which, in turn, act as an "active heat bath" which causes the random forcing and dissipation of the longest waves. In contrast to weak-turbulence theory (which can be viewed as a stochastic description of the active heat bath), "effective stochastic dynamics" depends critically on properties of the nonlinearity because it demands the presence of long-wave instabilities. For example focusing, rather than defocusing, nonlinearity is required.

Recently, this issue of "non-equilibrium fluctuation-dissipation theorems" has received renewed interest in statistical physics, particularly in the connection between the hydrodynamic limit of the Kuramoto-Sivashinsky equation and the Burgers-KPZ universality class [200, 193, 172, 38, 32, 100, 93]. The formalism used to describe the coarse-grained effective stochastic dynamics is a natural extension to a dissipative system of the Zwanzig-Mori projection formalism for a Hamiltonian system in thermal equilibrium [182]. When applied to the Kuramoto-Sivashinsky model in the spatiotemporal chaotic regime, a noisy Burgers equation results as the effective long-range, large-time dynamics [200, 193, 172, 38, 32].

There are two questions: (i) Does an effective stochastic dynamics exist which provides a macroscopic description of long waves in a chaotic deterministic system? (ii) Can a closure theory be developed which derives the effective stochastic equations from the original deterministic system? Most of the work in the literature assumes an affirmative answer to the first question, and develops formal closure schemes to address the second. Often, these heuristic arguments are based on ideas from renormalization group methodology [76, 193, 194], and are very difficult to convert into precise asymptotic analyses. In this article, we address the first question with numerical experiments designed to validate some necessary conditions for the existence of an effective stochastic dynamics.

In [35, 34] we extend the methods of reference [200] to the perturbed NLS equation (5.1), focusing upon which aspects of chaoticity are necessary for the validity of its effective stochastic dynamics. Specifically, is spatiotemporal chaos necessary or is temporal chaos sufficient for an effective stochastic dynamics? Surprisingly, we find that numerical tests of necessary conditions for an effective stochastic dynamics for the perturbed NLS equation require only temporal chaos, in contrast to the Kuramoto-Sivashinsky equation

for which spatiotemporal chaos is believed to play a crucial role for the validity of the effective stochastic dynamics [200, 193, 172, 38, 32]. But effective stochastic dynamics fails for quasi-periodic behavior.

The representation of the perturbed NLS equation (5.1) in the Fourier space is

$$i\dot{a}_k = (k^2 - i\alpha)a_k - \frac{2}{\ell^2}\sum_{q,p} a_q a_p \bar{a}_{p+q-k} + \ell\Gamma e^{i(\omega t+\gamma)}\delta_{k,0}, \tag{6.24}$$

where

$$a_k = \int_0^\ell q(x)e^{ikx}dx$$

with $k = 2\pi m/\ell$, m being an integer. The effective dynamics is concerned with the dynamics for a_k in the long wavelength limit. In other words, the aim is to construct an effective dynamics for the macroscopic observable

$$\tilde{q}(x) = \frac{1}{\ell}\sum_{|k|<\Lambda} a_k e^{-ikx},$$

where Λ is a (small) cutoff parameter.

Zaleski [200] developed a numerical procedure to test the possibility of an effective stochastic dynamics for the Kuramoto-Sivashinsky equation. We will illustrate the method for the perturbed NLS equation. For a fixed cutoff Λ and any $\tilde{\alpha}_k$, we can rewrite equation (6.24) in an equivalent form:

$$\begin{aligned} i\dot{a}_k &= (k^2 - i\tilde{\alpha}_k)a_k - \frac{2}{\ell^2}{\sum}^{<} a_q a_p \bar{a}_{p+q-k} + \ell\Gamma e^{i(\omega t+\gamma)}\delta_{k,0} + F_k(t), \\ F_k(t) &= -i(\alpha - \tilde{\alpha}_k)a_k - \frac{2}{\ell^2}{\sum}' a_q a_p \bar{a}_{q+p-k}, \end{aligned} \tag{6.25}$$

where $\sum^<$ denotes summation over all $|q|$, $|p|$, $|q+p-k| < \Lambda$ and $\sum'$, a summation in which at least one of wavenumbers $|q|$, $|p|$, $|q+p-k|$ is larger than Λ.

In this setting, equation (6.25) can be viewed as the effective stochastic dynamics, *provided* we regard $F_k(t)$ as a stochastic force and $\tilde{\alpha}_k$ as an correction to dissipation and/or dispersion, (e.g., a k-dependent $\mathrm{Re}\tilde{\alpha}_k$ will represent an effective k-dependent damping while $\mathrm{Im}\tilde{\alpha}_k$ an effective dispersion).

If $F_k(t)$ truly acts as an "external" stochastic force, it cannot depend on the solution $q(s)$ in the past; i.e., for $s < t$. This "causality condition"

$$\langle F_k(t)\bar{a}_k(t-s)\rangle_t = 0 \ \text{ for } s > 0, \tag{6.26}$$

where $\langle\cdots\rangle_t$ is the time average over t, determines an expression for the effective dissipation parameter:

$$\tilde{\alpha}_k = \alpha - \frac{2i}{\ell^2}{\sum}' \frac{\langle a_q(t)a_p(t)\bar{a}_{q+p-k}(t)\bar{a}_k(t-s)\rangle_t}{\langle a_k(t)\bar{a}_k(t-s)\rangle_t}. \tag{6.27}$$

Relation (6.27) implies explicit s-dependence, which we denote as $\alpha_k(s)$. The existence of an effective stochastic dynamics requires s-independence — at least over a coarse-grained time scale. The numerical computation of the full dynamics (5.1) shows that equation (6.27) is indeed s-independent for the perturbed NLS equation, even in the regime of *only temporal chaos* [see Fig. 10 (left panel)]. No spatiotemporal chaos is

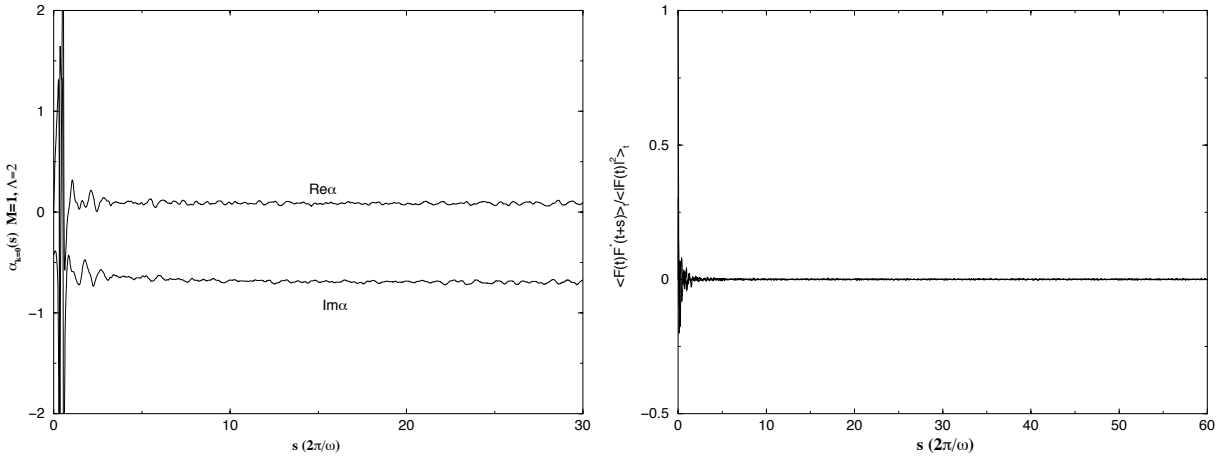

Figure 10: Numerical validation of effective stochastic dynamics: the s-independence of $\alpha_k(s)$ (left panel) and rapid decay of the force-force correlation (right panel) (Note that $\langle F(t)\bar{F}(t+s)\rangle_t/\langle|F(t)|^2\rangle_t = 1$ for $s = 0$). Time unit is normalized by $2\pi/\omega$.

required. In view of the the usual belief that an effective stochastic dynamics requires spatiotemporal chaos, this result is rather surprising. Of course, as is expected, this s-independence also applies in the regime of spatiotemporal chaos. However, an effective stochastic description is not valid for quasiperiodic dynamics, since quasiperiodic temporal behavior introduces a long memory time. And indeed, this was borne out in the numerical simulations [34].

In the presence of temporal chaos alone, the numerical construction shows that the effective $\mathrm{Re}\tilde{\alpha}_k$ gives rise to a renormalization of dissipation for the longest waves ($k = 0, 1$). In general, $\mathrm{Im}\tilde{\alpha}_k$ has the form of $\beta_0 + \beta_2 k^2 + \beta_4 k^4$, leading to an additional modification of the Schrödinger dispersion $\omega = k^2$ to

$$\omega \sim (1 + \beta_1)k^2 + \beta_2 k^4, \tag{6.28}$$

with β_1 and β_2 determined from a numerical construction.

In addition to this test that $\alpha_k(s)$ is independent of s, another necessary criterion for stochastic dynamics is that the effective stochastic force should have no long-time correlation. This is satisfied in the perturbed NLS case: it has been (numerically) shown that $\langle F_k(t)\bar{F}_k(t+s)\rangle_t$ decays rapidly, and can be regarded as no correlation over the coarse-grained time-scale [see Fig. 10 (right panel)]. The construction procedure only demands the causality (6.26), which only involves correlations for the same k. For $k \neq k'$, $\langle F_k(t)\bar{a}_{k'}(t-s)\rangle_t$ is left unconstrained by the determination of the effective dissipation. However, the numerical results also show that, for the $F_k(t)$ constructed above, $\langle F_k(t)\bar{a}_{k'}(t-s)\rangle_t \approx 0$ also holds for $k \neq k'$. The fulfillment of causality in this general form is indicative of a deep self-consistency, and goes toward the validation of the interpretation of $F_k(t)$ as an external stochastic forcing. Of course, whether a Gaussian white noise can be used to replace $F_k(t)$ in the effective dynamics requires a further statistical characterization of higher orders of correlations in the stochastic forcing.

Finally, we emphasize that a significant separation of scales lies in the heart of the validity of effective stochastic dynamics. And we note in passing that the numerical simulations show that effective stochastic dynamics also works well with even symmetry imposed. For example, for one linearly unstable mode, with or without even symmetry, the effective α_k are the same within numerical errors.

In summary, these numerical studies have clarified the nature of the chaoticity which is required for effective stochastic dynamics, i.e., temporal chaos seems sufficient for the validity of the effective equation for perturbed NLS, while the absence of chaos invalidates effective stochastic dynamics.

6.4 Nonlinear Localization

In this survey, we have described deterministic chaos, together with some discussion (in the section on weak-turbulence theory) of the stochastic behavior induced by random initial conditions. However, stochastic waves can also be generated by a random environment. In contrast to the decoherence effects caused by spatiotemporal chaos, the spatial disorder of a random environment can cause the waves to localize. This phenomena is particularly striking for linear waves — where it can convert conductors into insulators [2], and prevent sound from propagating [169]!

For example, consider the very idealized model for an electron propagating in a metal — the one dimensional linear Schrödinger equation of quantum mechanics:

$$iq_t = -q_{xx} + gV(x)q, \quad -\infty < x < +\infty.$$

Here $V(x)$ is a random potential which models impurities in the metal. This problem can be completely understood by analyzing the time-independent spectral problem

$$-q_{xx} + gV(x)q = Eq.$$

Following the original work of Anderson [2], it is now understood (with complete mathematical rigor) that the spectrum of this *one dimensional* problem consists of only point spectrum with no continuous spectrum. (See, for example, [177].) *Any amount* of randomness converts a problem with only continuous spectrum ($g = 0$) into one with *dense* point spectrum ($g \neq 0$)! All eigenfunctions in the random system are exponentially localized in space, since they are associated with the discrete eigenvalues in the point spectrum. As such, the extended generalized eigenfunctions of the continuous spectrum in the deterministic $g = 0$ case (which are associated with conduction) are all destroyed by the randomness, and replaced by localized eigenfunctions which do not conduct. Extended waves are localized by the random environment.

While this problem is completely understood for linear waves, it is essentially open in the presence of nonlinearity. Focusing nonlinearity causes waves to localize into solitary waves, while defocusing causes nonlinear spreading. Numerical experiments show that the competition between these deterministic nonlinear processes and the linear localization caused by spatial disorder produces some interesting phenomena — phenomena which, as yet, is not well understood analytically.

For the nonlinear Schrödinger equation,

$$iq_t = -q_{xx} + V(x)q + 2g|q|^2 q, \tag{6.29}$$

where $V(x)$ is a random potential, some theoretical results [55, 108] related to localization have been obtained using a time-harmonic ansatz,

$$\begin{aligned} q(x,t) &= \exp(-ik^2 t)u \\ k^2 u &= -u_{xx} + V(x)u + 2g|u|^2 u, \end{aligned}$$

to study the resulting time-independent nonlinear Schrödinger equation. However, in the presence of nonlinearity, this nonlinear eigenvalue problem approach inherited from the linear theory may not be sufficient. These time-independent solutions may be dynamically unstable, and hence irrelevant for the description of long-time behavior. This is indeed the case [28]: For both the focusing and defocusing nonlinearities, the time harmonic solutions of the random NLS equation are often unstable.

Furthermore, it has been demonstrated numerically [28] that the disordered NLS equation exhibits rather different dynamics, depending on whether the nonlinearity is focusing or defocusing. For the focusing case, the final attractor of the dynamics is a state which consists of interacting, highly localized solitary waves, with widths far narrower than the localization lengths of the corresponding linear system. For the defocusing case, in contrast, the system settles down to a nearly monochromatic state with a spatial profile which can be approximately described by

$$2g|q(x)|^2 \sim k^2 - V(x).$$

This profile is slaved to the random potential and its form indicates a lack of localization.

Finally we mention that similar issues arise in the discrete NLS equation

$$i\dot{q}_n = -J(q_{n+1} + q_{n-1}) - \omega q_n + V_n q_n + 2g|q_n|^2 q_n, \tag{6.30}$$

in the presence of disorder V_n, where J and ω are constants. Similar localization phenomena have been observed. In the discrete case, the localized states are intimately related to *discrete breathers*, which are ubiquitous, robust nonlinear excitations in discrete nonlinear systems [6]. For the focusing case, in the weak nonlinearity limit, the localization is still "Anderson-like". With increasing of nonlinearity, the excitations become highly localized and are controlled by the nucleation of discrete breathers. This scenario suggests the existence of a phase diagram in disorder-nonlinearity space describing a crossover between a disorder controlled attractor and a nonlinearity controlled attractor. Again, as in the continuous case, it has been shown that the effect of nonlinearity on localization depends sensitively on the class of nonlinearities: the nonlinearity enhances the localization in the focusing case, whilst suppressing the localization in the defocusing case.

7 Asymptotic Long-Time Behavior of NLS Waves

In final two sections we return to the completely integrable NLS equation, in order to exhibit the level of precision in asymptotic description of nonlinear waves which can be extracted from the inverse spectral representation. In this section we will describe the Riemann–Hilbert formulation of the inverse spectral problem for the defocusing NLS equation. Then we will use this formulation to establish long time asymptotics for the defocusing NLS equation. The results described here are due to Deift, Its, and Zhou [45]. A more detailed description of the analysis contained in [45] is presented in [53].

7.1 Statement of the Riemann–Hilbert Problem

Before defining the Riemann–Hilbert problem, we begin with an auxiliary matrix-valued function: Given a function $r(\lambda) \in \mathbf{S}(\mathbb{R})$, the Schwarz space of C^∞ functions which decay faster than any power as $|\lambda| \to \infty$, we build a matrix $v_{x,t}(\lambda)$ via

$$v_{x,t}(\lambda) = e^{-i(2t\lambda^2 - x\lambda)\sigma_3} \begin{pmatrix} 1 & \overline{r(\lambda)} \\ -r(\lambda) & 1 - |r(\lambda)|^2 \end{pmatrix} e^{i(2t\lambda^2 - x\lambda)\sigma_3}. \tag{7.1}$$

The goal of the Riemann–Hilbert problem is to determine the unique 2x2 matrix valued function $m(\lambda, x, t)$ satisfying (7.2)-(7.4) below:

$$m \text{ is analytic in } \mathbb{C} \setminus \mathbb{R}, \tag{7.2}$$

with continuous boundary values for $\lambda \in \mathbb{R}$, $m_\pm(\lambda, x, t) = \lim_{\epsilon \downarrow 0} m(\lambda \pm i\epsilon, x, t)$, satisfying

$$m_+(\lambda, x, t) = m_-(\lambda, x, t) v_{x,t}(\lambda). \tag{7.3}$$

Finally, m possesses the following asymptotics for x and t fixed:

$$m \to I \text{ as } \lambda \to \infty. \tag{7.4}$$

The fact of the matter is that if $r(\lambda)$ is the reflection coefficient associated with $q_0(x)$ as defined in (3.8), then the solution $q(x,t)$ to the defocusing NLS equation is obtained from the matrix m via

$$q(x,t) = 2 \left[\lim_{\lambda \to \infty} \lambda \left(I - m(\lambda, x, t) \right) \right]_{12}. \tag{7.5}$$

That is, if m possesses the asymptotic description $m = I + \frac{m_1}{\lambda}$ as $\lambda \to \infty$, then $q(x,t) = -2\,(m_1)_{12}$.

Remark: In this section we have replaced t in the defocusing NLS equation with $-t$, and the equation becomes

$$iq_t + q_{xx} - 2|q|^2 q = 0.$$

The above Riemann–Hilbert problem (7.2)-(7.4) is one formulation of the integral equations of inverse scattering theory, as mentioned in Section 3. Indeed, if we set

$$\Psi(\lambda, x, t) \equiv m(\lambda, x, t) e^{i\lambda x \sigma_3}, \tag{7.6}$$

then it turns out that for $\lambda \in \mathbb{C} \setminus \mathbb{R}$, Ψ is a fundamental matrix solution of the differential equation (3.3), normalized by the following two conditions:

$$\Psi e^{-ix\lambda\sigma_3} \to I, \text{ as } x \to +\infty, \tag{7.7}$$

$$\Psi e^{-ix\lambda\sigma_3} \text{ remains bounded as } x \to -\infty. \tag{7.8}$$

The jump relation (7.3) expresses the fact that while $\Psi(\lambda, x, t)$ satisfying (7.7)-(7.8) is defined *a priori* for $Im\lambda \neq 0$ only, it turns out that $\Psi(\lambda, x, t)$ has continuous boundary values for $\lambda \in \mathbb{R}$,

$$\Psi_\pm(\lambda, x, t) = \lim_{\epsilon \downarrow 0} \Psi(\lambda \pm i\epsilon, x, t).$$

Since Ψ_+ and Ψ_- represent two fundamental matrix solutions of (3.3), they must be related, i.e.,

$$\Psi_+(\lambda, x, t) = \Psi_-(\lambda, x, t) v(\lambda, t),$$

for some jump matrix v which is independent of x.

Remark: If one starts with this jump relation, and then uses (7.6), one arrives at a jump relation for m, which appears a bit different than (7.3), because the time-dependence is not explicit. However, one can compute the evolution of the matrix $v(\lambda, t)$ explicitly (see, for example, [53]), and (7.3) can be derived in this fashion.

Remark: The connection between the Riemann–Hilbert problem (7.2)-(7.4) and a set of integral equations for inverse scattering theory is classical: it turns out that existence and uniqueness of the solution of a Riemann–Hilbert problem is equivalent to invertibility of an associated integral operator. This is explained in many papers; we refer the reader to [53], where the connection is made particularly clearly.

7.2 Long-Time Behavior

In this subsection we will explain the Riemann–Hilbert approach to the problem of computing the long-time asymptotics of the solution to the defocusing NLS equation. The idea is to describe the solution to the Riemann–Hilbert problem (7.2)-(7.4) for $t \to \infty$, and then use the reconstruction formula (7.5) to compute asymptotics for $q(x, t)$.

To avoid technical issues, we will assume for the remainder of this section that the reflection coefficient $r(\lambda)$ can be continued analytically to a strip containing the real axis. This is satisfied, for example, if $q_0(x)$ is analytic, with sufficient decay as $x \to \infty$.

From a calculational point of view, the basic idea behind the method is that if we have a Riemann–Hilbert problem which is simple:

$$\begin{aligned} &n(\lambda) \text{ analytic in } \mathbb{C} \setminus \Sigma, \\ &n_+(\lambda) = n_- \left(I + \text{err}(\lambda)\right), \ \lambda \in \Sigma \\ &n(\lambda) \to I, \text{ as } \lambda \to \infty, \end{aligned}$$

where Σ is some oriented contour, and $\mathrm{err}(\lambda)$ is uniformly small on Σ [$O\left(\frac{1}{t}\right)$ in the $L^1(\Sigma) \cap L^\infty(\Sigma)$ norm, for example], then the solution to this Riemann–Hilbert problem can be obtained by solving an associated integral equation. It turns out that because the term err is uniformly small, this integral equation can be solved by Neumann series. Unraveling this connection between the Riemann–Hilbert problem and the integral equation, one arrives at an asymptotic expansion for the solution of the Riemann–Hilbert problem (in powers of $\frac{1}{t}$). In the present setting, rather than arriving at a "simple" Riemann–Hilbert problem as described above, we will arrive at a simplified model Riemann–Hilbert problem which can be solved exactly ([45], see also [53]).

Now we will explain how one arrives at a "simple" Riemann–Hilbert problem. The fundamental observation is that we have the factorization of the matrix $v_{x,t}(\lambda)$

$$v_{x,t}(\lambda) = \begin{pmatrix} 1 & 0 \\ -r(\lambda)e^{2it\theta} & 1 \end{pmatrix} \begin{pmatrix} 1 & \overline{r(\lambda)}e^{-2it\theta} \\ 0 & 1 \end{pmatrix}, \tag{7.9}$$

$$it\theta = it\theta(\lambda, x, t) = it\left(2\lambda^2 - t^{-1}x\lambda\right) = it(2\lambda^2 - 4\lambda_0\lambda), \tag{7.10}$$

$$\lambda_0 = \frac{x}{4t}. \tag{7.11}$$

Now although $v_{x,t}(\lambda)$ possesses rapidly oscillating terms (as $t \to \infty$), we observe that for $\lambda < \lambda_0$, the second factor on the right hand side in (7.9) can be analytically continued above the real axis, and $\mathrm{Re}\{-2it\theta\} < 0$, i.e. the rapidly oscillating term becomes exponentially decaying! Furthermore, the first factor on the right hand side of (7.9) can be analytically continued below the axis, where the oscillatory term again becomes exponentially decaying. (These properties of $it\theta$ can be seen by noting that if $\lambda = u + iv$, then $\mathrm{Re}\ it\theta = -4tv(u - \lambda_0)$.)

We now indicate how one splits a part of the real axis into two contours, deformed above and below the real axis, in order to exploit the exponential decay indicated above. We begin by re-writing the jump relation (7.3), using the factorization (7.9),

$$m_+ = m_- \begin{pmatrix} 1 & 0 \\ -r(\lambda)e^{2it\theta} & 1 \end{pmatrix} \begin{pmatrix} 1 & \overline{r(\lambda)}e^{-2it\theta} \\ 0 & 1 \end{pmatrix}.$$

Now using the analyticity discussed above, we may write this equation (for $\mathrm{Re}\ \lambda < \lambda_0$) as follows,

$$\left(m \begin{pmatrix} 1 & -\overline{r(\lambda)}e^{-2it\theta} \\ 0 & 1 \end{pmatrix} \right)_+ = \left(m \begin{pmatrix} 1 & 0 \\ -r(\lambda)e^{2it\theta} & 1 \end{pmatrix} \right)_-,$$

and so if we define n_1 via

$$n_1 = m \begin{pmatrix} 1 & -\overline{r(\lambda)}e^{-2it\theta} \\ 0 & 1 \end{pmatrix} \text{ for } \lambda \text{ above the axis, } \mathrm{Re}\ \lambda < \lambda_0,$$

$$n_1 = m \begin{pmatrix} 1 & 0 \\ -r(\lambda)e^{2it\theta} & 1 \end{pmatrix} \text{ for } \lambda \text{ below the axis, } \mathrm{Re}\ \lambda < \lambda_0,$$

then n_1 possess no jump across $(-\infty, \lambda_0)$. Since r and $\overline{r}$ can only be continued to a strip containing the real axis, we cannot make this definition globally, and so we define n_1 as shown in Fig. 7.1.

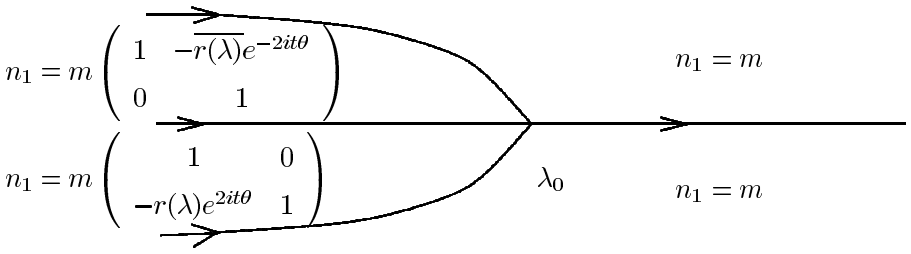

Figure 7.1. The definition of the matrix n_1.

Now n_1 is analytic for $\lambda \in \mathbb{C} \setminus \Sigma_1$, where Σ_1 is shown in Fig. 7.2. Observe that the jump across the real axis for $\lambda < \lambda_0$ has been removed by this factorization.

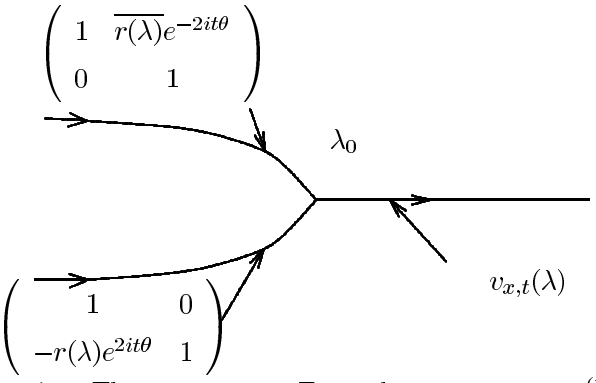

Figure 7.2. The new contour Σ_1, and jump matrices $v^{(1)}$.

Putting this all together, we have *transformed* the first Riemann–Hilbert problem for m, into a new Riemann–Hilbert problem, for n_1:

(7.12) $\quad n_1$ is analytic in $\mathbb{C} \setminus \Sigma_1$,

(7.13) $\quad (n_1)_+(\lambda, x, t) = (n_1)_-(\lambda, x, t) v^{(1)}_{x,t}(\lambda)$ for $\lambda \in \Sigma_1$, $\qquad$ ($v^{(1)}_{x,t}$ is defined in Fig. 7.2),

(7.14) $\quad n_1 \to I$ as $\lambda \to \infty$,

which is equivalent to the original problem: if we have a solution to the new problem, then by using Fig. 7.1, we have a solution to the original problem.

Remark: The contour Σ_1 is oriented as shown in Fig. 7.2, and we use the convention that the plus side of an oriented contour lies to the left as one traverse the contour. The $+(-)$ subscript in (7.13) denotes the boundary value taken from the $+(-)$ side of the contour Σ_1.

The second, and more fundamental, thing to observe is that now, for $\mathrm{Re}\ \lambda < \lambda_0$, the off-diagonal entries in the jump matrices $v^{(1)}$ are exponentially decaying, and so the jump matrices are exponentially close to I.

Unfortunately, for λ to the right of λ_0, this procedure does not work immediately. Indeed, for $\mathrm{Re}\ \lambda > \lambda_0$,

and λ below the real axis, $e^{2it\theta}$ is *exponentially growing*, and for $\operatorname{Re}\lambda > \lambda_0$, and λ above the real axis, $e^{-2it\theta}$ is also exponentially growing. However, we can switch the order of the factors that appear through a lower/upper factorization:

$$v_{x,t}(\lambda) = \begin{pmatrix} 1 & \frac{\overline{r(\lambda)}}{1-|r(\lambda)|^2}e^{-2it\theta} \\ 0 & 1 \end{pmatrix} \begin{pmatrix} \frac{1}{1-|r(\lambda)|^2} & 0 \\ 0 & 1-|r(\lambda)|^2 \end{pmatrix} \begin{pmatrix} 1 & 0 \\ -\frac{r(\lambda)}{1-|r(\lambda)|^2}e^{2it\theta} & 1 \end{pmatrix}. \tag{7.15}$$

Now for λ to the right of λ_0, the first term on the right hand side of (7.15) can be deformed below the real axis, and the off-diagonal entry becomes exponentially decaying, while the third term can be deformed above the real axis, and again the off-diagonal entry becomes exponentially decaying. (It turns out that since the reflection coefficient is analytic in a strip containing $\mathbb{R}$, the quantity $\overline{r(\lambda)} = \overline{r(\overline{\lambda})}$, $\lambda \in \mathbb{R}$, possesses an analytic continuation to a strip, as does $1-|r(\lambda)|^2$.) So now we define n_2 using Fig. 7.3.

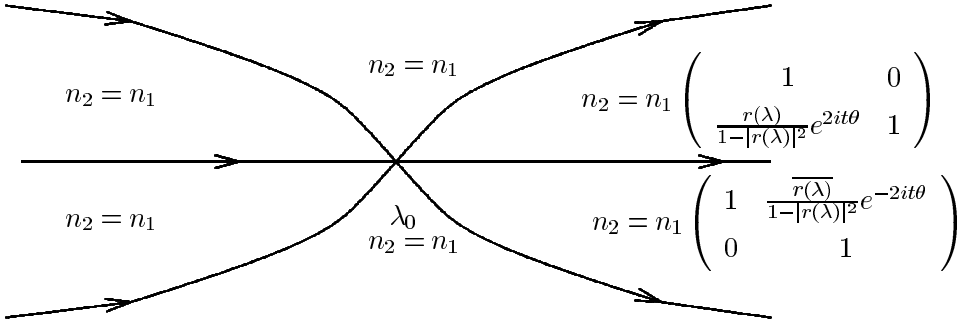

Figure 7.3. The definition of n_2.

We thus arrive at the following Riemann–Hilbert problem for n_2:

$$\begin{aligned} &n_2 \text{ is analytic in } \mathbb{C} \setminus \Sigma_2, \\ &(n_2)_+(\lambda,x,t) = (n_2)_-(\lambda,x,t)v^{(2)}_{x,t}(\lambda), \quad \lambda \in \Sigma_2, \\ &n_2 \to I \text{ as } \lambda \to \infty, \end{aligned}$$

where the new contour Σ_2 is shown in Fig. 7.4, along with the jump matrices $v^{(2)}_{x,t}$.

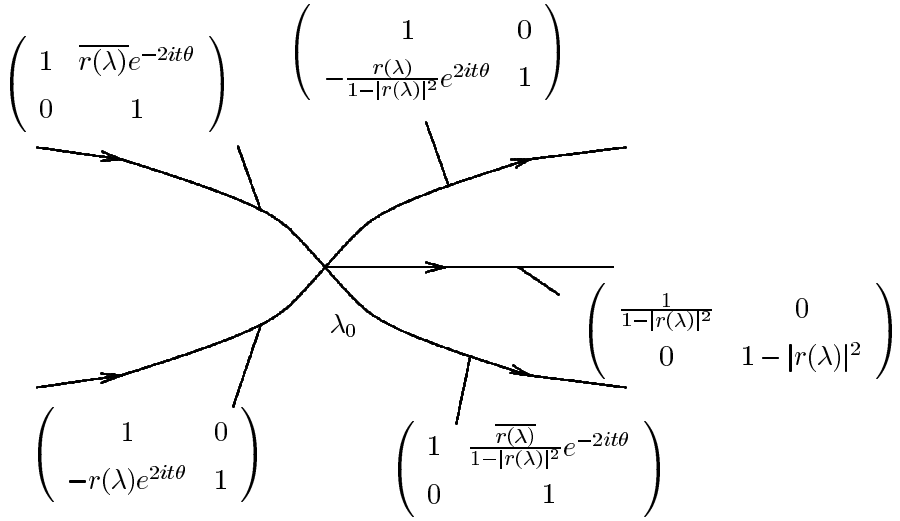

Figure 7.4. The contour Σ_2, and the jump matrices $v^{(2)}_{x,t}$.

There remains a diagonal jump matrix, for $\lambda \in (\lambda_0, \infty)$, which, it seems, cannot be deformed away. Even if we attempt to deform this term off of the axis, there is no hope to gain exponential decay, because this jump matrix has no t-dependence. This piece of the puzzle is handled by first solving the following scalar Riemann–Hilbert problem: find δ analytic in $\mathbb{C} \setminus \mathbb{R}$ such that

$$\delta_+(\lambda) = \begin{cases} \delta_-(\lambda)\left(1 - |r(\lambda)|^2\right), & \lambda > \lambda_0, \\ \delta_-(\lambda), & \lambda < \lambda_0, \end{cases}$$
$$\delta \to I, \text{ as } \lambda \to \infty.$$

It turns out that this problem can be solved by formula:

$$\delta(\lambda) = \exp\left[\frac{1}{2\pi i}\int_{\lambda_0}^{\infty} \frac{\log\left(1 - |r(s)|^2\right)}{s - \lambda} ds\right], \quad \lambda \notin \mathbb{R}.$$

Now, using this, we define

$$n_3(\lambda) = n_2(\lambda) \begin{pmatrix} \delta & 0 \\ 0 & \delta^{-1} \end{pmatrix}. \tag{7.16}$$

One may verify directly that the matrix valued function n_3 solves the Riemann–Hilbert problem

$$n_3 \text{ is analytic in } \mathbb{C} \setminus \Sigma_3,$$
$$(n_3)_+(\lambda, x, t) = (n_3)_-(\lambda, x, t) v^{(3)}_{x,t}(\lambda), \ \lambda \in \Sigma_3,$$
$$n_3 \to I \text{ as } \lambda \to \infty,$$

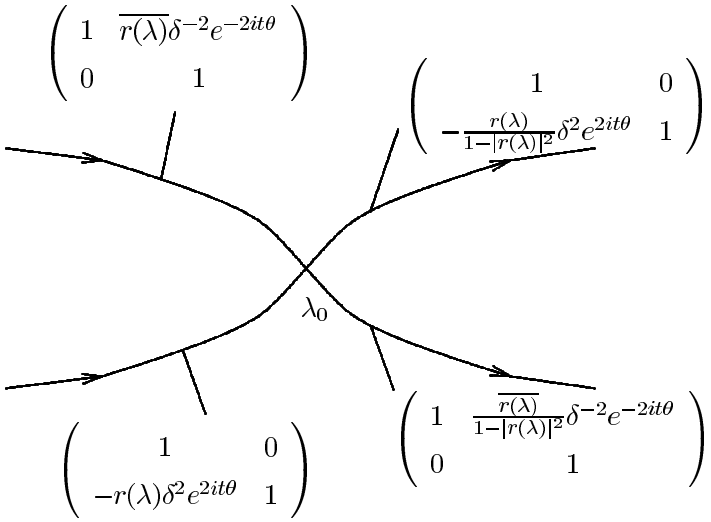

Figure 7.5. The contour Σ_3 and the jump matrices $v^{(3)}_{x,t}$.

Now we have finally arrived at a Riemann–Hilbert problem which is in the fortunate situation that away from one point, λ_0, the jump matrices are uniformly close to I. The last step to arrive at a Riemann–Hilbert problem which is "simple" in the manner described above, is to isolate the local nature of the Riemann–Hilbert problem for n_3.

To do this, we introduce the scaling transformation,

$$\zeta(\lambda) \equiv (8t)^{1/2}(\lambda - \lambda_0),$$

which is a map from $\mathbb{C}$ to $\mathbb{C}$, sending Σ_3 to Σ_4, shown in Fig. 7.6. This figure also shows the new jump matrices, $v^{(3)}(\lambda(\zeta))$.

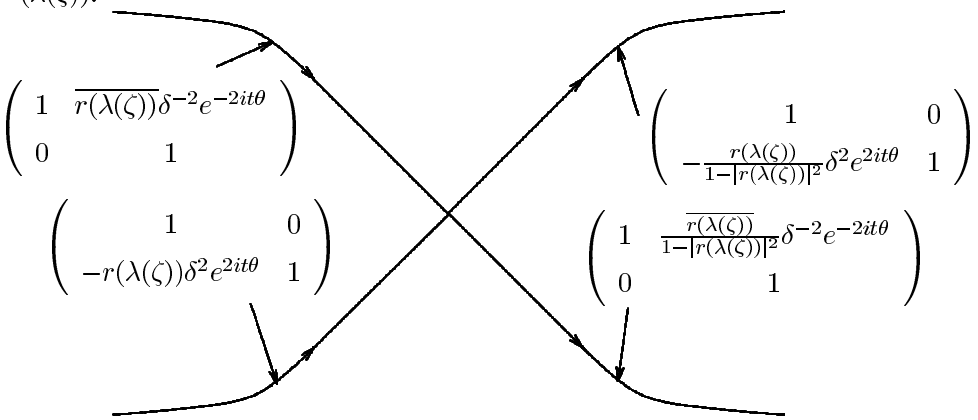

Figure 7.6. The contour Σ_4, and jump matrices $v^{(3)}(\lambda(\zeta))$.

Remark 1: We have chosen the contour Σ_3 so that for a small neighborhood of λ_0, the contour consists of 4 straight lines emanating from λ_0, forming angles of $\pi/4$ radians with the real axis. Because of this, on a large neighborhood of $\zeta = 0$ (of size $O(t^{1/2})$), the new contour Σ_4 consists of 4 straight lines forming angles of $\pi/4$ radians with the real axis.

Remark 2: For ζ on the contour Σ_4, we have the following representation for $\delta(\lambda(\zeta))e^{it\theta}$:

$$\begin{aligned} \delta(\lambda(\zeta))e^{it\theta} &= \frac{\zeta^{i\nu}}{(8t)^{i\nu/2}} e^{i\zeta^2/4} e^{-2it\lambda_0^2} e^{\kappa(\lambda_0+\zeta/(8t)^{1/2})} \\ &= \frac{\zeta^{i\nu}}{(8t)^{i\nu/2}} e^{i\zeta^2/4} e^{-2it\lambda_0^2} e^{\kappa(\lambda_0)} e^{\kappa(\lambda_0+\zeta/(8t)^{1/2})-\kappa(\lambda_0)}, \\ &= \delta^{(0)}\delta^{(1)}, \end{aligned} \tag{7.17}$$

where

$$\begin{aligned} \kappa(\lambda) &= -\frac{1}{2\pi i}\int_{\lambda_0}^{\infty} \log(\lambda - s) d\log\left(1 - |r(s)|^2\right), \\ \nu &= \frac{1}{2\pi}\log\left(1 - |r(\lambda_0)|^2\right), \\ \delta^{(0)} &= \frac{e^{\kappa(\lambda_0)} e^{-2it\lambda_0^2}}{(8t)^{i\nu/2}}, \\ \delta^{(1)} &= \zeta^{i\nu} e^{i\zeta^2/4} e^{\kappa(\lambda_0+\zeta/(8t)^{1/2})-\kappa(\lambda_0)}. \end{aligned} \tag{7.18}$$

We now make one further transformation, by defining $n_4(\zeta)$:

$$n_4(\zeta) = \begin{pmatrix} \delta^{(0)} & 0 \\ 0 & \left(\delta^{(0)}\right)^{-1} \end{pmatrix} n_3(\lambda(\zeta)) \begin{pmatrix} \left(\delta^{(0)}\right)^{-1} & 0 \\ 0 & \delta^{(0)} \end{pmatrix} \tag{7.19}$$

(recall from the definition (7.18) that $\delta^{(0)}$ is a constant). The matrix n_4 then solves the following Riemann–Hilbert problem:

$$\begin{aligned}
&n_4 \text{ is analytic in } \mathbb{C} \setminus \Sigma_4, \\
&(n_4)_+(\zeta, x, t) = (n_4)_-(\zeta, x, t) v^{(4)}_{x,t}(\zeta), \quad \zeta \in \Sigma_4, \\
&n_4 \to I \text{ as } \lambda \to \infty,
\end{aligned}$$

where Σ_4 and $v^{(4)}$ are shown in Fig. 7.7. Notice that $v^{(4)}$ is obtained from $v^{(3)}(\lambda(\zeta))$ by replacing $\delta e^{it\theta}$ by $\delta^{(1)}$.

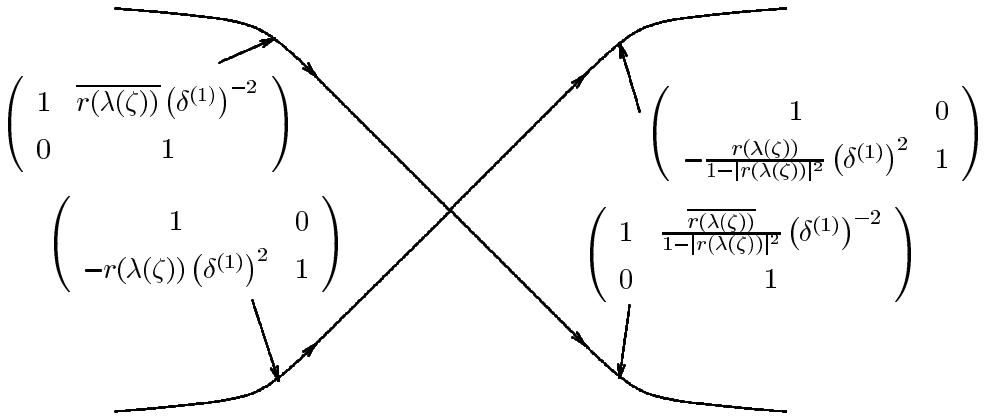

Figure 7.7. The contour Σ_4, and the jump matrices $v^{(4)}(\zeta)$.

The last step is to solve this final Riemann–Hilbert problem for n_4. Observe that $r(\lambda(\zeta)) = r(\lambda_0 + \frac{\zeta}{(8t)^{1/2}})$. It turns out that one can show that the solution to this problem is well approximated by the solution to the problem obtained by replacing $r(\lambda(\zeta))$ with $r(\lambda_0)$, and $\delta^{(1)}(\lambda(\zeta))$ with $\delta^{(1)} = \zeta^{i\nu} e^{-i\zeta^2/4}$. This model problem can be solved through the use of parabolic cylinder functions. Thus the final problem for n_4 can be solved asymptotically. We will omit these details, and refer the reader to [53]. We now assume that we have obtained n_4 by this procedure.

In summary, by explicit, invertible transformations, $m \to n_1 \to n_2 \to n_3 \to n_4$, we have arrived at a simple problem whose solution can be approximated easily. We can unravel all of these transformations, and hence we have obtained an approximation for the solution of the original Riemann–Hilbert problem (7.2)-(7.4). For example, if we take λ to lie in the region of the upper half-plane which is above the contour Σ_3, then we find

$$m(\lambda) = \begin{pmatrix} \left(\delta^{(0)}\right)^{-1} & 0 \\ 0 & \delta^{(0)} \end{pmatrix} n_4(\zeta(\lambda)) \begin{pmatrix} \delta^{(0)} & 0 \\ 0 & \left(\delta^{(0)}\right)^{-1} \end{pmatrix} \begin{pmatrix} \delta(\lambda)^{-1} & 0 \\ 0 & \delta(\lambda) \end{pmatrix}.$$

In this region of the complex plane, one can compute asymptotics for $\lambda \to \infty$, and from those asymptotics, read off the asymptotics for $q(x,t)$, using (7.5). We refer the reader to [53] for the details, and here only state the final result.

Let

$$n_4^{(1)} = \lim_{\zeta \to \infty} \zeta \left(n_4(\zeta) - I\right).$$

If $q(x,t)$ is the solution of the defocusing NLS equation, then there is a constant M so that as $t \to \infty$,

$$q(x,t) = -(2t)^{-1/2} \left(\delta^{(0)}\right)^{-2} \left(n_4^{(1)}\right)_{12} + O\left(\frac{\log t}{t}\right), \quad \text{for } |\lambda_0| = \left|\frac{x}{4t}\right| \leq M. \tag{7.20}$$

In [53], the explicit asymptotic description of n_4 is carried out. If we use this, and formula (7.18), then we have the following result:

Theorem 7.1 *If $q(x,t)$ is the solution of the defocusing NLS equation, then there is a constant M so that as $t \to \infty$,*

$$q(x,t) = -(2t)^{-1/2}(8t)^{i\nu} e^{i\frac{|x|^2}{4t}} e^{-2\kappa(\lambda_0)} \frac{-i(2\pi)^{1/2} e^{i\pi/4} e^{-\pi\nu/2}}{r(\lambda_0)\Gamma(-i\nu)} + O\left(\frac{\log t}{t}\right), \quad \textit{for } |\lambda_0| = \left|\frac{x}{4t}\right| \leq M. \tag{7.21}$$

Such uniform long-time asymptotics is unprecedented in the theory of nonlinear waves, and can only be obtained because of the deep connection between the linear spectral theory and the complete integrability of NLS. Similar results have been obtained for other soliton equations (see, for example, [45]). We close this section by reiterating that a key step in the argument is understanding how to handle rapidly oscillating terms in Riemann—Hilbert problems.

8 Semi-Classical Behavior

Consider the NLS equation in the form

$$\begin{aligned} i\epsilon q_t &= \epsilon^2 q_{xx} - 2g\left(q\bar{q}\right) q \\ q(x,0) &= A_{in}(x) \exp\left[\frac{i}{\epsilon} S_{in}(x)\right], \end{aligned} \tag{8.1}$$

where $0 < \epsilon \ll 1$. The limiting behavior of $q(x,t;\epsilon)$ for fixed x and t, as $\epsilon \to 0$, is known as the "semi-classical" or "vanishing dispersion" limit. This limit is very natural in the linear ($g = 0$) case, where it describes the semi-classical reduction of nonrelativistic quantum mechanics. In this setting, the parameter ϵ denotes *Planck's constant* $\hbar$, and the limit describes the reduction of Schrödinger quantum mechanics to Newtonian classical mechanics as $\hbar \to 0$. In the nonlinear cases ($g \neq 0$), the limit describes vanishing dispersion. In this limit, beautiful rapidly oscillating wavetrains form and propagate. The goal of the "small dispersion" problem is to characterize and describe these nonlinear wavetrains.

Remark: Physically, the nonlinear Schrödinger equation provides an asymptotic description [164] of the slowly varying envelope of a rapidly oscillating nonlinear wavetrain, which is (i) strongly dispersive, (ii) nearly monochromatic, and (iii) weakly nonlinear (of small amplitude). As such, properties of NLS solutions such as "blow-up in finite time" and "the development of rapid oscillations" tend to violate the assumptions of the NLS representation — assumptions such as slowly varying envelopes and small amplitude waves.

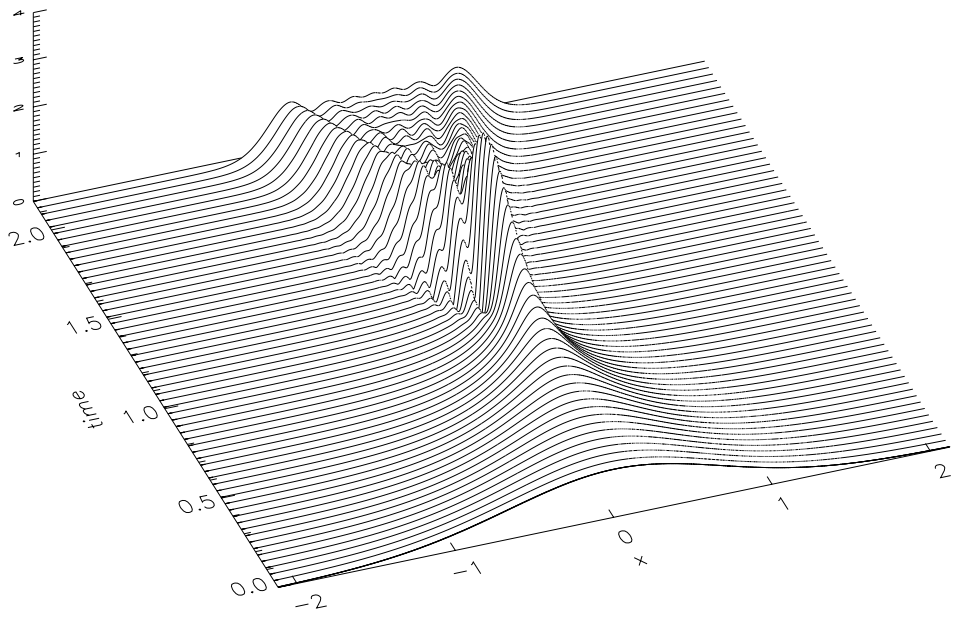

Figure 11: Semi-classical behavior: Linear case

Thus, the physical importance of these properties of NLS is not immediate; nevertheless, laser beams do filament and they can develop oscillations (which are associated to "optical shocks"). The validity of NLS in capturing such physical phenomena is a matter of scales — which can be short on the envelop scale, while still long on the scale of the underlying wavetrain. In any case, often there is a correlation between beautiful NLS wavetrains and observable behavior in laserbeams [31, 163, 162, 109, 75].

8.1 Sample Numerical Simulations

Figures 11, 12, and 13 illustrate the formation of rapid oscillations in the magnitude $|q(x,t;\epsilon)|$ for three cases: (i) linear ($g = 0$), (ii) defocusing nonlinearity ($g > 0$), and (iii) focusing nonlinearity ($g < 0$). The *same* initial data is used for each case:

$$q(x,0) = A_{in}(x) \exp\left[\frac{i}{\epsilon} S_{in}(x)\right],$$

where

$$A_{in}(x) = \exp(-x^2), \qquad \frac{d}{dx} S_{in}(x) = -\tanh(x).$$

In the figures, $\epsilon = 0.02$. Notice that initially there are no oscillations in the data $|q(x,0)| = A_{in}(x)$, but they form temporally in $|q(x,t;\epsilon)|$.

In the linear case, Fig. 11 shows a severe focus of intensity, and the emergence of caustics which bound a region in space-time which supports rapid oscillations. These phenomena are well understood in this linear

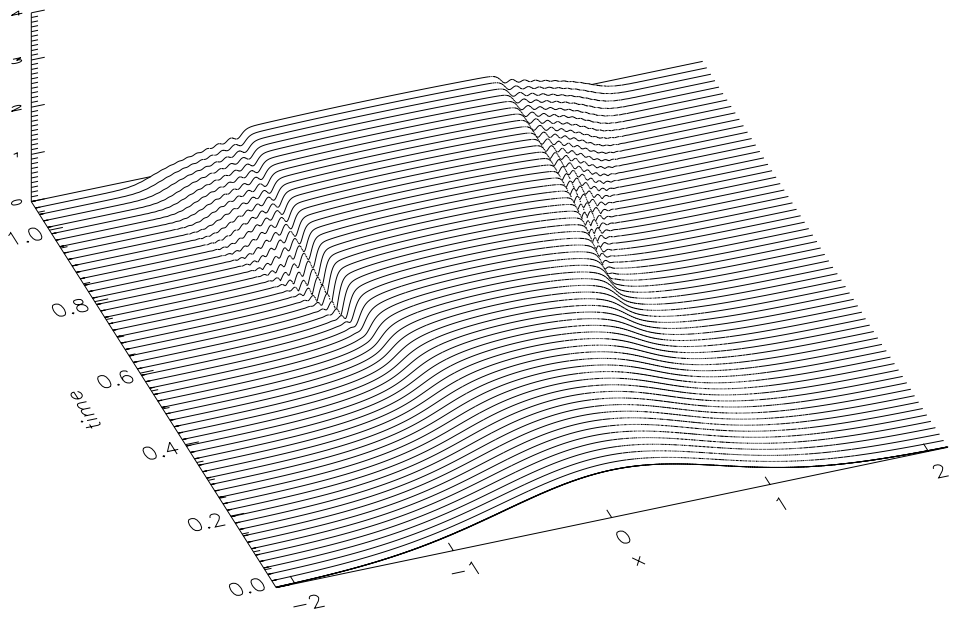

Figure 12: Semi-classical behavior: Defocusing nonlinearity

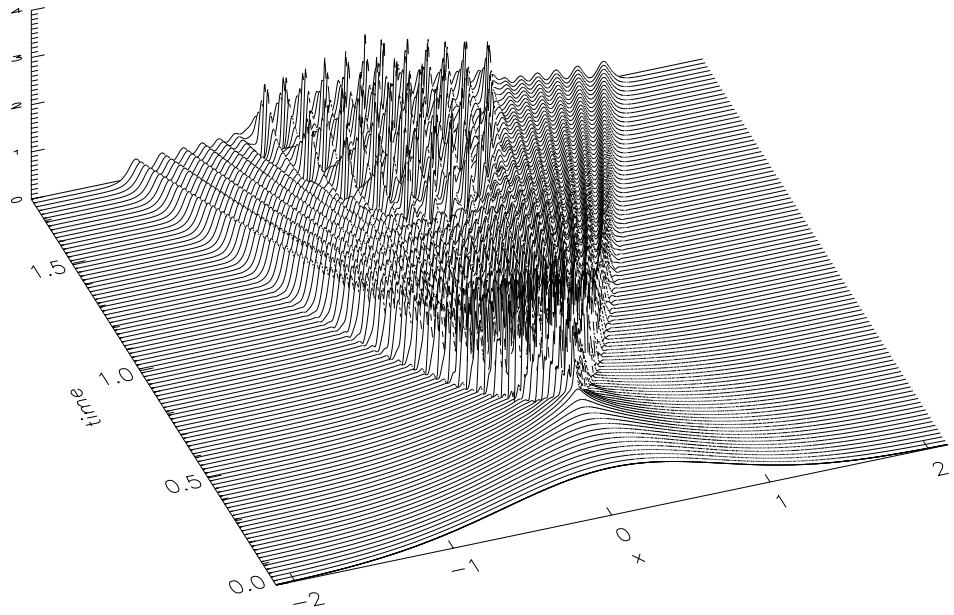

Figure 13: Semi-classical behavior: Focusing nonlinearity

case, and can be easily calculated using elementary stationary phase evaluation of

$$q(x,t;\epsilon) = \sqrt{\frac{i}{4\pi\epsilon t}} \int \exp\left\{\frac{i}{\epsilon}\left[\frac{(x-y)^2}{4t} - S_{in}(y)\right]\right\} A_{in}(y)\ dy.$$

The oscillations are the consequences of phase-interference of the quantum mechanical wave function $q(x,t;\epsilon)$. The mathematical theory of Lagrangian manifolds [4] was invented to describe such semi-classical phenomena in the presence of a potential.

The behavior for defocusing nonlinearity is milder — with no focus of intensity, but with two distinct regions of space-time which support rapid oscillations (Fig. 12). In these oscillatory regions (for both the linear and defocusing cases), the convergence of $|q(x,t;\epsilon)|$ as $\epsilon \to 0$ is only weak convergence. As $\epsilon \to 0$, the wave-length of the oscillations goes to zero linearly with ϵ, but their amplitude does not vanish. Rather, the amplitude itself converges to a nonvanishing limit, and the oscillations fill-in an "envolope" defined by the amplitude. This prevents strong convergence of $|q(x,t;\epsilon)|$.

The focusing case, Fig. 13, exhibits the most severe behavior. (The intriguing second region of distinct oscillations was also observed in [150].) To summarize, the oscillations may be ordered by their severity — from the least severe defocusing nonlinearity, through the intermediate linear case, to the most severe case of focusing nonlinearity.

8.2 Formal Semi-Classical Asymptotics

This ordering can be understood by the following formal asymptotic calculation [31], which applies before the onset of oscillations: We make the ansatz

$$q(x,t;\epsilon) \simeq A(x,t)\ \exp\left[\frac{i}{\epsilon}S(x,t)\right], \tag{8.2}$$

insert it into NLS equation, and balance powers of ϵ to obtain

$$\begin{aligned} P_t &= 2PP_x + 4gAA_x, \\ A_t &= 2PA_x + P_xA, \end{aligned}$$

where $P \equiv S_x$. This is a first order system of pde's for A and P. It can be placed in Riemann invariant form:

$$\Gamma^{\pm}_t = C^{\pm}\Gamma^{\pm}_x, \tag{8.3}$$

where the Riemann invariants $\Gamma^{\pm}$ are defined by

$$\Gamma^{\pm} \equiv P \pm 2\sqrt{g}\ A, \tag{8.4}$$

and where the characteristic speeds are given by

$$C^{\pm} = 2\big[P \pm \sqrt{g}A\big]. \tag{8.5}$$

From these characteristic speeds (or "nonlinear group velocities"), one can understand the "ordering". In the defocusing case, the speeds are real and distinct, and the system of equations (8.3) is "strictly hyperbolic" [122]. As such, the unknowns A and P are bounded; hence, the intensity A^2 cannot blow-up. (However, its derivatives can.)

On the other hand, in the linear case, the two real speeds are identical and the system (8.3) is "degenerate hyperbolic". When the hyperbolic system is degenerate, it can have foci at which its solutions diverge. In fact, this linear NLS case is particularly simple: The equation $P_t = 2PP_x$ can be easily solved by the method of characteristics [96], which can then be used to solve $A_t = 2PA_x + P_xA$, whose amplitude $A(x,t)$ is seen explicitly to diverge at a focus of the characteristics.

In the focusing case, the speeds are complex. The system is not hyperbolic, and the Cauchy problem is not well-posed. Instabilities are present which are related to the "modulational instability" as was described earlier. The situation is unclear, and quite unstable.

Returning to the case of defocusing nonlinearity, the modulation equations (8.3) describe the propagation of the waveform (8.2), until it "breaks at a focus of the characteristics". Moreover, by replacing the waveform ansatz (8.2) with one based upon slowly varying elliptic functions [74], one can use the modulation theory of Whitham [189, 190] to anticipate the evolution of those oscillations which form beyond "break-time". While this modulation theory provides beautiful representations of the oscillations, it is based upon the local ansatz of a modulating waveform — an assumption which is not connected to, nor derived from, the nonlinear initial value problem. As such, modulation theory provides only a partial description — although a very detailed one.

8.3 The Weak Limit in the Defocusing Case

In the defocusing integrable case, inverse spectral theory can be used to characterize completely the weak limit (8.1). This characterization connects the weak limit to the initial data; moreover, it characterizes the (phase) transition boundaries in space-time, across which the nature of the oscillations changes (See Fig. 12).

Lax and Levermore [123, 125, 124] first used inverse spectral theory to describe vanishing dispersion nonlinear wave problems in the setting of the Korteweg deVries (KdV) equation. That initial work, together with subsequent studies, is summarized in the survey [126]. The heart of the matter is a closed formula for the solution of the KdV equation obtained by neglecting the reflection coefficient (the formula involves only the solitons). A remarkable calculation then shows that, asymptotically as the dispersion parameter tends to zero, this formula is governed by an associated maximization problem in function space, in which x and t appear as external parameters. These methods were adapted in [94, 95] to study the semi-classical limit of the defocusing cubic NLS equation, where the steps in, and organization of, the proof of the Lax-Levermore construction is clarified significantly.

Today, the modern approach to these semi-classical limits combines the methods of Lax-Levermore with

those of Riemann-Hilbert problems with rapidly oscillating kernels. (Here, the oscillations arise as the coefficient of dispersion vanishes, rather than as $t \to \infty$.) Recently, Deift, Venakides, and Zhou [51] have completed a Riemann-Hilbert analysis of the small dispersion limit of the KdV equation. They are able to obtain a very detailed asymptotic description of the solution. It is remarkable to note that the maximization problem identified by Lax and Levermore appears as an essential component for this Riemann-Hilbert analysis: the support of the maximizer determines the limiting subset of the real axis on which a model Riemann-Hilbert problem must be solved. Moreover, if this limiting set consists of finitely many (but more than one) intervals, then the asymptotic description of the solution involves an associated theta function, and one is able to connect the initial value problem with the higher genus modulation equations of [70].

So far such a Riemann-Hilbert analysis has not been carried out for the case of the semi-classical limit of the NLS equation, and there are some difficulties. One particularly interesting aspect is that in [51], the authors assume that there are no solitons present, and work exclusively with the reflection coefficient. The situation in which there are N solitons, and $N \to \infty$ in the small dispersion limit (the easiest case for the Lax-Levermore approach), seems somewhat more difficult in the Riemann-Hilbert setting.

8.4 More on the Modulation Equations

In spite of the success in the characterization of the semi-classical limit through inverse spectral theory, modulation theory still provides the quickest method to display the local space-time structure of the oscillations. While significant work [126, 184, 51] has been carried out toward extracting this local structure from the Lax-Levermore/Riemann-Hilbert framework, the modulation approach is still far more direct. Moreover, inverse spectral theory is restricted to the very special case of integrable nonlinear waves, and it would seem that the modulation approach will form the basis for studies of more general nonintegrable waves.

In the completely integrable setting, a particularly beautiful representation of the modulation equations exists — an "invariant representation" in terms of meromorphic differentials. These are developed, and their consequences explored, in some detail in the KdV setting [70, 144]. Similar results could certainly be developed for defocusing NLS [74].

One begins with an N-phase, quasi-periodic waveform and its associated Zakharov-Shabat spectral theory. Let $\{\lambda_1, \lambda_2, \ldots, \lambda_{2N}\}$ denote the simple eigenvalues, and consider the hyperelliptic Riemann surface defined through these branch points:

$$R \equiv \left(\lambda, \sqrt{\left(\prod(\lambda - \lambda_j)\right)}\right).$$

The modulation of the waveform is described by letting the parameters be (slowly varying) functions of space-time, $\{\lambda_j(x,t),\ j = 1, \ldots, 2N\}$. Then, as shown in [74, 95], the modulation equations take the compact form

$$\partial_t\, \Omega^{(x)}(\lambda) \;=\; \partial_x\, \Omega^{(t)}(\lambda), \tag{8.6}$$

where $\Omega^{(x)}$ and $\Omega^{(t)}$ denote differentials of the form

$$\Omega^{(\alpha)} \equiv \frac{P^{(\alpha)}}{R}\, d\lambda, \quad \alpha = x, t, \tag{8.7}$$

and where $P^{(\alpha)}$ denote polynomials which are uniquely defined in terms of the branch points $\{\lambda_j(x,t),\ j = 1, \ldots, 2N\ \}$ through normalization conditions [74, 95]. Thus, these differentials are uniquely specified by the branch points $\{\lambda_j(x,t),\ j = 1, \ldots, 2N\ \}$, and they depend upon (x,t) only through these branch points. Moreover, these differentials characterize physical features of the wave — such as its frequencies of oscillation and its nonlinear group velocities. Thus, the modulation equations (8.6) may be viewed as evolution equations for the branch points.

As described in detail in [70, 144] for the KdV case, equation (8.6) is a particularly compact form of the modulation equations. All other forms may be extracted from it:

1. Expansion of the modulation equations (8.6) near $\lambda \simeq \lambda_j$ produces the Riemann invariant form of the equations. The branch points are shown to be Riemann invariants, and explicit formulas for the characteristic speeds are deduced:
$$C^j = \left.\frac{P^{(t)}}{P^{(x)}}\right|_{\lambda=\lambda_j}.$$

2. Expansion of equations (8.6) as $\lambda \to \infty$ produces the "averaged conservation law" form of the modulation equations, as first deduced by Whitham [189].

3. Integration of representation (8.6) around certain cycles on the Riemann surface produces a "canonical Hamiltonian-system form" of the modulation equations [70, 61].

8.5 The Focusing Case

While the semi-classical limit of the defocusing integrable NLS equation is rather completely characterized through inverse spectral theory, the semi-classical limit for the focusing case remains open — which many regard as *the* open problem in integrable nonlinear wave theory [95, 126]. In the focusing case, it is not even clear that the weak limit exists. Recently, there has been some progress:

1. By analysing the modified KdV hierarchy, Ercolani, Jin, Levermore and MacEvoy [62] showed that the obstruction is not the nonself-adjointness of the Zakharov-Shabat operator.

2. Bronski [29] has computed numerically a fascinating "Y-configuration" in the Zakharov-Shabat spectrum in the semi-classical limit for one type of data.

3. Consequences of this Y-configuration in the spectrum have been observed recently in laboratory experiments in nonlinear optics [113].

4. Miller and Kamvissis [150] have studied numerically the semiclassical limit for special analytic data. Their numerics indicates that the weak limit appears to exist and to be described, prebreaking, by the elliptic modulation theory.

5. Tian [180] has developed some numerical evidence toward the existence of a weak limit, as well as a particularly clean form of the log-determinant N-soliton formula in the focusing case.

Given this recent progress on the semi-classical limit for focusing nonlinearity, we are optimistic that this central problem of integrable nonlinear wave theory will soon be solved.

On the other hand, when the waves are not integrable, the semi-classical limit is completely open. The only known mathematical result is due to Grenier [81], who characterizes the prebreaking limit for defocusing nonlinearities. In this more general setting, the semi-classical limit and its generation of rapid oscillations is one example of the nonlinear transitions of excitations between spatial scales. As such, it is related to theories of turbulence (see Section 6.2). Recent promising mathematical approaches [116, 117, 118, 119, 18, 24] to such transitions between scales combine pde and dynamical systems methods.

9 Conclusion

In this survey, we have used a class of nonlinear Schrödinger equations to display typical qualitative properties of nonlinear dispersive waves, and to illustrate the interplay between the methods of partial differential equations and those of dynamical systems theory by which these properties can be understood mathematically. Specifically, for the study of global behavior for evolutionary pde's, we advocate implementing intuition from the theory of dynamical systems with methods natural for the pde. In addition, the central importance of scientific computation to the process is also emphasized throughout the survey, as is stochastic behavior.

One very special NLS equation is the integrable case of cubic nonlinearity in one spatial dimension. As one of the soliton equations, it represents the most spectacular success of dynamical systems methods for pde's. The miraculous properties of the soliton, which were discovered numerically, have been understood through the realization that these soliton equations are completely integrable Hamiltonian systems in infinite dimensions. However, this understanding did not follow solely through intuition from dynamical systems theory. Rather it resulted from a totally new mathematical idea — the deep connection between certain special nonlinear wave equations and the spectral theory of linear differential operators. Moreover, for the rigorous calculation of asymptotic limits, the full exploitation of this deep connection requires the proper setting, skills, and methods from mathematical analysis — the Riemann-Hilbert formulation of inverse spectral theory.

With the full power of the mathematical methods of the spectral and inverse spectral theory of linear differential operators, complete integrability (which seems so special from the viewpoint of nonlinear waves) has been shown to be quite universal throughout mathematical analyses where, in addition to the representation of integrable waves, it has been used: to solve classical problems regarding the asymptotic description of orthogonal polynomials [46]; to resolve open conjectures about the universality of random matrix theories [47]; to provide an understanding of sorting algorithms and of matrix factorizations [49] such as the "LU" and "singular-value" decompositions of numerical analysis; and, most recently, the solution of certain counting

problems in number theory [8] which may indicate a relation of these integrable methods to the zeros of the Riemann ζ function. Again, we emphasize that this remarkable breadth of integrable techniques follows from *both* the new mathematical idea and its natural analytic framework.

For nonlinear waves, integrable examples illustrate rich and fascinating global behavior; however, they do not indicate the generality of the phenomena. Once integrability is broken by perturbations of the equation, very little is known mathematically. In this survey we described some initial steps toward persistence, and toward the characterization and description of temporal and spatiotemporal chaos. However, most important non-integrable problems remain open, and we anticipate that the interplay between dynamical systems, pde, and stochastic analysis will play significant roles in their resolution.

References

[1] M. J. Ablowitz, B. M. Herbst, and C. M. Schober. The nonlinear Schrödinger equation: asymmetric perturbations, traveling waves and chaotic structures. *Math. Comput. Simulation*, 43:3–12, 1997.

[2] P. Anderson. Absence of diffusion in certain random lattices. *Phys. Rev.*, 109:1492, 1958.

[3] V. I. Arnold. Instabilities of systems with several degrees of freedom. *Sov Math Dokl*, 5:581–585, 1964.

[4] V. I. Arnold. *Mathematical Methods of Classical Physics*. Springer-Verlag (New York), 1978.

[5] V. I. Arnold and A. Avez. *Ergodic problems of classical mechanics*. W. A. Benjamin, Inc., New York-Amsterdam, 1968. Translated from the French by A. Avez.

[6] S. Aubry. Breathers in nonlinear lattices: Existence, linear stability and quantization. *Physica D*, 103:201–250, 1997.

[7] A.V. Babin and L.A. Bunimovich. Stable chaotic waves generated by hyperbolic pdes. *Nonlinearity*, 9:853, 1996.

[8] J. Baik, P. Deift, and K. Johansson. On the distribution of the length of the longest increasing subsequence of random permutations. *submitted to J. Amer. Math. Soc.*, 1999.

[9] P. W. Bates, K. Lu, and C. Zeng. Existence and persistence of invariant manifolds for semiflows in Banach space. *Mem. Amer. Math. Soc.*, 1999.

[10] R. Beals and R. Coifman. Scattering and inverse scattering for first-order operators. *Comm. Pure and Appl. Math.*, 37:39–90, 1984.

[11] R. Beals, P. Deift, and C. Tomei. *Direct and Inverse Scattering on the Line*. Amer. Math. Soc., Providence, 1988.

[12] T.B. Benjamin and J.F. Feir. The disintegration of wave trains on deep water. *J. Fluid Mech.*, 27:417–430, 1967.

[13] R. F. Bikbaev and S. B. Kuksin. A periodic boundary value problem for the sine-Gordon equation, its small Hamiltonian perturbations, and KAM-deformations of finite-gap tori. *Algebra i Analiz*, 4:42–78, 1992.

[14] B. Birnir, H. P. McKean, and A. Weinstein. The rigidity of sine-Gordon breathers. *Comm. Pure Appl. Math.*, 47:1043–1051, 1994.

[15] A. R. Bishop, M. G. Forest, D. W. McLaughlin, and E. A. Overman II. A quasiperiodic route to chaos in a near-integrable pde. *Physica D*, 23:293–328, 1986.

[16] R.E. Blahut. *Principles and Practice of Information Theory.* Addison-Wesley, New York, 1988.

[17] A. I. Bobenko and S. B. Kuksin. Small-amplitude solutions of the sine-Gordon equation on an interval under Dirichlet or Neumann boundary conditions. *J. Nonlinear Sci.*, 5:207–232, 1995.

[18] J Bourgain. Approximation of solutions of the cubic nonlinear Schrödinger equations by finite-dimensional equations and nonsqueezing properties. *Internat. Math. Res. Notices*, pages 79–88, 1994.

[19] J. Bourgain. Periodic nonlinear Schrödinger equation and invariant measures. *Comm. Math. Phys.*, 166:1–26, 1994.

[20] J. Bourgain. Construction of periodic solutions of nonlinear wave equations in higher dimension. *Geom. Funct. Anal.*, 5:629–639, 1995.

[21] J. Bourgain. Harmonic analysis and nonlinear partial differential equations. In *Proceedings of the International Congress of Mathematicians, Vol. 1, 2 (Zürich, 1994)*, pages 31–44, Basel, 1995. Birkhäuser.

[22] J. Bourgain. Construction of approximative and almost periodic solutions of perturbed linear Schrödinger and wave equations. *Geom. Funct. Anal.*, 6:201–230, 1996.

[23] J. Bourgain. Invariant measures for the 2D-defocusing nonlinear Schrödinger equation. *Comm. Math. Phys.*, 176:421–445, 1996.

[24] J. Bourgain. On growth in time of Sobolev norms of smooth solutions of nonlinear Schrödinger equations in $\mathbb{R}^D$. *J. Anal. Math.*, 72:299–310, 1997.

[25] J. Bourgain. On Melnikov's persistency problem. *Math. Res. Lett.*, 4:445–458, 1997.

[26] J. Bourgain. Refinements of Strichartz' inequality and applications to 2D-NLS with critical nonlinearity. *Internat. Math. Res. Notices*, 1998:253–283, 1998.

[27] J. Bourgain. Global wellposedness of defocusing critical nonlinear Schrödinger equation in the radial case. *J. Amer. Math. Soc.*, 12:145–171, 1999.

[28] J. Bronski, D. McLaughlin, and M. Shelley. On the stability of time harmonic localized states in a disordered nonlinear medium. *J. Stat. Phys.*, 88:1077–1115, 1997.

[29] J. C. Bronski. Semiclassical eigenvalue distribution of the Zakharov-Shabat eigenvalue problem. *Phys. D*, 97:376–397, 1996.

[30] J. C. Bronski. Nonlinear scattering and analyticity properties of solitons. *J. Nonlinear Sci.*, 8:161–182, 1998.

[31] J. C. Bronski and D. W. McLaughlin. Semiclassical behavior in the NLS equation: optical shocks—focusing instabilities. In *Singular limits of dispersive waves (Lyon, 1991)*, pages 21–38. Plenum, New York, 1994.

[32] J.C. Bronski. *Aspects of Randomness in nonlinear wave propagation.* PhD thesis, Princeton University, 1994.

[33] R.K. Bullough, Y.Z. Chen, and J.T. Timonen. Thermadynamics of Toda lattice models: Application to DNA. *Physica D*, 68:83–92, 1992.

[34] D. Cai, D. McLaughlin, and J. Shatah. Spatial temporal chaos for perturbed NLS equations. *In preparation for submission to J. Nonlinear Sci.*, 1998.

[35] D. Cai, D. McLaughlin, and J. Shatah. Spatiotemporal chaos and effective stochastic dynamics for a near integrable nonlinear system. *Phys Lett A, in press*, 1999.

[36] T. Cazenave. *An Introduction to Nonlinear Schrödinger Equations*, volume 22. IMUFRJ Rio De Janeiro, 1989.

[37] A. J. Chorin, A. P. Kast, and R. Kupferman. Optimal prediction of underresolved dynamics. *Proc. Natl. Acad. Sci. USA*, 95:4094–4098 (electronic), 1998.

[38] C.C. Chow and T. Hwa. Defect-mediated stability: an effective hydrodynamic theory of spatiotemporal chaos. *Physica D*, 84:494–512, 1995.

[39] S. Ciliberto and M. Caponeri. Thermodynamics of spatiotemporal chaos: An experimental approach. *Phys. Rev. Lett.*, 64:2775–2778, 1990.

[40] W. Craig and C. E. Wayne. Periodic solutions of nonlinear Schrödinger equations and the Nash-Moser method. In *Hamiltonian mechanics (Toruń, 1993)*, pages 103–122. Plenum, New York, 1994.

[41] M. Cross and P. Hohenberg. Pattern formation outside of equilibrium. *Rev. Mod. Phys.*, 65:851–1112, 1993.

[42] G. Cruz Pacheco, C.D. Levermore, and B. Luce. Melnikov methods for Pde's with applications to perturbed nonlinear Schroedinger equations. *submitted Physica D.*

[43] E. Date and S. Tanaka. Periodic multi-soliton solutions of Korteweg-de Vries equation and Toda lattice. *Prog Theor Phys Supp*, 59:107–125, 1976.

[44] A. Degasperis. Resource letter sol-1: Solitons. *Am. J. Phys.*, 66:486–497, 1998.

[45] P. Deift, A. Its, and X. Zhou. *Long-time asymptotics for integrable nonlinear wave equations.* Important developments in soliton theory, 19980-1990. Springer-Verlag (New York), 1993.

[46] P. Deift, T. Kriecherbauer, K. T-R McLaughlin, S. Venakides, and X. Zhou. Asymptotics for polynomials orthogonal with respect to varying exponential weights. *Internat. Math. Res. Notices*, 1997:759–782, 1997.

[47] P. Deift, T. Kriecherbauer, K. T.-R. McLaughlin, S. Venakides, and X. Zhou. Uniform asymptotics for orthogonal polynomials. In *Proceedings of the International Congress of Mathematicians, Vol. III (Berlin, 1998)*, volume 1998, pages 491–501 (electronic), 1998.

[48] P. Deift, C. D. Levermore, and C. E. Wayne, editors. *Dynamical systems and probabilistic methods in partial differential equations*, Providence, RI, 1996. American Mathematical Society.

[49] P. Deift, L.C. Li, and C. Tomei. Symplectic aspects of some eigenvalue algorithms. In *Important developments in soliton theory*, pages 511–536. Springer, Berlin, 1993.

[50] P. Deift and E. Trubowitz. Inverse scattering on the line. *Comm. Pure Appl. Math.*, 32:121–251, 1979.

[51] P. Deift, S. Venakides, and X. Zhou. New results in small dispersion kdv by an extension of the steepest descent method for riemann–hilbert problems. *International Mathematics Research Notices*, pages 286–299, 1997.

[52] P. Deift and X. Zhou. A steepest descent method for oscillatory Riemann-Hilbert problems. Asymptotics for the MKdV equation. *Ann. of Math. (2)*, 137:295–368, 1993.

[53] P. Deift and X. Zhou. Long time behavior of the non-focusing nonlinear Schroedinger equation - a case study. *Lectures in Mathematical Sciences, Univ. of Tokyo*, pages 1–61, 1994.

[54] P. Deift and X. Zhou. Near integrable systems on the line. A case study — perturbation theory of the defocusing nonlinear Schrödinger equation. *Math. Res. Lett.*, 4:761–772, 1997.

[55] P. Devillard and B. Souillard. Polynomially decaying transmission for the nonlinear Schroedinger equation. *Journal of Statistical Physics*, 43:3–4, 1986.

[56] P.G. Drazin and R.S. Johnson. *Solitons: An Introduction*. Cambridge U.P., Cambridge, 1989.

[57] D.A. Egolf and H.S. Greenside. Dependence of extensive chaos on the spatial correlation length. *Nature (London)*, 369:129–131, 1994.

[58] D.A. Egolf and H.S. Greenside. Characterization of the transition from defect to phase turbulence. *Phys. Rev. Lett.*, 74:1751–1754, 1995.

[59] H. Epstein, J.-P. Eckmann, and C.E. Wayne. Normal forms for parabolic partial differential equations. *Ann. Inst. H. Poicare Phys. Theor.*, 58:287, 1993.

[60] N. Ercolani, M. Forest, and D. McLaughlin. Geometry of the modulational instability, III: Homoclinic orbits for the periodic sine Gordon equation. *Physica D*, 43:348–84, 1990.

[61] N. Ercolani, M. G. Forest, D. W. McLaughlin, and R. Montgomery. Hamiltonian structure for the modulation equations of a sine-Gordon wavetrain. *Duke Math. J.*, 55:949–983, 1987.

[62] N. Ercolani, S. Jin, D. Levermore, and W. MacEvoy. The zero dispersion limit of the NLS-MKdV hierarchy for the nonselfadjoint ZS operator. *Preprint*, 1992.

[63] N. M. Ercolani and D. W. McLaughlin. *Toward a topological classification of integrable PDE's.* The Geometry of Hamiltonian Systems. Springer-Verlag (New York), 1991.

[64] L.D. Faddeev and L.A. Takhtajan. *Hamiltonian methods in the theory of solitons.* Springer-Verlag (Heidelberg), 1987.

[65] N. Fenichel. Persistence and smoothness of invariant manifolds for flows. *Ind University Math J*, 21:193–225, 1971.

[66] N. Fenichel. Asymptotic stability with rate conditions. *Ind Univ Math J*, 23:1109–1137, 1974.

[67] N. Fenichel. Asymptotic stability with rate conditions II. *Ind Univ Math J*, 26:81–93, 1977.

[68] N. Fenichel. Geometric singular perturbation theory for ordinary differential equations. *J Diff Eqns*, 31:53–98, 1979.

[69] H. Flaschka. On the Toda lattice II. Inverse scattering solution. *Prog. Theor. Phys.*, 51:703–706, 1974.

[70] H. Flaschka, M. G. Forest, and D. W. McLaughlin. Multiphase averaging and the inverse spectral solution of the Korteweg de Vries equation. *Comm. Pure Appl. Math.*, 33:739–784, 1980.

[71] H. Flaschka and D. W. McLaughlin. Canonically conjugate variables for the Korteweg-de Vries equation and the Toda lattice with periodic boundary conditions. *Progr. Theoret. Phys.*, 55:438–456, 1976.

[72] A. S. Fokas and V. E. Zakharov, editors. *Important developments in soliton theory.* Springer-Verlag, Berlin, 1993.

[73] M. G. Forest, C. G. Goedde, and A. Sinha. Chaotic transport and integrable instabilities in a near-integrable, many-particle, Hamiltonian lattice. *Phys. D*, 67:347–386, 1993.

[74] M. G. Forest and J.E. Lee. Geometry and modulation theory for the periodic nonlinear Schrödinger equation. In *Oscillation theory, computation, and methods of compensated compactness (Minneapolis, Minn., 1985)*, pages 35–69. Springer, New York, 1986.

[75] M.G. Forest and K.T.R. McLaughlin. Onset of oscillations in nonsoliton pulses in nonlinear dispersive fibers. *J. Nonlinear Sci.*, 7:43–62, 1998.

[76] D. Forster, D. Nelson, and M. Stephen. Large distance and long time properties of a randomly stirred fluid. *Phys. Rev. A*, 16:732–749, 1977.

[77] C. S. Gardner, J. M. Greene, M. D. Kruskal, and R. M. Miura. Method for solving the Korteweg-de Vries equation. *Phys. Rev. Lett.*, 19:1095–1097, 1967.

[78] C. S. Gardner, J. M. Greene, M. D. Kruskal, and R. M. Miura. Korteweg-deVries equation and generalization. VI. Methods for exact solution. *Comm. Pure Appl. Math.*, 27:97–133, 1974.

[79] R. T. Glassey. On the blowing up of solutions to the Cauchy problem for nonlinear Schrödinger equations. *J. Math. Phys.*, 18:1794–1797, 1977.

[80] G. Goren, J. Eckmann, and I. Procaccia. Scenario for the onset of space-time chaos. *Phys. Rev. E*, 57:4106–4134, 1998.

[81] E. Grenier. Semiclassical limit of the nonlinear Schroedinger equation in small time. *Proc American Math Soc*, 126:523–530, 1998.

[82] R.O. Grigoriev and H.G. Schuster. Solvable model for spatiotemporal chaos. *Phys. Rev. E*, 57:388–396, 1998.

[83] M. Grillakis, J. Shatah, and W. Strauss. Stability theory of solitary waves in the presence of symmetry. I. *J. Funct. Anal.*, 74:160–197, 1987.

[84] M. Grillakis, J. Shatah, and W. Strauss. Stability theory of solitary waves in the presence of symmetry. II. *J. Funct. Anal.*, 94:308–348, 1990.

[85] J. Guckenheimer and P. Holmes. Nonlinear Oscillations, Dynamical Systems, and Bifurcations of Vector Fields. *Appl Math Sci*, 42, 1983.

[86] G. Haller. Homoclinic jumping in the perturbed nonlinear Schroedinger equation. *Comm. Pure and Appl. Math*, 1998.

[87] G. Haller. Multi-dimensional homoclinic jumping and the discretized NLS equation. *Comm. Math. Phys.*, 193:1–46, 1998.

[88] G. Haller and S. Wiggins. Multi-pulse jumping orbits and homoclinic trees in a modal truncation of the damped-forced nonlinear Schroedinger equation. *Physica D*, 85:311–347, 1995.

[89] D. Hansel and H. Sompolinsky. Solvable model of spatiotemporal chaos. *Phys. Rev. Lett.*, 71:2710–2713, 1993.

[90] A Hasegawa and Y Kodama. *Solitons in Optical Communications*. Oxford U.P., New York, 1995.

[91] P.C. Hohenberg and B.I. Shraiman. Chaotic behavior of an extended system. *Physica D*, 37:109, 1989.

[92] L. N. Howard and N. Kopell. Slowly varying waves and shock structures in reaction-diffusion equations. *Studies in Appl. Math.*, 56:95–145, 1976/77.

[93] C. Jayaprakash, F. Hayot, and R. Pandit. Universal properties of the two-dimensional Kuramoto-Sivashinsky equation. *Phys. Rev. Lett.*, 71:12–15, 1993.

[94] S. Jin, C. D. Levermore, and D. W. McLaughlin. The behavior of solutions of the NLS equation in the semiclassical limit. In *Singular limits of dispersive waves (Lyon, 1991)*, pages 235–255. Plenum, New York, 1994.

[95] S. Jin, C. D. Levermore, and D. W. McLaughlin. Semi-classical limits of defocusing NLS hierarchy. *Comm. Pure and Applied Math*, 52, 1999.

[96] F. John. *Partial differential equations*. Springer-Verlag, New York, 1971. Applied Mathematical Sciences, Vol. 1.

[97] C. Jones. Geometric singular perturbation theory. In *Dynamical systems (Montecatini Terme, 1994)*, pages 44–118. Springer, Berlin, 1995.

[98] T. Kappeler and Makarov M. On Birkhoff coordinates for KdV. *Univ. Zurich preprint*, 1999.

[99] T. Kappeler and J Poschel. *Perturbations of KdV in preparation*.

[100] M. Kardar, G. Parisi, and Y.C. Zhang. Dynamical scaling of growing interfaces. *Phys. Rev. Lett.*, 56:889–892, 1986.

[101] J. P. Keener and D. W. McLaughlin. Solitons under perturbations. *Phys. Rev. A (3)*, 16:777–790, 1977.

[102] J. B. Keller and D. W. McLaughlin. The Feynman integral. *Amer. Math. Monthly*, 82:451–465, 1975.

[103] R. Klein and A. J. Majda. Self-stretching of a perturbed vortex filament. I. The asymptotic equation for deviations from a straight line. *Phys. D*, 49:323–352, 1991.

[104] R. Klein and A. J. Majda. Self-stretching of perturbed vortex filaments. II. Structure of solutions. *Phys. D*, 53:267–294, 1991.

[105] R. Klein and A. J. Majda. An asymptotic theory for the nonlinear instability of antiparallel pairs of vortex filaments. *Phys. Fluids A*, 5:369–379, 1993.

[106] R. Klein, A. J. Majda, and K. Damodaran. Simplified equations for the interaction of nearly parallel vortex filaments. *J. Fluid Mech.*, 288:201–248, 1995.

[107] R. Klein, A. J. Majda, and R. M. McLaughlin. Asymptotic equations for the stretching of vortex filaments in a background flow field. *Phys. Fluids A*, 4:2271–2281, 1992.

[108] B. Knapp, G. Papanicolaou, and B. White. Nonlinearity and localization in one dimensional random media. *Journal of Statistical Physics*, 63:567, 1991.

[109] Y. Kodama. The Whitham equations for optical communications: Mathematical theory of NRZ. *SIAM J. of Appl. Math. in press*, 1999.

[110] N. Kopell. Waves, shocks, and target patterns in an oscillating chemical reagent. *Nonlinear Diffusion, Research Note in Math.*, 14:129–154, 1977.

[111] G. Kovacic. Dissipative dynamics of orbits homoclinic to a resonance band. *Phys. Lett. A*, 167:143–150, 1992.

[112] R.H. Kraichnan and S. Chen. Is there a statistical mechanics of turbulence? *Physica D*, 37:160, 1989.

[113] D. Krylov, L. Leng, K. Bergman, J. Kutz, and J. Bronski. Chirped pulse propagation and break-up in low dispersion optical fibers. *preprint*, 1999.

[114] S. B. Kuksin. *Nearly integrable infinite-dimensional Hamiltonian systems.* Springer-Verlag, Berlin, 1993.

[115] S. B. Kuksin. KAM-theory for partial differential equations. In *First European Congress of Mathematics, Vol. II (Paris, 1992)*, pages 123–157. Birkhäuser, Basel, 1994.

[116] S. B. Kuksin. Infinite-dimensional symplectic capacities and a squeezing theorem for Hamiltonian PDEs. *Comm. Math. Phys.*, 167:531–552, 1995.

[117] S. B. Kuksin. On squeezing and flow of energy for nonlinear wave equations. *Geom. Funct. Anal.*, 5:668–701, 1995.

[118] S. B. Kuksin. Growth and oscillations of solutions of nonlinear Schrödinger equation. *Comm. Math. Phys.*, 178:265–280, 1996.

[119] S. B. Kuksin. On turbulence in nonlinear Schrödinger equations. *Geom. Funct. Anal.*, 7:783–822, 1997.

[120] G.L. Lamb. *Elements of Soliton Theory.* Wiley, New York, 1980.

[121] P. D. Lax. Integrals of nonlinear equations of evolution and solitary waves. *Comm. Pure Appl. Math.*, 21:467–, 1968.

[122] P. D. Lax. *Hyperbolic Systems of Conservation Laws and the Mathematical Theory of Shock Waves.* Society for Industrial and Applied Mathematics. J W Arrowsmith Ltd England, 1973.

[123] P. D. Lax and C. D. Levermore. The small dispersion limit of the Korteweg-de Vies Equation I. *Comm. Pure and Applied Math*, 36(253-290), 1983.

[124] P. D. Lax and C. D. Levermore. The small dispersion limit of the Korteweg-de Vries Equation III. *Comm Pure and Applied Math*, 36:809–830, 1983.

[125] P. D. Lax and C. D. Levermore. The small dispersion limit of the Korteweg-de VSeries Equation II. *Comm. Pure and Applied Math*, 36:571–593, 1983.

[126] P. D. Lax, C. D. Levermore, and S. Venakides. The generation and propagation of oscillations in dispersive initial value problems and their limiting behavior. In *Important developments in soliton theory*, pages 205–241. Springer, Berlin, 1993.

[127] J. Lebowitz, H. Rose, and E. Speer. Statistical mechanics of a nonlinear Schroedinger equation. *Journal Statistical Physics*, 50:657–687, 1988.

[128] J. Lebowitz, H. Rose, and E. Speer. Statistical mechanics of the nonlinear Schroedinger equation. II Mean field approximation. *Journal Statistical Physics*, 54:17–56, 1989.

[129] Y. Li. Symbol dynamics for models of NLS equations. *to appear J. Nonlinear Sci*, 1999.

[130] Y. Li and D. W. McLaughlin. Morse and Melnikov functions for NLS pdes. *Commun. Math. Phys.*, 162:175–214, 1994.

[131] Y. Li, D. W. McLaughlin, J. Shatah, and S. Wiggins. Persistent homoclinic orbits for a perturbed nonlinear Schrödinger equation. *Comm. Pure Appl. Math.*, 49:1175–1255, 1996.

[132] Y. Li and S. Wiggins. Homoclinic orbits and chaos in discretized perturbed NLS systems II Symbol dynamics. *J. Nonlinear Science*, 7:315–370, 1997.

[133] Y. Li and S. Wiggins. *Invariant Manifolds and Their Fibrations for Perturbed NLS Pdes Graph Transform Approach.* Springer-Verlag (New York), 1997.

[134] P. L. Lions and A. J. Majda. Equilibrium statistical mechanics for nearly parallel vortex filaments. *Comm. Pure Appl Math*, 1999.

[135] W. Magnus and W. Winkler. *Hill's Equation.* Interscience-Wiley (New York), 1966.

[136] A. Majda, D. McLaughlin, and E. Tabak. A one dimensional model for dispersive wave turbulence. *J. Nonlinear Sci*, 7:9–44, 1997.

[137] P. Manneville. Liapounov exponents for the Kuramoto-Sivashinski model. In U. Frisch, J.B. Keller, G. Papanicolaou, and O. Pironneau, editors, *Macroscopic Modeling of Turbulent, Lecture Notes in Physics Vol. 230*, pages 319–326. Springer-Verlag, New York, 1985.

[138] F. Marchesoni and C. Lucheroni. Soliton density in an infinite toda lattice. *Phys. Rev. B*, 44:5303–5305, 1991.

[139] V.B. Matveev and M.A. Salle. *Darboux Transformations and Solitons.* Springer-Verlag, Berlin, 1991.

[140] H. P. McKean. Stability for the Korteweg - de Vries equation. *Comm. Pure Appl. Math*, 30:347–353, 1977.

[141] H. P. McKean. Erratum: "Statistical mechanics of nonlinear wave equations. IV. Cubic Schrödinger". *Comm. Math. Phys.*, 173:675, 1995.

[142] H. P. McKean. Statistical mechanics of nonlinear wave equations. IV. Cubic Schrödinger. *Comm. Math. Phys.*, 168:479–491, 1995.

[143] H. P. McKean and K. L. Vaninsky. Cubic Schrödinger: the petit canonical ensemble in action-angle variables. *Comm. Pure Appl. Math.*, 50:593–622, 1997.

[144] D. W. McLaughlin. Modulations of KdV wavetrains. *Physica D*, 3(1):335–343, 1981.

[145] D. W. McLaughlin, II Overman, E. A., S. Wiggins, and C. Xiong. Homoclinic orbits in a four-dimensional model of a perturbed NLS equation: a geometric singular perturbation study. In *Dynamics Reported*, pages 190–287. Springer, Berlin, 1996.

[146] D. W. McLaughlin and A. Scott. Perturbation analysis of fluxon dynamics. *Phys. Rev. A*, 18:1652 – 1679, 1976.

[147] D. W. McLaughlin and J. Shatah. Melnikov analysis for PDE's. In *Dynamical systems and probabilistic methods in partial differential equations (Berkeley, CA, 1994)*, pages 51–100. Amer. Math. Soc., Providence, RI, 1996.

[148] D. W. McLaughlin and J. Shatah. Homoclinic orbits for PDE's. In *Recent advances in partial differential equations Venice 1996*, pages 281–299. Amer. Math. Soc., Providence, RI, 1998.

[149] D.W. McLaughlin and E. A. Overman. Whiskered tori for integrable pdes and chaotic behavior in near integrable pdes. *Surveys in Appl Math 1*, pages 83–203, 1995.

[150] P. D. Miller and S. Kamvissis. On the semiclassical limit of the focusing nonlinear Schrödinger equation. *Phys. Lett. A*, 247:75–86, 1998.

[151] R.M. Miura. The Korteweg-de Vries equation: a survey of results. *SIAM Review*, 18:412–459, 1976.

[152] L.F. Mollenauer, E. Lichtman, G.T. Harvey, M.J. Neubelt, and B.M. Nyman. Demonstration of error-free soliton transmission over more than 15,000 km. *Electron. Lett.*, 27:792–794, 1992.

[153] J. Moser. *Stable and Random Motion in Dynamical Systems.* Princeton University Press, 1987.

[154] V. Muto, A. C. Scott, and P. L. Christiansen. A Toda lattic model for DNA: Thermally generated solitons. *Physica D*, 44:75–91, 1990.

[155] V. Muto, A.C. Scott, and P.L. Christiansen. Thermally generated solitons in a Toda lattice model of dna. *Phys. Lett. A*, 136:33–36, 1989.

[156] A.C. Newell. *Solitons in Mathematics and Physics.* SIAM, Philadelphia, 1985.

[157] A.C. Newell and J.V. Moloney. *Nonlinear Optics*. Addison-Wesley, Redwood City, 1992.

[158] S.P. Novikov, S.V. Manakov, L.P. Pitaevskii, and V.E. Zakharov. *Theory of Solitons. The Inverse Scattering Method*. Plenum, New York, 1984.

[159] C.S. O'Hern, D.A. Egolf, and H.S. Greenside. Lyapunov spectral analysis of a nonequilibrium ising-like transition. *Phys. Rev. E*, 53:3374–3386, 1996.

[160] C.-A. Pillet and C.E. Wayne. Invariant manifolds for a class of dispersive Hamiltonian partial differential equations. *J. Diff. Eqns*, 131:310, 1997.

[161] J. Poschel and E. Trubowitz. *Inverse Spectral Theory*. Academic Press (New York), 1987.

[162] J. E. Rothenberg. Observation of the buildup of modulational instability from wave breaking. *Optics Lett*, 16:18–20, 1990.

[163] J. E. Rothenberg and D. Grischkowsky. Observation of the formation of an opitcal intensity shock and wave breaking in the nonlinear propagtion of pulses in optical fibers. *Phys. Rev. Lett.*, 62:531–534, 1989.

[164] H. Segur. Solitons as approximate descriptions of physical phenomena. *Rocky Mountain J. Math.*, 8:15–24, 1978. Conference on the Theory and Application of Solitons (Tucson, Ariz., 1976).

[165] H. Segur. Asymptotics beyond all orders—a survey. In *Chaos in Australia (Sydney, 1990)*, pages 150–172. World Sci. Publishing, River Edge, NJ, 1993.

[166] H. Segur and M. D. Kruskal. Errata: "Nonexistence of small-amplitude breather solutions in ϕ^4 theory". *Phys. Rev. Lett.*, 58:1158, 1987.

[167] H. Segur and M. D. Kruskal. Nonexistence of small-amplitude breather solutions in ϕ^4 theory. *Phys. Rev. Lett.*, 58:747–750, 1987.

[168] J. Shatah and C. Zeng. Homoclinic orbits for perturbed sine Gordon equation. *Submitted to Comm. Pure Appl. Math.*, 1998.

[169] P. Sheng. *Introduction to Wave Scattering, Localization, and Mesoscopic Phenomena*. Academic Press, New York, 1995.

[170] B.I. Shraiman, A. Pumir, W. van Saarloos, P.C. Hohenberg, H. Chaté, and M. Holen. Spatiotemporal chaos in the one-dimensional complex ginzburg-landau equation. *Physica D*, 57:241–248, 1992.

[171] S. Smale. Differential Dynamical Systems. *Bull Amer Math Soc*, 73, 1967.

[172] K. Sneppen, J. Krug, M.H. Jensen, C. Jayaprakash, and T. Bohr. Dynamic scaling and crossover analysis for the Kuramoto-Sivashinsky equation. *Phys. Rev. A*, 46:R7351–7354, 1992.

[173] A. Soffer and M. I. Weinstein. Multichannel nonlinear scattering for nonintegrable equations. *Comm. Math. Phys.*, 133:119–146, 1990.

[174] A. Soffer and M. I. Weinstein. Multichannel nonlinear scattering for nonintegrable equations. II. The case of anisotropic potentials and data. *J. Differential Equations*, 98:376–390, 1992.

[175] A. Soffer and M. I. Weinstein. Resonances, radiation damping and instability in Hamiltonian nonlinear wave equations. *to appear in Invent. Math.*, 1999.

[176] H. Sompolinsky and A. Crisanti. Chaos in random neural networks. *Phys. Rev. Lett.*, 61:259–262, 1988.

[177] T. Spencer. The Schroedinger equation with a random potential: A mathematical review. *Gibbs Lecture of American Mathematical Society*, 1987.

[178] W.A. Strauss. *Nonlinear wave equations.* Published for the Conference Board of the Mathematical Sciences, Washington, DC, 1989.

[179] N. Theodorakopoulos and N.C. Bacalis. Thermal solitons in the Toda chain. *Phys. Rev. B*, 46:10706–10709, 1992.

[180] F. Tian. Private communication.

[181] M. Toda. *Theory of Nonlinear Lattices.* Springer-Verlag, Berlin, 1981.

[182] M. Toda, R. Kubo, and N. Saito. *Statistical physics.* Springer-Verlag, New York, 1983.

[183] J.A. Vastano and H.L. Swinney. Information trasport in spatiotemporal systems. *Phys. Rev. Lett*, 60:1773–1776, 1988.

[184] S. Venakides. The Korteweg-de Vries equation with small dispersion: higher order Lax-Levermore theory. *Comm. Pure Appl. Math.*, 43:335–361, 1990.

[185] C. E. Wayne. An introduction to KAM theory. In *Dynamical systems and probabilistic methods in partial differential equations (Berkeley, CA, 1994)*, pages 3–29. Amer. Math. Soc., Providence, RI, 1996.

[186] M. I. Weinstein. Modulational instability of ground-states of nonlinear schrödinger-equations. *SIAM J. of Appl. Math.*, 1985.

[187] M. I. Weinstein. Lyapunov stability of ground states of nonlinear dispersive evolution equations. *Comm. Pure and Applied Math*, 39:51–68, 1986.

[188] M.I. Weinstein. Asymptotic stability of nonlinear bound states in conservative dispersive systems. *Mathematical problems in the theory of water waves, contemporary mathematics*, 200, 1996.

[189] G.B. Whitham. Non-linear dispersive waves. *Proc. Roy. Soc. Ser. A*, 283:238–261, 1965.

[190] G.B. Whitham. *Linear and Nonlinear Waves*. John Wiley and Sons, 1974.

[191] S. Wiggins. *Global Bifurcations and Chaos: Analytical Methods*. Springer-Verlag (New York), 1988.

[192] R. W. Wittenberg. *Local dynamics and spatiotemporal chaos - the Kuramoto-Sivashinsky equation: a case study*. PhD thesis, Princeton University, 1998.

[193] V. Yakhot. Large scale properties of unstable systems governed by the Kuramoto Sivashinski equation. *Phys. Rev. A*, 24, 1981.

[194] V. Yakhot and S. Orszag. Renormalization group analysis of turbulence: Basic theory. *Journal of Scientific Computing*, 1:3–51, 1986.

[195] V. E. Zakharov, editor. *Nonlinear waves and weak turbulence*. American Mathematical Society, Providence, RI, 1998. Advances in the Mathematical Sciences, 36.

[196] V. E. Zakharov and A. B. Shabat. Exact theory of two-dimensional self- focusing and one-dimensional self-modulation of waves in nonlinear media. *Sov. Phys. JETP*, 34(1):62–69, 1972.

[197] V.E. Zakharov. Kolmogorov spectra in weak turbulence problems. *Handbook Plasma Phys.*, 2, 1984.

[198] V.E. Zakharov, V. Lvov, and G. Falkovich. *Wave Turbulence*. Springer-Verlag, New York, 1992.

[199] V.E. Zakharov, S.L. Musher, and A.M. Rubenchik. Hamiltonian approach to the description of nonlinear plasma phenomea. *Physics Reports*, 129:285–366, 1985.

[200] S. Zaleski. A stochastic model for the large scale dynamics of some fluctuating interfaces. *Physica D*, 34:427, 1989.